



PALEODYNAMICS OF THE GREEN POND OUTLIER,
NEW JERSEY HIGHLANDS: EVIDENCE FOR
NONCOAXIAL DEFORMATION DURING
LATE PALEOZOIC OROGENESIS


By JAMES PORTER MITCHELL

A thesis submitted to
The Graduate School-New Brunswick
Rutgers, The State University of New Jersey
in partial fulfillment of the requirements
for the degree of
Master of Science
Graduate Program in Geological Sciences

Written under the direction of
Professor Randall Forsythe
and approved by







New Brunswick, New Jersey

January, 1985

ABSTRACT OF THE THESIS

Paleodynamics of the Green Pond outlier,
New Jersey Highlands: evidence for
noncoaxial deformation during
late Paleozoic orogenesis
by JAMES PORTER MITCHELL

Thesis Director: Professor Randall Forsythe

A paleostress analysis of folds using echelon vein arrays and slickenfiber faults was conducted in Siluro-Devonian strata in the Green Pond outlier of northern New Jersey. Results indicate that slickenfiber faults principally record NW-SE trending compression oriented perpendicular to the dominant structural trend and that echelon vein arrays record a greater variation with a N-S maximum oriented oblique to the structural trend. The N-S compression, however, is oriented normal to an E-W trending locally developed second cleavage recognized for the first time in the Green Pond outlier. The two cleavages combined with the paleostress results indicates that noncoaxial deformation occurred in the Green Pond outlier. Additional field evidence suggests a clockwise rotation from a NW-SE direction of compression and shortening towards a N-S direction.

In the Allegheny Plateau in eastern Pennsylvania two noncoaxial phases of deformation with structural trends parallel to those in the Green Pond (NE-SW and E-W) are

clearly Alleghenian in age. The two noncoaxial structural trends may be followed discontinuously across the intervening provinces of the Great Valley and Valley and Ridge. Therefore, it is concluded that noncoaxial deformation in the Green Pond outlier is Alleghenian in age and provides the first evidence of phase II Alleghenian deformation in the Highlands province.

Regional correlations also indicate that noncoaxial deformation is locally restricted to the New York promontory and occurs on every promontory in the central and southern Appalachians. A rigid indenter model is presented to explain the noncoaxial deformation on the New York promontory and the corresponding rotation in the stress field recorded in the Green Pond outlier.

ACKNOWLEDGEMENTS

I wish to express sincere thanks to Dr. Forsythe, Dr. Olsson, and Dr. Flynn for their conscientious and helpful criticism of this work. I am especially grateful for the many stimulating conversations with Dr. Forsythe and for his patient and thorough direction during this project. Finally, a heartfelt thanks to Bob, a coach, and most especially to my wife Anna.

TABLE OF CONTENTS

ABSTRACT.....	ii
ACKNOWLEDGEMENTS.....	iv
TABLE OF CONTENTS.....	v
LIST OF TABLES.....	vii
LIST OF ILLUSTRATIONS.....	viii
LIST OF PLATES.....	xii
INTRODUCTION.....	1
BACKGROUND TO ECHELON VEIN ARRAYS AND SLICKENFIBER FAULTS.....	10
ECHELON VEIN ARRAYS.....	10
SLICKENFIBER FAULTS.....	28
METHODOLOGY FOR DYNAMIC ANALYSIS IN THE GREEN POND OUTLIER.....	38
RATIONAL FOR DYNAMIC ANALYSIS.....	38
ECHELON VEIN ARRAYS IN THE OUTLIER.....	41
SLICKENFIBER FAULTS IN THE OUTLIER.....	53
PALEODYNAMIC RESULTS.....	58
GENERAL TRENDS.....	58
NW-SE S1 TREND ORIENTED NORMAL TO FOLD HINGES.....	65
S1 TRENDS ORIENTED OBLIQUE TO FOLD HINGES AND THOSE ORIENTED PARALLEL TO FOLD HINGES.....	75
TECTONIC MODEL FOR THE OUTLIER.....	87
TIMING OF DEFORMATION: ALLEGHENIAN?.....	90
RELATION TO THE CENTRAL APPALACHIANS.....	95
AN INDENTOR MODEL FOR THE COLLISION OF GONDWANALAND AND LAURASIA AND DEVELOPMENT OF ZONES OF NONCOAXIAL DEFORMATION.....	105
CONCLUSIONS.....	116

APPENDIX.....	120
REFERENCES.....	121
VITA.....	129

LIST OF TABLES

TABLE 1. THE RELATION OF PRINCIPAL STRESS AXES TO CONJUGATE BRITTLE SHEARS.....	23
TABLE 2. THE RELATION OF PRINCIPAL STRESS AXES TO EVA AS ASSUMED IN THIS STUDY.....	47
TABLE 3. BRACHIOPODS OF MIDDLE DEVONIAN AGE COLLECTED FROM THE LOWER BELLVALE SANDSTONE AND MARCELLUS SHALE BY KUMMEL AND WELLER (1902) AND WILLARD AND CLEAVES (1933).....	92

LIST OF ILLUSTRATIONS

FIGURE 1. GEOLOGIC MAP OF NORTHERN NEW JERSEY.....	3
FIGURE 2. A) GEOLOGIC MAP OF THE GREEN POND OUTLIER WITH STRUCTURE (MAP FROM GEOLOGIC OVERLAY SERIES SHEET #22 OF THE NEW JERSEY GEOLOGICAL SURVEY; STRUCTURE AFTER BARNETT, 1976). B) STRATIGRAPHIC COLUMN OF PALEOZOIC ROCKS IN THE GREEN POND OUTLIER (AFTER BARNETT, 1976).....	4-6
FIGURE 3. THREE DIMENSIONAL REPRESENTATION OF THE GREEN POND FORMATION (S) AND SKUNNEMUNK CONGLOMERATE (D) SHOWING FOLDS AND CROSS- SECTIONS (CONSTRUCTED USING TECHNIQUES FROM RAGAN, 1973).....	8
FIGURE 4. SCHEMATIC ILLUSTRATION OF AN EVA WITH THE SENSE OF SHEAR INDICATED.....	11
FIGURE 5. TWO IDEALIZED CONJUGATE EVA GEOMETRIES (AFTER BEACH, 1975): A) TYPE I, B) TYPE II.....	11
FIGURE 6. EVA TYPES RELATED TO MASTER FRACTURES: A) PINNATE EVA, B) DILATANT ECHELON CRACKS, C) EVA AT FAULT AND VEIN TIPS.....	14
FIGURE 7. COMPLEX VEINING RELATED TO PROGRESSIVE SHEAR..	18
FIGURE 8. FOUR DYNAMIC MODELS FOR VEIN FORMATION RELATED TO EVA DEVELOPMENT: A) THE MODELS (AFTER RICKARD AND RIXON, 1983), B) RANGE OF POSSIBLE PRIMARY S1 ORIENTATIONS WITH RESPECT TO VEINS.....	26
FIGURE 9. DEVELOPMENT OF SFF (A AND B) AND THE EXPOSED SURFACE (C) (AFTER DURNEY AND RAMSAY, 1973)...	29
FIGURE 10. RELATION OF SFF TO PRINCIPAL STRESS AXES FOR ISOTROPIC ROCK.....	34
FIGURE 11. RELATION OF SFF TO PRINCIPAL STRESS AXES FOR ANISOTROPIC ROCKS.....	36
FIGURE 12. PHOTO TRACINGS OF EVA IN THE GREEN POND (ROCK HAMMER AND LENS CAP FOR SCALE).....	42
FIGURE 13. THREE DIMENSIONAL SHAPES OF EVA IN THE GREEN POND: A) RECTANGULAR, B) ELLIPTICAL....	43

FIGURE 14. TWO STEREOGRAMS OF THE SAME EVA DATA (SITE #2) SHOWING THAT DIFFERENT APPROACHES GIVE SIMILAR RESULTS (LINES=S1, CIRCLES=S3, DOTS=POLES TO BEDDING).....	49
FIGURE 15. VIEWING ONLY ONE EXPOSED SECTION WHEN MEASURING EVA SHEAR ZONES MAY LEAD TO AN ERRONEOUS MEASUREMENT. A THIRD POINT ON THE PLANE (OR SECOND SECTION) IS REQUIRED IN ORDER TO MEASURE THE TRUE ATTITUDE.....	52
FIGURE 16. SFF AND EVA ASSOCIATIONS IN THE GREEN POND...	55
FIGURE 17. ROAD MAP SHOWING PRINCIPAL SITES WHERE EVA AND SFF DATA WERE COLLECTED.....	59
FIGURE 18. THREE-DIMENSIONAL REPRESENTATION OF THE GREEN POND FORMATION SHOWING THE POSITIONS OF SITES IN THE FOLD STRUCTURES. SITES 1-4 ACTUALLY OCCUR ON MODERATE TO STEEPLY DIPPING LIMBS OF THE SKUNNEMUNK CONGLOMERATE AND, IN PART, THE BELLVALE SANDSTONE. ALMOST ALL OF THE REMAINING DATA COMES FROM THE GREEN POND FORMATION.....	60
FIGURE 19. CUMULATIVE S1-S3 PLOTS FOR ALL SFF AND EVA DATA: A) FROM SE DIPPING LIMBS, B) FROM HINGES, C) FROM NW DIPPING LIMBS (SHORT LINE=S1, CIRCLE=S3, DOTTED LINE= FIELD OF POLES TO BEDDING).....	62
FIGURE 20. S1 TRENDS FROM SFF: A) AT INDIVIDUAL SITES, B) CUMULATIVE PLOT OF ALL SFF.....	63
FIGURE 21. S1 TRENDS FROM EVA: A) AT INDIVIDUAL SITES, B) CUMULATIVE PLOT OF ALL EVA.....	64
FIGURE 22. OUTCROP DRAWING OF NUMEROUS EVA AND SFF WITH COMMON S1 ORIENTATIONS (ROUTE 23, NEWFOUNDLAND, NEW JERSEY).....	66
FIGURE 23. STEREOGRAMS EXEMPLIFYING S1 PATTERNS FOR NW-SE TRENDING DATA (EXAMPLES FROM SE DIPPING LIMBS): A) EVA-SITE 7 (MINOR FOLD), B) SFF- SITE 7 (MINOR FOLD), C) EVA-SITE 17, D) SFF- SITES 1 AND 3 COMBINED.....	69
FIGURE 24. OUTCROP DRAWING OF EVA AND SFF ON A MINOR FOLD (ROUTE 23, NEWFOUNDLAND,NJ).....	70

FIGURE 25.	A MODEL FOR THE STRESS HISTORY OF FOLDING AND DEVELOPMENT OF THE "S1 GAP": A) CROSS-SECTION OF FOLD LIMBS SHOWING ROTATION OF SIGMA 1 RELATIVE TO BEDDING, B) STEREOGRAM SHOWING SIGMA 1 PATTERN AND RELATIVE TIMING, C) SFF-SITES 1 AND 2 COMBINED (SHORT LINE= SIGMA 1, DOT=POLE TO BEDDING).....	73
FIGURE 26.	COMPUTER GENERATED S1 TRAJECTORIES DURING PROGRESSIVE FOLDING OF LAYERS WITH HIGH VISCOSITY CONTRAST (FROM DIETERICH AND CARTER, 1969).....	74
FIGURE 27.	SOME SITES WITH A LARGE SIGMA 1 POPULATION TRENDING: A) N-S (SITES 9,5,1, AND 3), B) NE-SW (SITES 12,11,1, AND 3).....	76
FIGURE 28.	A) CURVILINEAR S1 DISTRIBUTIONS MODELED BY SUBJECTING A FOLD LIMB TO OBLIQUE HORIZONTAL COMPRESSION DURING PROGRESSIVE FOLDING. S1 "PATHS" ARE SHOWN FOR TWO ORIENTATIONS OF OBLIQUE COMPRESSION (LINE=S1, CIRCLE=S3) B) EVA-SITE 3; NNW-SSE TRENDING SIGMA 1 AND SIGMA 3 "PATHS" COMPARE WITH THOSE IN THE MODEL.....	80
FIGURE 29.	POLES TO CROSS-CLEAVAGE (LARGE DOTS) AND BEDDING (SMALL DOTS) FROM SITES 1 AND 2 OF THE MAIN SYNCLINE. NOTE THE DISCORDANCE OF TRENDS.....	82
FIGURE 30.	SUMMARY OF NONCOAXIAL DEFORMATION RECORDED BY STRUCTURES IN THE GREEN POND OUTLIER INDICATES A CLOCKWISE ROTATION OF THE MAXIMUM SHORTENING AND COMPRESSION DIRECTION FROM NW-SE TO ALMOST N-S.....	86
FIGURE 31.	THREE POSSIBLE MODELS OF STAGE II DEFORMATION IN THE GREEN POND OUTLIER RELATED TO STRIKE-SLIP FAULTING DURING N-S DIRECTED COMPRESSION (E=EXTENSION, C=COMPRESSION).....	88
FIGURE 32.	SITES OF PREVIOUS STUDIES THAT HAVE REPORTED NONCOAXIAL STRUCTURAL TRENDS OF PROBABLE ALLEGHENIAN AGE.....	96
FIGURE 33.	FOLD TRACES IN THE CENTRAL APPALACHIANS (PRIMARILY AFTER GEISER AND ENGELDER, 1983, AND COHEE ET AL., 1976). DOTTED LINES= LACKAWANA SYNCLINE AND GREEN POND "SYNCLINE".	97
FIGURE 34.	CLEAVAGE TRENDS IN THE NORTHERN CENTRAL APPALACHIANS (PRIMARILY AFTER GEISER AND ENGELDER, 1983).....	98

FIGURE 35.	CONTINENT-CONTINENT COLLISION MODEL FOR THE NEW YORK PROMONTORY AND PENNSYLVANIA REENTRANT: A) CONVERGING CONTINENTAL MARGINS OF GONDWANALAND AND LAURASIA, B) INITIAL CONTACT ON LEADING EDGE OF PROMONTORY MARGIN, C) SUBSEQUENT CONTACT ALONG THE PROMOTORY SIDE(S), D) CONTACT AND OCEAN CLOSURE IN THE REENTRANT.....	108
FIGURE 36.	A) FOLD AND THRUST DEVELOPMENT ON THE INDIAN CRATON ORIENTED PARALLEL TO WRENCH FAULTS ALONG THE INDIA-ASIA SUTURE, B) SLIP LINES PREDICTED IN RIGID INDENTOR MODEL (AFTER TAPPONNIER AND MOLNAR, 1976).....	110
FIGURE 37.	A MAJOR RIGHT-LATERAL WRENCH FAULT SYSTEM ON A PERMO-TRIASSIC RECONSTRUCTION (ADAPTED FROM VAN DER VOO, 1981).....	112
FIGURE 38.	NONCOAXIAL STRUCTURAL TRENDS OF PROBABLE ALLEGHENIAN AGE REPORTED ON PROMONTORIES IN THE CENTRAL AND SOUTHERN APPALACHIANS....	114

LIST OF PLATES

- PLATE 1. QUARTZ FIBERS ON A SFF SURFACE (SITE #1).
TWO STAGES OF DISPLACEMENT ARE INDICATED.
THE FIRST TRENDS NW AND THE LATER TRENDS
MORE NORTHERLY.....79
- PLATE 2. EVA ORIENTATIONS INDICATE MAXIMUM
COMPRESSION DIRECTED N-S AND NORMAL
TO CLEAVAGE CONSISTENT WITH COEVAL
DEVELOPMENT DURING A PERIOD OF
OBLIQUE COMPRESSION AND SHORTENING
(SITE #1).....83

INTRODUCTION

Structural geologists typically restrict their field studies to geometric and kinematic (ie. strain) information recorded in naturally deformed rocks without addressing the dynamics (ie. stresses) that caused the deformation. However, particular structural features are locally developed in orogenic belts which, with some reasonable assumptions, can be used directly for dynamic analysis. Such a unique set of dynamic features is developed in the Green Pond outlier in northern New Jersey. These features are 1) echelon vein arrays (EVA) and 2) "slickenfiber" faults (SFF) (terminology of Wise et al., 1984). They are two distinct types of brittle and semi-brittle shear zones that have geometric attributes that can be assumed to bear a direct relation to the direction of applied stress that caused them to form. Previous field studies in other areas have utilized them for kinematic information (EVA: Shainin, 1950; Hancock, 1964; Ramsay and Graham, 1970; SFF: Cloos, 1971) and more recently for dynamic information (EVA: Dalziel and Stirewalt, 1975; Etchecopar, 1981; Rispoli and Vasseur, 1983; SFF: Marshak, 1981; Etchecopar, 1981; Rispoli and Vasseur, 1983; Bristol et al., 1984).

Many dynamic studies have been conducted by using quartz deformation lamellae and calcite twins (see review

of eight studies in Dieterich and Carter, 1969) as well as by using fracture patterns (Burger and Thompson, 1970; Friedman and Stearns, 1971). However, in all cases cited, studies were restricted to a single fold. In this study numerous shear zones were measured (202 EVA and 130 SFF) from four large folds over an area of about 80 square miles within the Green Pond outlier of northern New Jersey. As such the data base provides regional information about the directions of principal stresses that operated in northern New Jersey during the structural evolution of the Green Pond outlier.

The study area covers most of the New Jersey portion of the Green Pond outlier (figure 1). It is about 20 miles long (Dover northeastward to West Milford) and less than 5 miles wide (NW-SE). Much of the stratigraphic and structural relations of the outlier have been mapped by Barnett (1976). Additional structural analysis has been conducted by Rowlands, but as yet is not published (Rowlands, personal communication). The outlier consists of Cambrian through Middle Devonian sedimentary rocks resting above and surrounded by Precambrian rocks of the Reading Prong (figure 2a). Cambrian and Ordovician strata occur discontinuously between the Precambrian and the Silurian and Devonian strata suggesting an angular unconformity in the sequence. In contrast, the Silurian and Devonian strata can be mapped continuously throughout

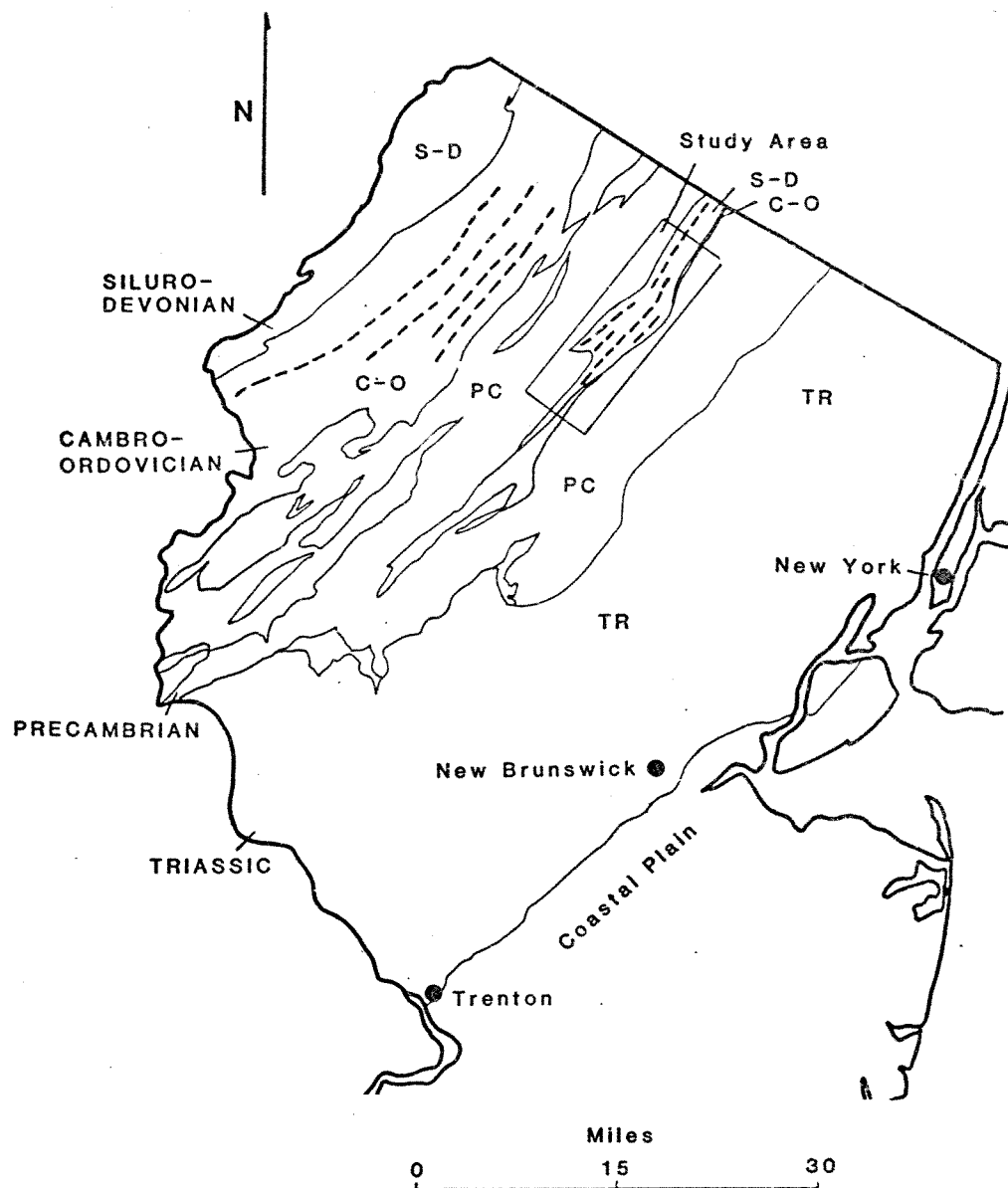


FIGURE 1. GEOLOGIC MAP OF NORTHERN NEW JERSEY.

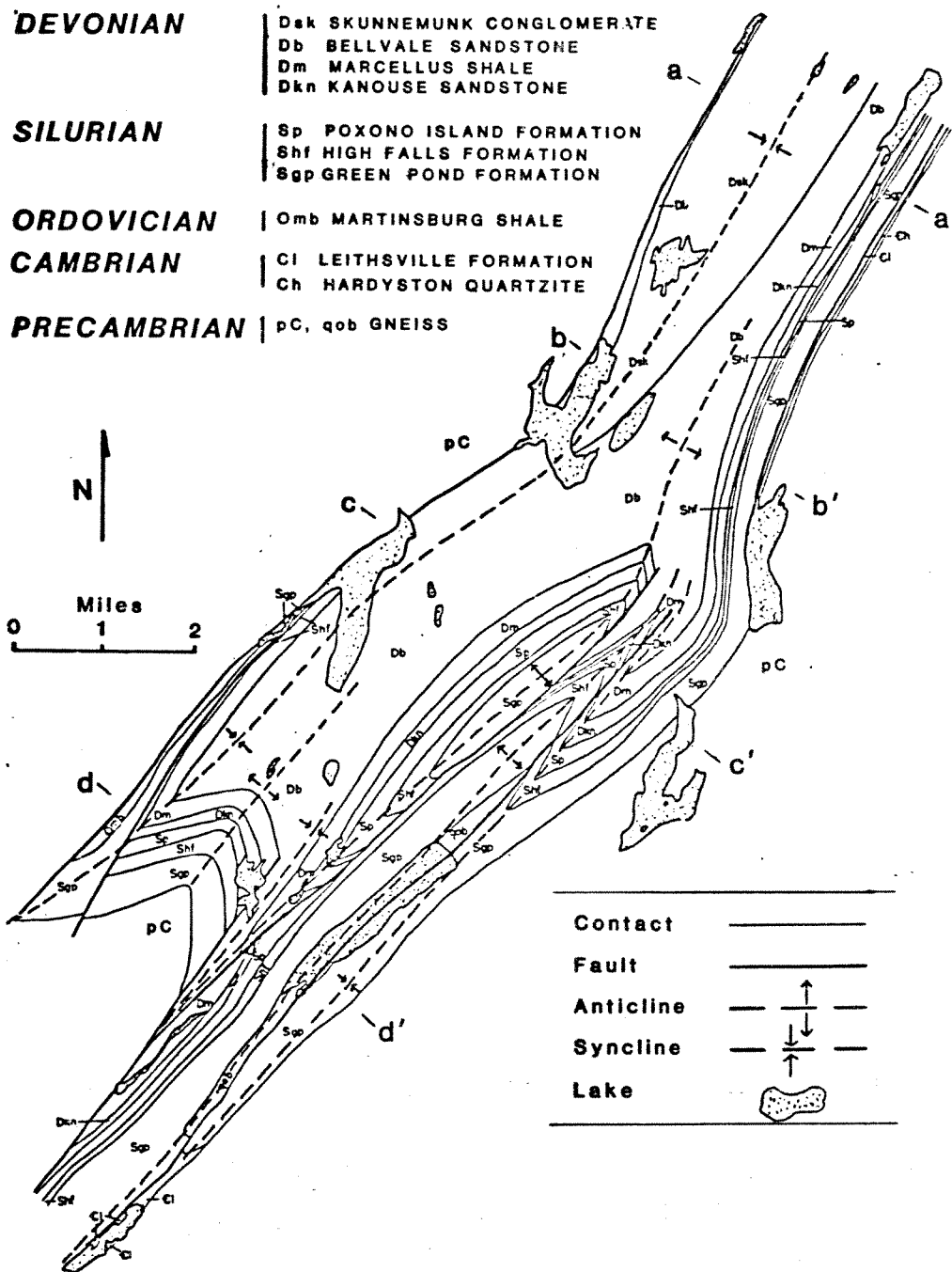
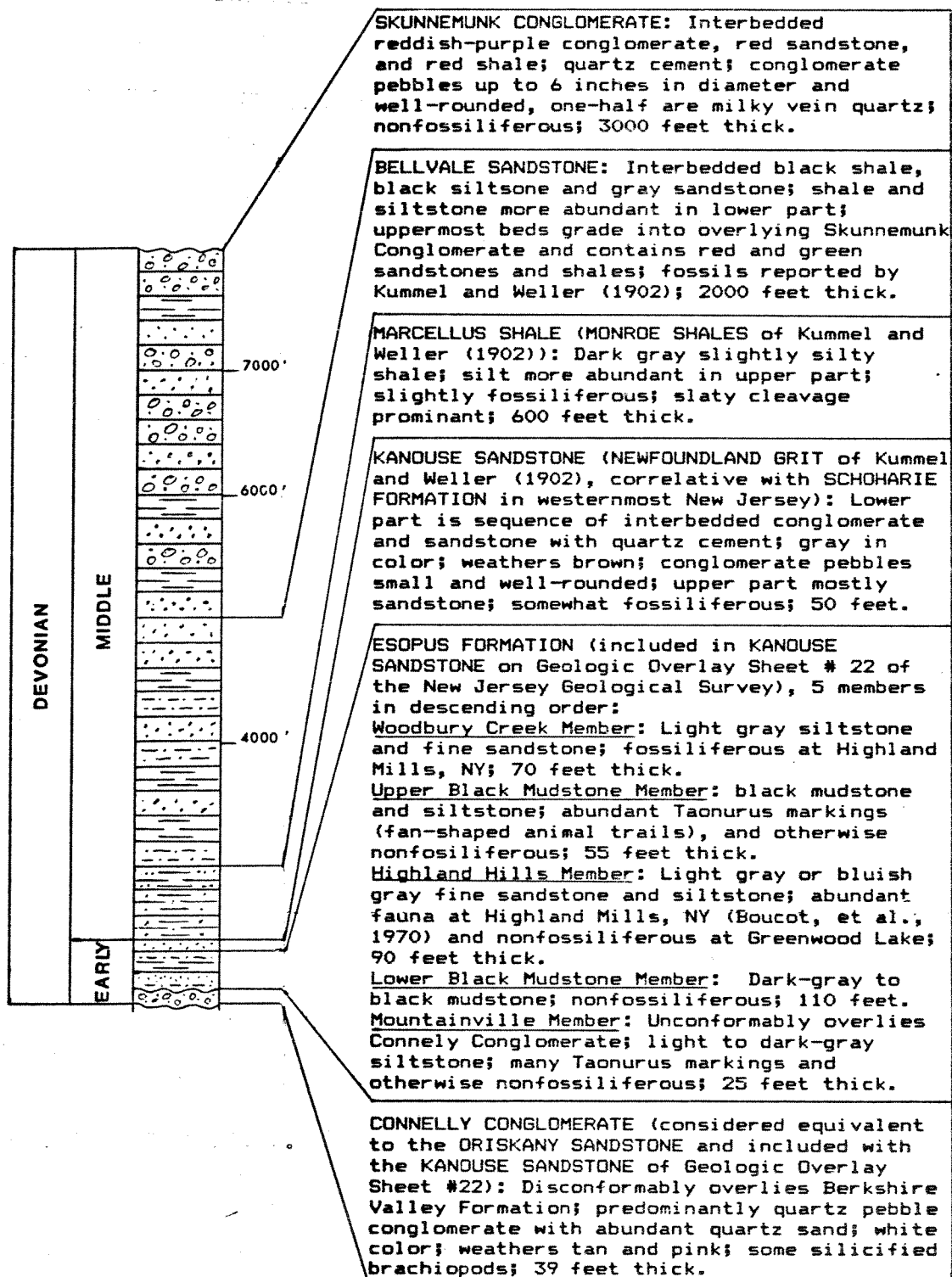
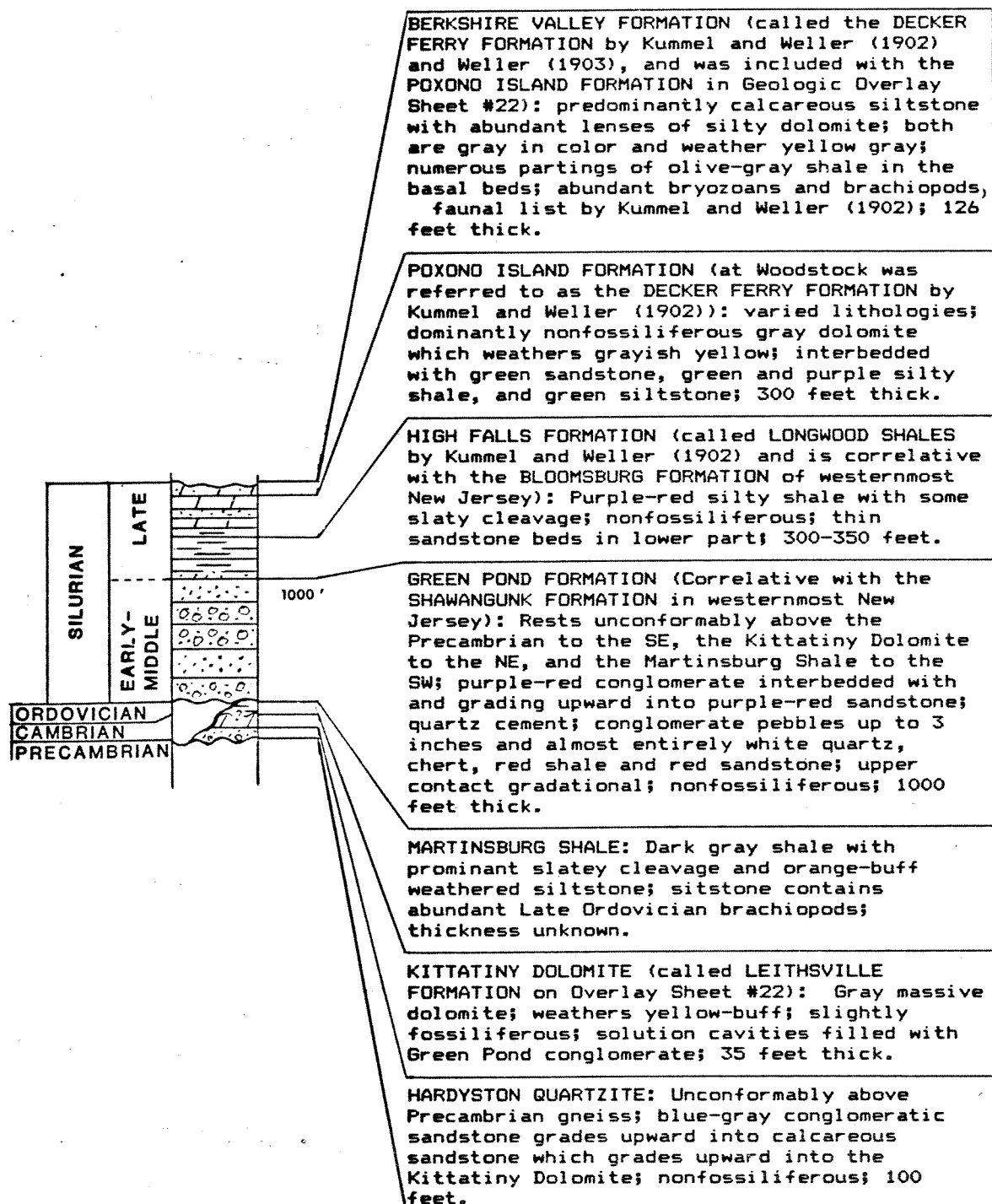


FIGURE 2. A) GEOLOGIC MAP OF THE GREEN POND OUTLIER WITH STRUCTURE (MAP FROM GEOLOGIC OVERLAY SERIES SHEET #22 OF THE NEW JERSEY GEOLOGICAL SURVEY; STRUCTURE AFTER BARNETT, 1976). B) STRATIGRAPHIC COLUMN OF PALEOZOIC ROCKS IN THE GREEN POND OUTLIER (AFTER BARNETT, 1976).





the outlier. The Silurian and Devonian strata consist of nine formations as shown in the stratigraphic column of figure 2b. Data were collected from the thickest and most exposed formations which are the Shawangunk Formation (Silurian), Bellvale Sandstone (Devonian), and Skunnemunk Conglomerate (Devonian) (Barnett, 1976).

The overall structure of the Green Pond is one of a series of upright northeast trending fold structures that have been down-faulted within the Highlands province between adjacent ranges of Precambrian rocks. Folds in general are doubly plunging with gently plunging hingelines. Fold geometry in the study area, as illustrated in figure 3, is characterized in the north by a large tightly folded asymmetric syncline with a steeply dipping eastern limb which is overturned in some regions. Southward it expands to include three smaller amplitude open folds separated by faults (Barnett, 1976). Axial surface cleavage, both slaty and spaced (?pressure solution) cleavage, is largely restricted to the finer units (shales and siltstones) and is subvertical at most sites. In addition, a locally developed second spaced cleavage has been observed in the large syncline and strikes nearly E-W at a high angle to the fold structure. Compared with deformation in equivalent age strata in the Valley and Ridge to the northwest, metamorphic grade is slightly higher in the outlier (Thompson, PhD) and there

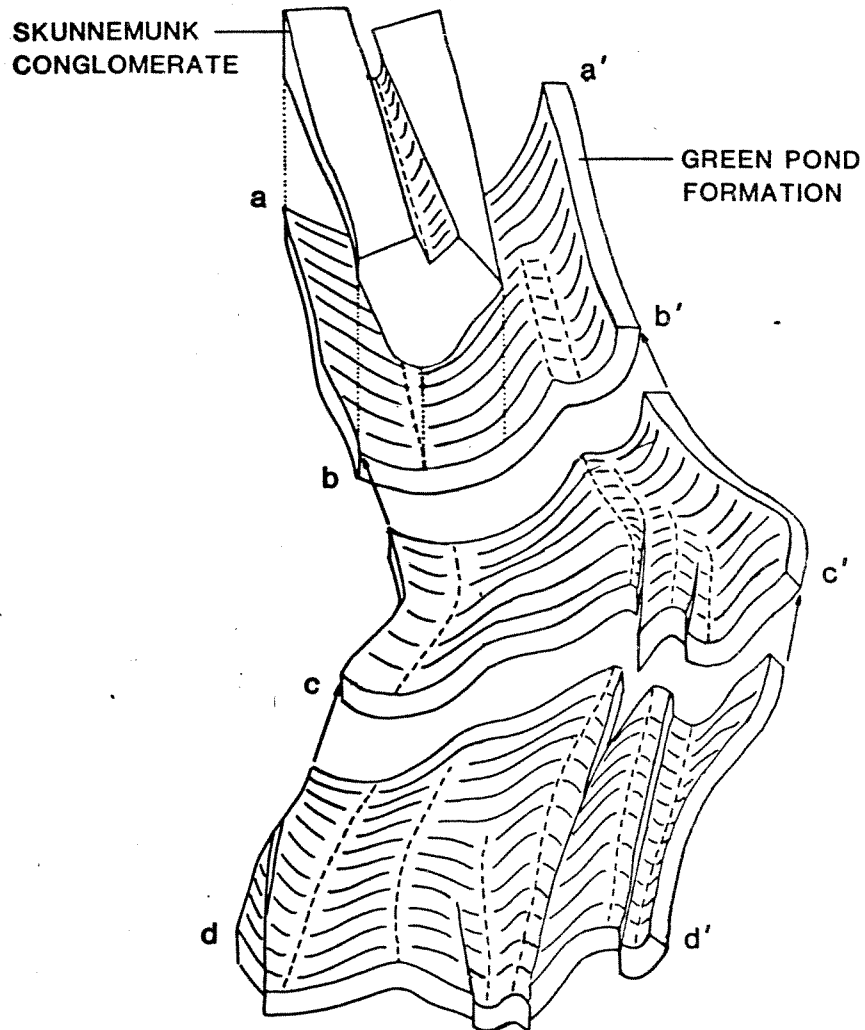


FIGURE 3. THREE DIMENSIONAL REPRESENTATION OF THE GREEN POND FORMATION (S) AND SKUNNEMUNK CONGLOMERATE (D) SHOWING FOLDS AND CROSS-SECTIONS (CONSTRUCTED USING TECHNIQUES FROM RAGAN, 1973).

is no strong fold vergence.

The overall approach of this study is to determine regional trends in paleostress directions that accompanied deformation of the Green Pond outlier and wherever possible to identify these trends with finite strain recorded by other structures (eg. folds and cleavages). The result is an integrated paleostress and structural history of the Green Pond outlier that may be compared with the structural history of the surrounding region. After these results are presented, they will first be discussed in light of late Paleozoic deformation in the Central Appalachians and then used as a dynamic complement to existing kinematic data in a discussion of recent models of the Alleghenian orogeny (?collision of Laurasia and Gondwanaland).

BACKGROUND TO ECHELON VEIN ARRAYS AND SLICKENFIBER FAULTS

INTRODUCTION

The purpose of this section is to provide a background understanding of echelon vein arrays and slickenfiber faults, as dynamic interpretations of these features form the basis of the present study. General geometric attributes and models of development are presented which are considered applicable to features in the Green Pond, though specific attributes observed in the Green Pond are discussed in a later section. Also in this section, background of the relation of applied stress directions to the formation of these structures is presented which provides a foundation for the dynamic assumptions and techniques used in this study.

ECHELON VEIN ARRAYS (EVA)

EVA Geometry

An echelon vein array (EVA), is a series of roughly parallel and overlapping veins or veinlets in an echelon arrangement as schematically illustrated in figure 4. Veins are oriented at relatively low angles to the array

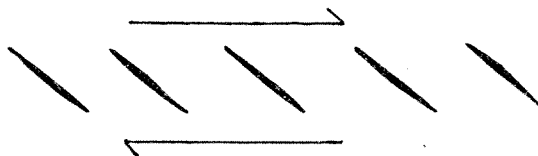


FIGURE 4. SCHEMATIC ILLUSTRATION OF AN EVA WITH THE SENSE OF SHEAR INDICATED.

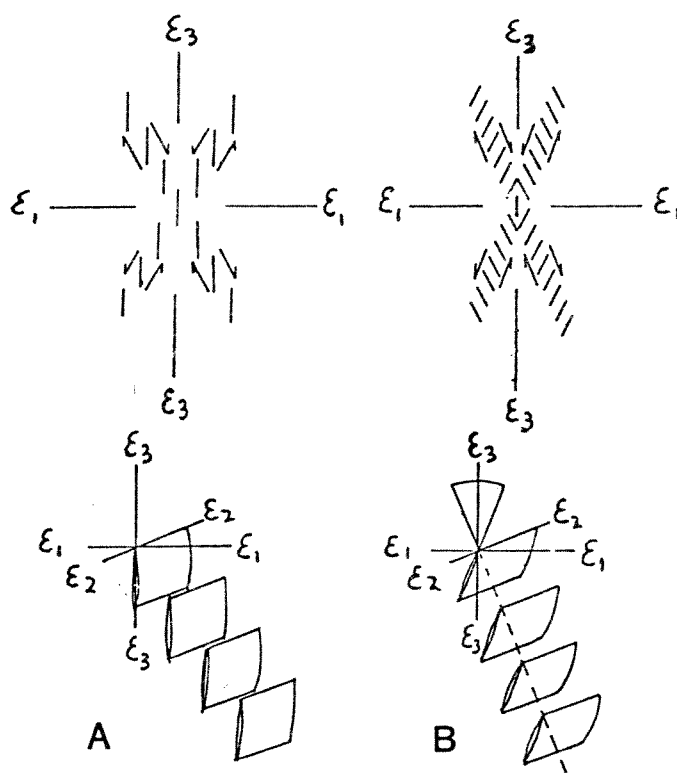


FIGURE 5. TWO IDEALIZED CONJUGATE EVA GEOMETRIES (AFTER BEACH, 1975): A) TYPE I, B) TYPE II.

(<45 degrees) indicating that development is related to shear in a tabular zone roughly defined by the array and vein dimensions. The sense of displacement is such that veins are rotated away from the shear zone during progressive shear (Ramsay and Graham, 1973). EVA have also been described as "tension gash arrays" (Roering, 1969), "tension gash bands" (Dalziel and Stirewalt, 1975), and "lens-belts" (Hancock, 1964).

EVA frequently occur in conjugate pairs (Ramsay and Graham, 1970). That is, two arrays intersect while displaying complementary senses of shear (figure 5) such that the bulk rock is shortened (minimum principal strain axis, e_3) in the acute angle between arrays and extended (maximum principal strain axis, e_1) in the obtuse angle (Shainin, 1950; Davis, 1984). Two conjugate EVA geometries that have been noted in the literature (Beach, 1975) are shown in figure 5 with the senses of shear and principal finite strain axes indicated. Some studies have recorded type I geometry (figure 5a) where individual veins parallel the maximum shortening direction (Beach, 1975; Roering, 1968) but most studies have reported type II geometry (figure 5b) where individual veins parallel complementary shear zones and hence lie at an angle to the bulk shortening direction (Shainin, 1950; Roering, 1968; Ramsay and Graham, 1970, figure 11; Beach, 1975; Rickard and Rixon, 1983; this study).

Other types of EVA form in relation to master fractures (ie. faults and larger veins). "Pinnate veins" (Hancock, 1972) or vein filled "feather joints" (Cloos, 1932; Dennis, 1972, p. 280) branch diagonally from a master vein or fault (figure 6a). EVA which create discontinuities along veins have been called "dilatant echelon cracks" (Pollard et al., 1982) (figure 6b). Also, EVA may occur at fault tips (Fletcher and Pollard, 1981; Rispoli, 1981) or vein tips (Roering, 1968; Beach, 1977) (figure 6c). To my knowledge, intersecting conjugates of these types have not been observed.

EVA Development

General Conditions: While not always the case, many EVA develop within the more competent beds of folded sedimentary sequences (Ramsay and Graham, 1970; Beach, 1977). Their development is believed on the basis of kinematic arguments to be an integral part of the deformation process that involves cleavage formation and buckling (Ramsay, 1967).

Also, due to the restricted nature of recrystallization of EVA it is likely that they develop at shallow depths, yet deep enough for greatly reduced permeabilities within the sedimentary pile (Beach, 1977; Rickard and Rixon, 1983). Since permeability and porosity versus depth functions depend on many factors (eg. thermal

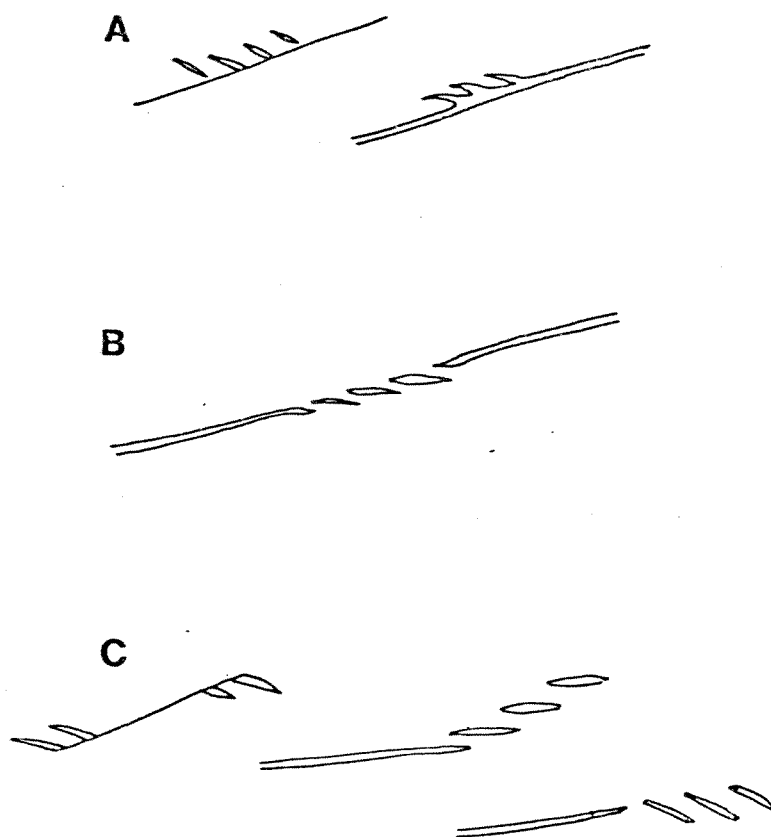


FIGURE 6. EVA TYPES RELATED TO MASTER FRACTURES:
A) PINNATE EVA, B) DILATANT ECHELON CRACKS,
C) EVA AT FAULT AND VEIN TIPS.

gradients, composition, and rates of burial), exact depths and conditions for EVA development are difficult to estimate. Rickard and Rixon (1983) conclude from stratigraphic considerations that EVA in an area of Australia developed at depths of less than 3 KM and probably at about 1 KM. Also, fluid pressures close to or greater than lithostatic pressures are likely to be necessary conditions for EVA formation.

The development of EVA is thought to be a continuous process involving both brittle (microfracturing and fracturing) and ductile deformation (crystal plasticity, grain boundary sliding and grain boundary diffusion) (Knipe and White, 1979). Therefore, what follows is not a discussion of a single process but a simplified sequence of interrelated and overlapping processes that dominate during the evolution of EVA. On the basis of micro- and mesostructural studies two characteristic stages of EVA development are presented. Then modern concepts of fluid dynamics are presented which provide a mechanism for vein formation and a commonality in all aspects of EVA development.

Two-Stage Formation: On the basis of observed structures the development of EVA appears to follow at least a two-stage evolution. This involves an early microcracking stage during incipient shear zone development which continues into a second stage of

incremental vein growth. Microcracks are thought to play an important role in early EVA development (Knipe and White, 1979). They have been found in shear zones which were thought to be precursors to EVA indicating that microcrack development preceeds vein formation (Knipe and White, 1979). In laboratory experiments microcracks have been observed to preceed shear failure (Hallbauer et al., 1973) and to grow by coalescence of pre-existing microcracks (Lajtai, 1971). Thus, a tabular zone of microcracks along a plane of shear probably establishes the EVA shear zone prior to vein formation.

During stage two, microcracks coalesce to form EVA veins. The available evidence suggests that this usually occurs incrementally. Studies of mineral filled veins show that mineral fibers filling veins of EVA have an incremental growth history of fissure propagation and dilation (Durney and Ramsay, 1973; Ramsay, 1980a). Ramsay (1980a) concludes that incremental vein growth involves a repeated process of 1) fracture formation and subsequent 2) sealing of the fracture by mineral growth in optical continuity with the pre-existing mineral species (usually quartz) resulting in incremental lengthening of fibers. In contrast to fibrous forms, massive mineral forms (eg. drusy quartz), sometimes accompanied by comb structure and vugs, have also been observed in veins of EVA (Beach, 1975). These latter textures reflect spacious quarters

during crystallization as well as formation during a single event or at least during a rather large increment of vein growth (Beach, 1977). In one study both fibrous and massive forms of quartz were observed in some veins of EVA which was interpreted as the result of unequal increments of dilation during vein formation (Beach, 1975). Since fibrous mineral forms have been reported in veins of EVA from most studies it appears that EVA generally evolve incrementally in accordance with this model.

The first increments of vein growth take place prior to significant displacement on the shear zone (Ramsay, 1979; Knipe and White, 1979). However, many EVA, though not all, record significant shear strains related to progressive shear (Ramsay and Graham, 1970). This shear resulted in complex vein formation coeval with dominately ductile deformation processes (stages two and three of Knipe and White, 1979). Examples of complex veining related to progressive shear are shown in figure 7. Pre-existing veins may rotate while at the same time continue to grow resulting in sigmoidal shaped veins containing curved fibers (Durney and Ramsay, 1970). Vein spurs may develop off of deformed veins (Shainin, 1950). And new veins may cut across pre-existing ones (Shainin, 1950; Durney and Ramsay, 1970). Also, vein tips may grow beyond the shear zone and turn into low angles to the

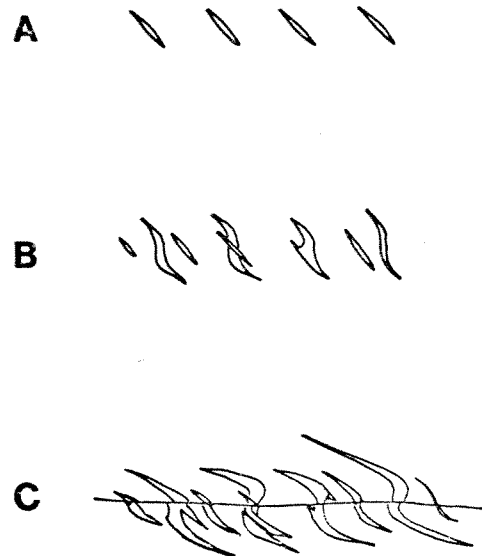


FIGURE 7. COMPLEX VEINING RELATED TO PROGRESSIVE SHEAR.

shear zone which accentuates the sigmoidal shape of deformed veins (Rickard and Rixon, 1983) (figure 7c). Meanwhile, ductile deformation processes are operating which result in deformation lamellae, undulatory extinction, and recrystallization (Knipe and White, 1979). Deformation within the shear zone sometimes culminates in development of minor cleavage restricted to the shear zone and oriented perpendicular to veins (Beach, 1975; Beach, 1977; Rickard and Rixon, 1983) and/or a late stage through-going fracture or fault (Knipe and White, 1979; Rickard and Rixon, 1983).

Fluids and EVA Formation: In recent years it has become apparent that fluids play an important role in many aspects of fold and thrust development in sedimentary terranes, including EVA development. High fluid pressures within pore spaces of rock may cause rock to fail at anomalously low strengths (Hobbs et al., 1976). This is in part because stress concentrations occur at crack tips such that fluids within a pre-existing crack may easily propagate the crack even at low fluid pressures. Furthermore, hydrofracturing experiments whereby pressurized fluids are injected into rock, demonstrate that fluids can create fractures in rock (Fyfe et al., 1978). These conditions are considered applicable to EVA vein formation (Beach, 1976; Beach, 1983) as well as jointing (Fyfe, 1978) and thrust (Hubbert and Rubey, 1959)

development. Also, fluids influence ductile deformation processes involved in cleavage development, recrystallization, and folding. Thus, dynamics of fluids when mobilized in a region of fold and thrust development touches on all rheologic aspects of structural development.

Likewise, fluids are likely to facilitate all aspects of EVA evolution described earlier. High fluid pressures facilitate microcrack development and may drive the coalescence of microcracks that leads to vein formation (Fyfe, 1978). Similarly, the reduction of fluid pressures tends to initiate mineralization and halt crack growth (Casey, 1980) resulting in the first increment of vein formation. Laboratory experiments have shown that the effect of microcrack and crack development is to dilate the rock. Dilation in turn increases pore volume which reduces fluid pressure. As a result, low pressure sinks in cracks create a pressure gradient in rocks which, in a manner analogous to suction, draws mineral rich fluids out of adjacent rock into vein fissures where minerals crystallize (Casey, 1980). Thus, the first increment of vein growth may involve a process of 1) hydrofracturing which propagates cracks and 2) dilation which halts crack growth and creates low pressure sinks that facilitate mineralization. Subsequent vein growth recorded by mineral fibers would occur as fluid pressures are

repeatedly restored to hydrofracture levels and dissipated by an increment of crack growth.

Relation of EVA to Applied Stresses

The geometry of EVA found in nature was shown previously in figures 4-6. In this section it is shown that the relation of conjugate EVA to the stress directions that cause them to form is relatively well constrained. This permits these features to be used as indicators of the paleostress directions at the time of their formation. Also, approaches to dynamic analysis using EVA in the absence of conjugates are discussed.

Since EVA occur as zones of shear with known displacement directions they must develop at some angle less than 90 degrees to the applied compression direction. While this in itself is not very useful, additional constraints are given based on experimental compression tests on natural rock where the relation of applied stress to the orientation of induced conjugate shears is well-documented. Specifically, samples of relatively isotropic and homogeneous rock under an applied axial load (maximum principal stress axis, s_1) often fail by the production of conjugate shear fractures oriented symmetrically about the principal stress directions such that s_1 bisects the acute angle between shears (Daubree, 1897; Shainin, 1950, fig. 7; Griggs and Handin, 1960;

Turner and Weiss, 1963, p. 293; Hobbs et al., 1976, p. 325; Davis, 1984, p. 306). The relation of the shears to the principal stress axes are listed in table 1. Inasmuch as the conjugate shear zones of EVA form in a manner analogous to the conjugate shear fractures, the stress directions responsible for the development of conjugate EVA are the same as that in table 1. Conjugate EVA and conjugate shear fractures in the same specimen have been produced in compressed clay (Davis, 1984, p. 306, fig. 9.63) which shows, at least qualitatively, that the geometric relations of stress and strain to conjugate fractures just described, also applies to conjugate EVA. Furthermore, under ideal conditions, principal stress axes parallel principal strain axes (Means, 1976, p. 252; Ramsay, 1980b; Davis, 1984, p. 306), hence, for EVA idealized earlier in figure 5 the direction of applied stress (s_1) parallels the bulk shortening direction (e_3).

Many EVA occur in nature without intersecting conjugates. This is not surprising since a single set of shear fractures, rather than conjugates, commonly occurs in laboratory experiments, even under "ideal" conditions (Handin, 1960; Turner and Weiss, 1963; Davis, 1984). Unfortunately, this means that the causal stress directions can not be determined using table 1. Rather, an additional assumption is required for isolated EVA in order to use them as a tool for measuring the paleostress

TABLE 1. THE RELATION OF PRINCIPAL STRESS
AXES TO CONJUGATE BRITTLE SHEARS.

S1 BISECTS THE ACUTE ANGLE BETWEEN SHEARS.

S2 PARALLELS THE INTERSECTION OF THE SHEAR
ZONES AND IS PERPENDICULAR TO THE
DIRECTION OF DISPLACEMENT ON EACH SHEAR.

S3 BISECTS THE OBTUSE ANGLE BETWEEN SHEARS.





directions. For example, since field studies consistently indicate that conjugate arrays form an acute angle of 40 degrees (Shainin, 1950; Roering, 1969; Rickard and Rixon, 1983), one may assume that s_1 lies about 20 degrees from the shear zone for all EVA, including isolated arrays. Or, one may find that isolated arrays occur in an area where only type II conjugates are found and therefore assume that s_1 bisects the acute vein-array angle for each EVA (see figure 5b). A third approach, is to assume that s_1 parallels individual veins (eg. Dennis, 1972, p. 302; Etchecopar, 1981). This approach is rather tempting since veins in EVA are reported to show more evidence of forming as tensile fractures rather than as shear fractures (Rickard and Rixon, 1983), and the assumption is consistent with type I conjugate geometry. However, this approach is clearly incorrectly applied to conjugate shear zones of type II conjugate EVA geometry for determining the principal stress directions that initiate the shear zones. Therefore, it is important to distinguish between type I and type II conjugate geometry in a study area when conducting a dynamic analysis.

If no conjugate EVA occur in a field area then there is little basis for making any of the assumptions just mentioned, in which case, only a range of possible s_1 orientations (eg. accurate to within 20 degrees) may be determined for isolated EVA. The problem corresponds to

two unresolved theoretical issues over the mechanics of EVA vein formation, namely 1) shear verses tensile mode of failure (alluded to earlier), and 2) primary verses secondary stress fields. The four different models are shown in figure 8a (after Rickard and Rixon, 1983). Each model may be correct for specific physical conditions, however, such conditions have not yet been delineated. The only certain generalization consistent with all four possible dynamic models is that the s_1 orientation which initiates a shear zone ("primary s_1 ") lies somewhere in the acute angle between, and including, each vein and its enclosing array (figure 8b).

The generalization just mentioned also applies to the dynamic interpretation of EVA along fault or vein surfaces. Since these features seldom occur as conjugates it appears that most, if not all, can only be used to constrain the "primary s_1 " direction to the acute vein-array angle. This is in contrast to other isolated EVA that occur in association, both in proximity and character, with conjugate EVA that can be used to better constrain s_1 .

Finally, in undertaking a dynamic analysis using EVA one should be aware of the possible effects of anisotropies, and perhaps should not include such EVA data in the analysis where possible. For example, veins may clearly form parallel to pre-existing planes of weakness

	PRIMARY STRESS	SECONDARY STRESS
TENSILE FRACTURE		
SHEAR FRACTURE		

A



B

FIGURE 8. FOUR DYNAMIC MODELS FOR VEIN FORMATION RELATED TO EVA DEVELOPMENT: A) THE MODELS (AFTER RICKARD AND RIXON, 1983), B) RANGE OF POSSIBLE PRIMARY S_1 ORIENTATIONS WITH RESPECT TO VEINS.

(Ramsay, 1967, figure 3-25) such as crossbedding. Also, the entire array orientation may occur along a fault or vein surface which follows pre-existing planes of weakness (Ramsay, 1967, figure 7-58). On the other hand, other EVA whose veins and shear zones crosscut rock anisotropies are good candidates for dynamic analysis. Also, whereas the natural geologic environment rarely approaches ideal conditions of isotropic and homogeneous rock presumed earlier, it does appear that conjugate EVA observed in most studies do approach the ideal conjugate geometries in figure 5. Thus, in general, EVA appear to be reliable tools for approximating paleostress directions in spite of the anisotropies common in nature.

In conclusion, the direction of applied stresses related to EVA geometry are well constrained for conjugate EVA. To incorporate isolated EVA into a paleostress study requires care in making appropriate assumptions. For all EVA, including EVA related to master fractures, the s_1 orientation is constrained to the acute vein-array angle for each array.

SLICKENFIBER FAULTS (SFF)

Geometry

A slickenfiber fault (SFF) is a fault wherein the surface of slip is characterized by the growth (or crystallization) of secondary minerals such as quartz or calcite. The crystals generally have a fibrous to prismatic habit and are aligned and overlapped with each other along the fault plane in a systematic manner dictated by irregularities of the fault surface and the sense of fault motion.

A systematic orientation of crystal fibers is apparent in cross-sections of SFF (figure 9). Sections cut parallel to fiber lineations reveal fibers that join the two fault blocks by attaching to wall rock at each end (Durney and Ramsay, 1970). But, unlike fibers in veins, they uniformly lean in one direction at a very low angle to the fault surface (less than 5 degrees) and overlap one another like shingles on a roof. For reasons discussed below their orientation and length represents the displacement vector, or fault movement.

An exposed SFF surface commonly exhibits lineated step-like surfaces due to breakage across the overlapping fibers (figure 9c). The geometry is such that one may use the conventional "rough-smooth" technique for determining the sense of displacement (Stoces and white, 1935; Durney

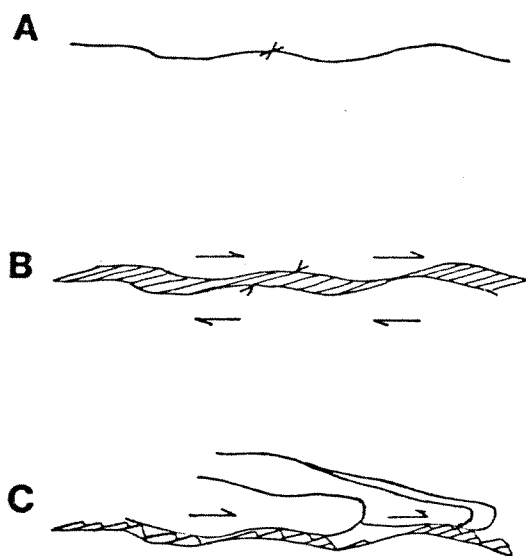


FIGURE 9. DEVELOPMENT OF SFF AND THE EXPOSED SURFACE
(AFTER DURNEY AND RAMSAY, 1973).

and Ramsay, 1973). This technique involves stroking the surface parallel to the lineations such that it feels relatively smooth in one direction and rough in the other. The fault block that is represented by the hand was displaced in the direction of hand motion that feels smooth to the touch (figure 9c). Movement in the opposite, and incorrectly interpreted, direction is rough to the touch as fingers encounter miniature escarpments. In recent years the reliability of the "rough-smooth" technique has been questioned. Debate has been aroused by the results of some fault studies in which the technique gave the incorrect sense of displacement. However, geologists have come full circle to accepting this technique for faults characterized by overlapping crystal fibers (eg. SFF) (see discussions by Durney and Ramsay, 1970, and by Hobbs et al., 1976, pp. 303-305). Indeed, inspection of the systematic orientation of overlapping fibers using a hand lens, as well as pinnate EVA, gives the same results as the rough-smooth technique. Thus, the sense of displacement can be determined with certainty on SFF as opposed to faults that do not have fibers.

SFF Development

General Occurrence: SFF may develop along any slip surface including faults and bedding plane flexural slip surfaces. They are particularly common in fold and thrust

belts where they are found in association with cleavage development as well as EVA. Like EVA, SFF are considered to form at relatively shallow depths (1 or 2 KM) but at depths sufficient to sustain high fluid pressures.

SFF Formation: Microstructural studies in rocks suggest that SFF development involves two stages which parallel the two-stage formation of EVA. These are: 1) microcracking related to initiation of the fault and 2) incremental displacements thereafter which corresponds to incremental fiber growth. Stage one microcracks coalesce to form a through-going fracture which in nature would be a fault. Subsequent displacements result in incremental fiber growth (stage 2) considered to proceed in accordance with the model of Durney and Ramsay (1973) described below.

The fracture surface prior to displacement usually contains small irregularities. Consequently, the first increments of displacement create small cavities along the fault surface as bumps on opposing surfaces ride over one another. These small spaces then fill with minerals and seal the fault. Later, a new fracture develops along the previously healed fracture surface and creates space for a new increment of fiber growth. Subsequent increments of displacement result in incremental growth of crystal fibers and overlapping of fibers at low angles to the shear zone. Depending on the site of recurring fractures

the actual growth of crystal fibers may take place at fiber tips adjacent to wall rock (oldest increment at fiber centers) termed "antitaxial growth" or at fiber centers along a central suture (oldest increment at fiber tips) called "syntaxial growth". In some cases growth may be a composite of antitaxial and syntaxial growth. In most faults studied by Durney and Ramsay (1973) syntaxial growth was particularly common.

This same repetitive process of 1) fracture formation followed by 2) dilation induced fiber growth also explains the formation of curved fibers that are occasionally seen along SFF surfaces. In these cases fiber curvature records a change in the direction of incremental displacements during progressive development of the SFF. In all cases fibers grow in the direction of displacement for each movement on a fault. Curved fibers, therefore, record rotations of movement directions, providing, care is taken when interpreting the sense of rotation. Antitaxial growth (last increment of displacement parallel to fiber ends) implies rotation of one sense (eg. clockwise) and syntaxial growth (last increment of growth parallel to fiber centers) implies rotation of the opposite sense (eg. counterclockwise) (Durney and Ramsay, 1970).

Fluid Dynamics and SFF Formation: Processes related to fluctuations of fluid pressures furnishes a mechanism

for SFF development as well as for EVA. In addition to aiding fracture formation, fluids under high pressure facilitate movement (ie. faulting) by reducing the effect of friction. Upon displacement the effect of dilation is to reduce fluid pressure which increases the effect of friction and tends to arrest displacement. Thus, incremental displacements involved in SFF formation (as recorded by mineral fibers) may be intimately related to a process whereby fluid pressures are repeatedly restored to hydrofracture levels and dissipated by an increment of displacement.

Relation of SFF to Applied Stress

As described earlier, natural rock experimentally compressed under ideal conditions commonly has produced conjugate shears oriented symmetrically about principal stress and strain axes as indicated in table 1 and figure 10a. Thus, inasmuch as conjugate faults in nature develop in a manner analogous to experimentally produced conjugate shear fractures, principal stress directions can be reasonably assumed for SFF that occur in conjugate sets.

For a single fault, in the absence of conjugate features, one must utilize a different approach. For example, one technique is to assume that each fault formed at a 30 degree angle to σ_1 (Ragan, 1973; Davis, 1984, pp. 314-318) (figure 10b). This reflects the fact that

experimentally produced conjugate shears commonly develop with an acute angle of 60 degrees such that s_1 lies at a 30 degree angle to each shear (Turner and Weiss, 1963, p. 293; Davis, 1984, pp. 306 and 309).

The above approach assumes ideal conditions (eg. isotropic and homogeneous mechanical rock properties), whereas naturally occurring rocks commonly contain anisotropies characterized by preferred planes of weakness. Compressive tests on anisotropic rock demonstrates the susceptibility of such rocks to failure along pre-existing planes of weakness at anomalous angles to s_1 . For example, compressed slates have resulted in failure along cleavage planes for all orientations to the applied stress from 25-40 degrees (Donath, 1961) (figure 11a). Also, Handin (1969) has shown that pre-existing fractures may fault at orientations to s_1 as high as 65 degrees. Consistent with Handins (1969) results, slip has been reported on pre-existing conjugate joints such that s_1 bisected the obtuse angle (Marshak et al., 1983) (figure 11b). Thus a SFF surface that developed along anisotropies in the rock may have formed at any of a number of possible s_1 orientations.

SFF that develop by reactivation of pre-existing fractures not only may form at a range of possible angles to s_1 but to s_2 as well. That is, s_2 may be positioned at an angle to the fault surface as illustrated in figure

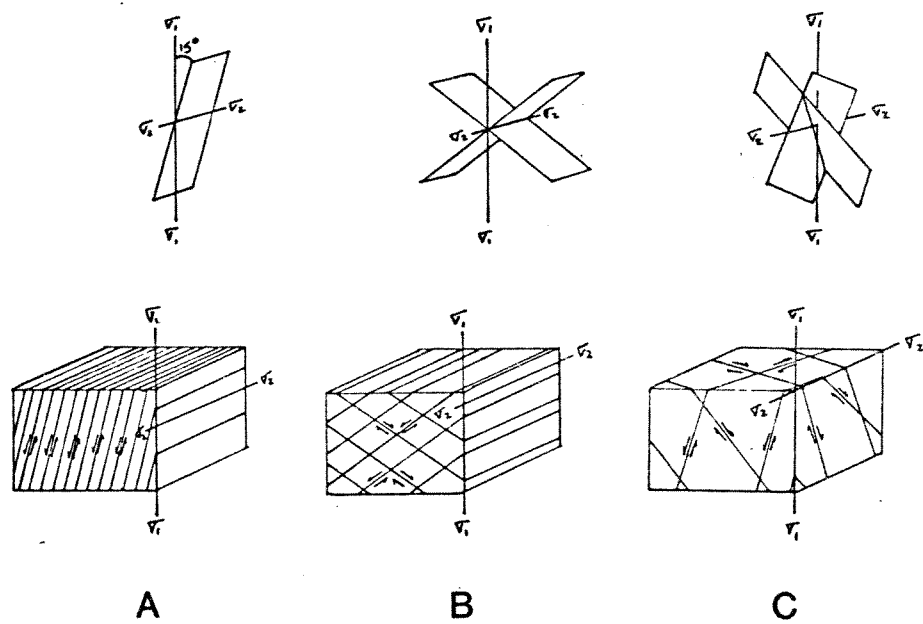


FIGURE 11. RELATION OF SFF TO PRINCIPAL STRESS AXES FOR ANISOTROPIC ROCKS.

11c, rather than lying in the plane of the fault as described for isotropic rock (table 1 and figure 10). This situation may be visualized by imagining a pile of disordered dice on a table which is squeezed horizontally in a vice beneath a glass plate. S_2 is vertical but not in the plane of all slip surfaces. Obviously, using the approach in figure 10 for slip surfaces that record movement in a manner analogous to the dice produces results that are erroneous on a detailed scale. Nonetheless, it is commonly accepted that the results may be used to provide a general window of possible s_1 orientations when a reasonable density of faults has been measured (Ragan, 1973; Compton, 1966).

Clearly, care must be exercised in using SFF for dynamic analysis. Conjugates and isolated SFF in isotropic rock may be used for detailed determinations of stress directions whereas SFF that developed along pre-existing fractures or anisotropies are less reliable but are also likely to provide at least a general window of stress directions.

METHODOLOGY FOR DYNAMIC ANALYSIS
IN THE GREEN POND OUTLIER

INTRODUCTION AND RATIONAL

The fundamental rational for using echelon vein arrays and slickenfiber faults for dynamic analysis is based on the assumption that they represent naturally occurring examples of brittle and semibrittle zones of shear that formed in manners analogous to brittle and semibrittle shears observed in experimentally deformed samples. The fact that they are often found in conjugate sets and in some cases with faults that indicate consistent stress orientations provides further support for this assumption. This is not to say that there are not pitfalls and many exceptions as discussed earlier in the context of rock anisotropies.

Nonetheless, due to the brittle nature of these features, they are more reliable indicators of stress than are most other deformation features. Experiments on the brittle deformation of rocks have shown that under an applied load above a critical yield stress, crack propagation occurs more or less instantaneously. This is true for hydraulic fracture experiments as well as axial load tests. In addition, as implied from the above discussion, these cracks grow at predictable orientations

to the applied stress. Therefore, because of the relative rapidity of crack growth, crack geometry generally reflects the instantaneous principal stress configuration that caused it to form. This is in contrast to the protracted history of deformation represented by cleavage and other deformation features formed strictly by a ductile mechanism. These deformation features can generally be used to determine the principal finite strains but not the instantaneous strains or instantaneous stresses that operated throughout the deformation history. Most strained objects are the end product of a summation of different incremental strain and stress states of unknown configurations and durations. Barring rare cases, only the finite strain state is generally measurable. Consequently, EVA and SFF are somewhat unique because they record a more instantaneous stress field.

In some areas one can find a co-occurrence of brittle and ductile features both likely to have formed during a protracted history of deformation. For example, in the Green Pond outlier EVA and SFF represent brittle deformation while cleavage and deformed reduction spots represent ductile features. All of these features, for reasons to be developed further on, are likely to have formed during the general folding event. The shear zones, represented by the EVA and SFF, have a protracted history of incremental displacements (via the previously discussed

crack-seal mechanism) which usually does not alter the planar nature of the shear zone. Thus, the orientation of the shear zone continues to record the relative principal stress configuration at the time of incipient shear zone development despite its possible rotation within the fold structure or with respect to an external reference frame. Thus, in contrast to most strained objects, the instantaneous principal stress configuration that initiates a shear zone is usually preserved even if the shear zone has a protracted history.

This means that in a progressive or polyphase deformed region a given shear zone orientation records the paleostress directions for a small finite period within the overall deformation history. For example, within a relatively tightly folded sequence in the Green Pond some shear zones are curved (deformed) while others are undeformed implying that each represents a different finite period in the fold history. Furthermore, although progressive folding leads to rotation of earlier formed shear zones with respect to the regional stress field the discontinuous, but sequential, formation of shear zones results in systematic patterns that may be related to the regional stress field through time. The measurement and analysis of such patterns is the goal of this research.

EVA IN THE GREEN POND

EVA Attributes in the Green Pond

EVA characteristics in the Green Pond appear to be typical of those described in the previous studies just reviewed. In the Green Pond outlier they occur predominately in sandstone and conglomerate beds as opposed to the less competent shale and siltstone beds. Most occur internal to massive units rather than along bedding surfaces and crosscut pre-existing crossbedding. This indicates that these features did not develop along pre-existing planes of weakness and are therefore good candidates for dynamic analysis. Furthermore, many conjugate EVA observed in the Green Pond closely approximate the ideal geometries previously described in figure 5.

Some EVA typical of those observed in the Green Pond are illustrated in figure 12. An array usually contains 10-20 veins spaced over a distance of less than 3 meters. The dimensions of individual veins in cross-section are commonly less than 30 CM long and less than 2 CM thick (note scale of hammers and lens cap in figure 12). The three dimensional shapes of veins are schematically illustrated in figure 13. In many cases veins of a given array are roughly rectangular and of equal length (figure 13a). In other cases veins in a given array are

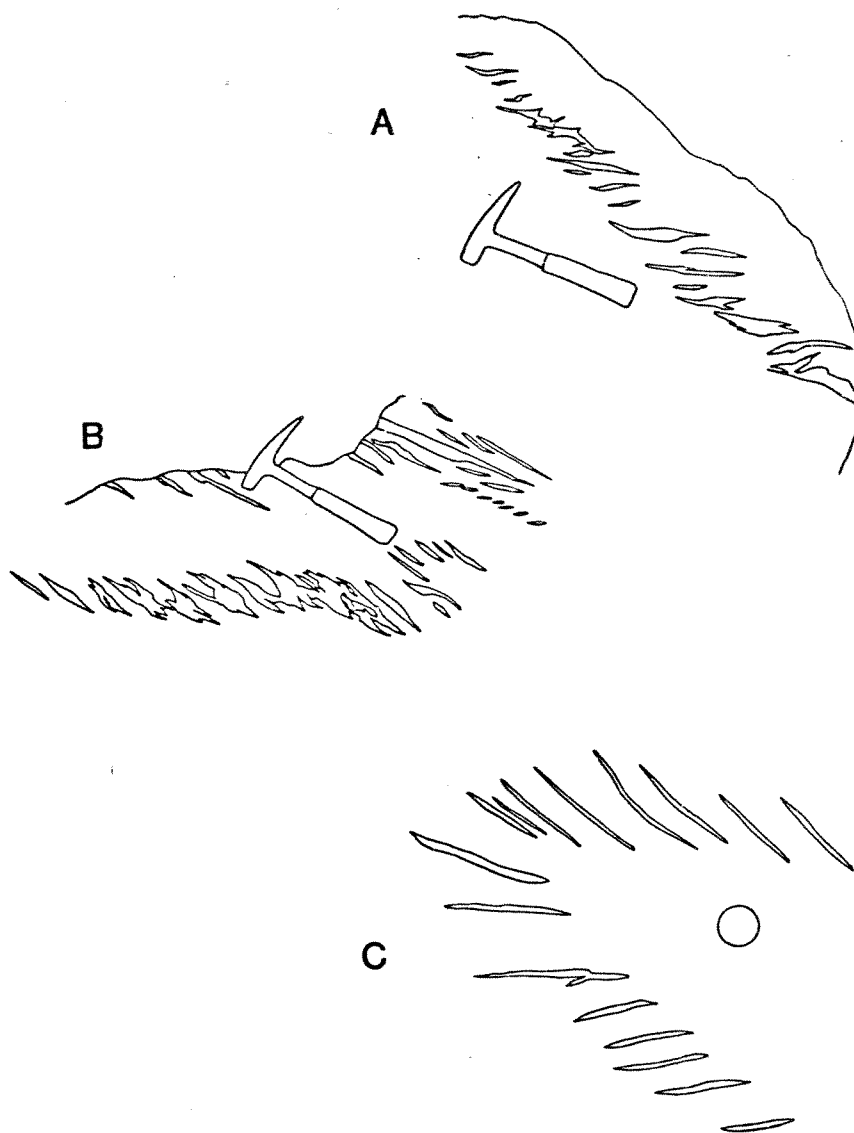


FIGURE 12. PHOTO TRACINGS OF EVA IN THE GREENPOND
(ROCK HAMMER AND LENS CAP FOR SCALE).

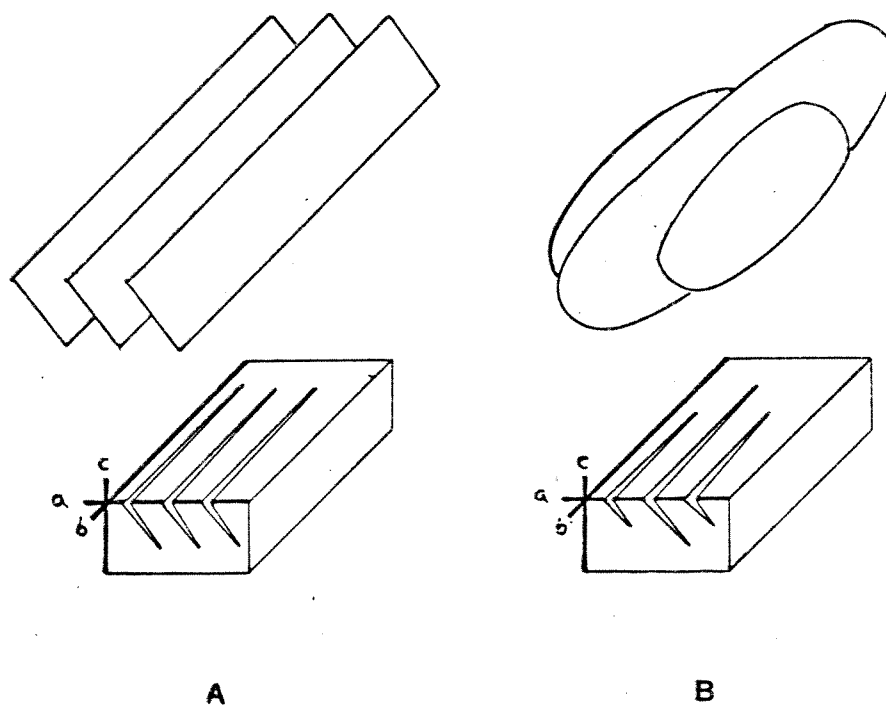


FIGURE 13. THREE DIMENSIONAL SHAPES OF EVA IN THE GREENPOND: A) RECTANGULAR, B) ELLIPTICAL.

elliptical in shape and of unequal length (longer in the array center) as in figure 13b. But in all cases, the longest dimension of veins (b axis in figure 13) is many times greater than the other two dimensions (a and c axes).

All EVA types were observed in the Green Pond although isolated and conjugate EVA associated with nondiscrete zones of shear (figures 4 and 5) outnumber those EVA associated with master fractures (figure 6). Over 200 EVA were included in the dynamic analysis which includes about 120 isolated arrays (ie. those isolated from conjugates, faults, or veins) and 60 conjugate arrays (ie. 30 pairs). Also, about 10 pinnate arrays along faults and about 10 relatively small "dilatant echelon cracks" along veins were measured. EVA associated with fault tips or vein tips, though observed, were not measured in this study. Conjugate EVA, in addition to isolated EVA, were found at almost all sites. Nearly all conjugates (28 out of 30 pairs) displayed type II geometry (ie. conjugate arrays developed at low dihedral angles, <40 degrees, and nonsigmoidal gashes parallel complementary conjugate shears) (figure 12). Clearly isolated arrays and type II conjugate arrays provide the bulk of the data used in the regional analysis.

Vein minerals are almost all quartz and most appear to have a fibrous form indicative of incremental vein

growth, though many veins contain massive quartz with comb structure and vugs. EVA development in the Green Pond is considered to follow the general model proposed earlier whereby fluids under pressure repeatedly fracture the rock, dilate the fissures, and facilitate mineralization to form EVA veins. Individual veins are commonly slightly sigmoidal such that vein tips turn into low angles to the shear zone (<30 degrees) (figure 12a and 12b). The sigmoidal shape is considered to be produced in part by progressive shear, as described earlier, and in part by complexities in the stress system discussed further below. Not infrequently, veins are highly sigmoidal and complex in shape due to overprinting of later veins and in some cases the development of a through-going fracture. A slight fanning of veins was consistently observed in the intersection of type II conjugates such that a central vein, one common to both arrays, bisects the acute array-array angle and parallels the inferred s_1 direction (figure 12c).

The preferred dynamic model of type II EVA development follows Rickard and Rixon (1983). This model is shown in figure 8 as one which favors vein formation by tension in a re-oriented stress field (ie. secondary s_1). First, the principal stress configuration initiates embryonic shear zones at a low angle to s_1 (about 20 degrees). Incipient shear zone development (eg.

microcracking, dilation, fluid mobilization) alters the physical conditions of the shear zone resulting in a re-oriented principal stress configuration rotated in the direction of displacement. Vein cracks subsequently propagate as extension cracks oriented parallel to secondary s_1 . Cracks which propagate beyond the shear zone curve into parallelism with s_1 of the primary stress field. Hence, s_1 trajectories at the time of vein growth parallel primary s_1 outside of the shear zone and secondary s_1 within the shear zone. Interference at array intersections produce a vein oriented parallel to s_1 as well as a slight fanning of adjacent veins. The data in the Green Pond appear to fit this model quite well. A possible weakness in the model is that the resulting geometry requires that the secondary s_1 consistently rotate approximately 20 degrees for each EVA.

EVA Methodology used in the Green Pond

Assumptions: For each EVA s_1 was assumed to bisect the acute vein-array angle consistent with type II conjugate geometry (figure 5b). The assumptions for all principal stress axes are listed in table 2. This interpretation is considered valid for the isolated arrays since they were associated, both in proximity and character, with type II conjugate arrays. Nonetheless, in consideration of possible effects of anisotropy and of

TABLE 2. THE RELATION OF PRINCIPAL STRESS
AXES TO EVA AS ASSUMED IN THIS
STUDY.

S1 IS ASSUMED TO BISECT, OR AT LEAST LIE
WITHIN, THE ACUTE VEIN-ARRAY ANGLE
FOR EACH EVA.

S2 IS ASSUMED TO LIE PARALLEL TO THE
INTERSECTION OF EACH VEIN WITH
THE PLANE OF THE ARRAY AND TO LIE
PERPENDICULAR TO THE DIRECTION OF
DISPLACEMENT ON THE SHEAR ZONE.

S3 IS ASSUMED TO BISECT, OR AT LEAST LIE
WITHIN, THE OBTUSE VEIN-ARRAY ANGLE
FOR EACH EVA

alternative dynamic models the range of possible s_1 orientations within each acute vein-array angle was determined for each EVA. The range plots on a stereogram as a line of finite length. When numerous shear zones are compiled the stereogram shows numerous criss-crossing lines as shown in figure 14a. When a plot for a given site is compared with a cumulative plot of the same data but using the assumption that s_1 bisects the vein-array angle for each EVA the general pattern is found to be the same (compare figure 14a with 14b). It appears that given a reasonable database the general pattern would be reproducible using any interpretation lying generally within the vein-array angle. This was found to be consistently true for compilation plots. Therefore it was concluded that whether one equates s_1 with the acute bisector or with a range of possible s_1 orientations for each EVA the results are insignificantly different for the purposes of the regional analysis made here.

Measurement Techniques: The attitude of the array (ie. shear zone) and a representative vein was measured for each EVA. With each measurement the degree of confidence (ie. error) was estimated qualitatively, based on the extent to which three points (two lines of site) could be established for each attitude. The orientation of most veins were measured with a relatively high degree of confidence (error of less than 15 degrees). Array

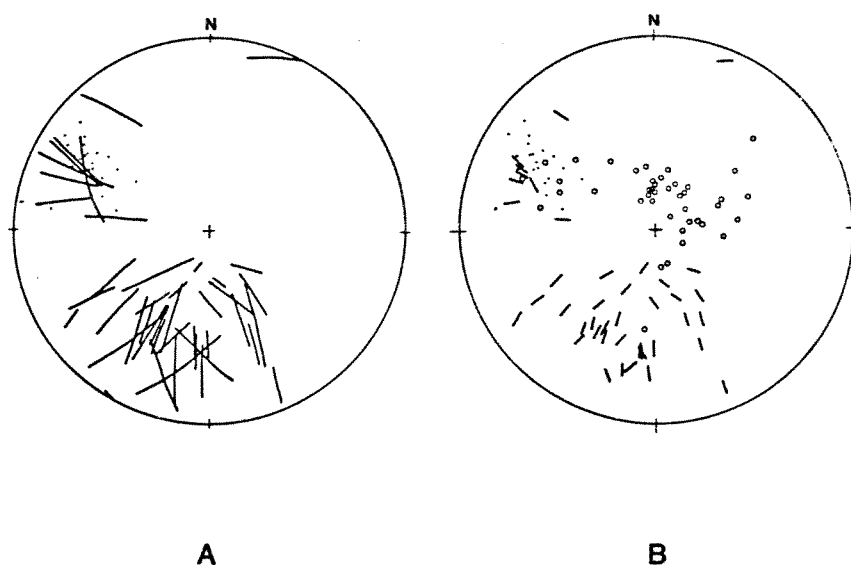


FIGURE 14. TWO STEREOGRAMS OF THE SAME EVA DATA (SITE #2) SHOWING THAT DIFFERENT APPROACHES GIVE SIMILAR RESULTS (LINES=S1, CIRCLES=S3, DOTS=POLES TO BEDDING).

orientations were commonly measured with a moderate degree of confidence (error of less than 30 degrees). Numerous EVA were measured with less than a moderate degree of confidence but were not used in the analysis and therefore not included in the EVA total (202) used in the regional analysis.

When measuring sigmoidal veins their tips were measured rather than vein centers because the centers may have been rotated during progressive shear. The actual measurement is not difficult since in nearly all cases small irregularities along the exposed surface can be used to establish the planar orientation. Unfortunately, measuring the shear zone is more difficult because two exposed sections are required for a confident measurement, not just one. The problem lies in determining the true inclination of the shear zone into the outcrop as illustrated in figure 15. Frequently, a second exposed section reveals the long dimension of a gash(s). Equally as often, a second section must be conceptually constructed by visually compiling information from outcrop irregularities as seen from different perspectives. This approach involves a lot of pacing back and forth. Another technique takes advantage of sigmoidal veins by establishing a down hinge view within the plane of the shear zone. In general one tries to establish several lines of site within the plane of the shear zone before

taking a measurement. Once two sections or lines of site are established the field notebook is placed parallel to the shear zone for a direct compass reading.

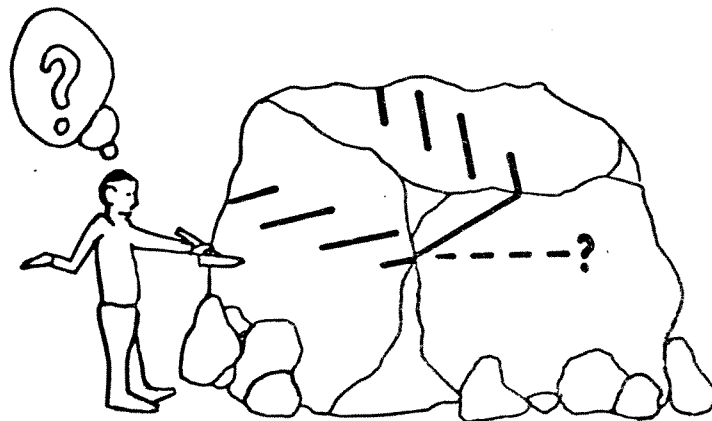


FIGURE 15. VIEWING ONLY ONE EXPOSED SECTION WHEN MEASURING EVA SHEAR ZONES MAY LEAD TO AN ERRONEOUS MEASUREMENT. A THIRD POINT ON THE PLANE (OR SECOND SECTION) IS REQUIRED IN ORDER TO MEASURE THE TRUE ATTITUDE.

SFF IN THE GREEN POND

SFF Attributes in the Green Pond

SFF in the Green Pond occur predominately along bedding and crossbedding surfaces although some do cut across layering at high angles. Most appear to have formed by flexural slip along bedding surfaces during folding. In addition, only a few conjugates have been observed. Thus in contrast to EVA, it appears that SFF formed predominately along pre-existing planes of weakness and therefore are considered less reliable measures of the paleostresses. Furthermore, presuming that SFF developed primarily in response to only those s_1 orientations which were likely to create slip on bedding surfaces, then they are likely to provide an incomplete record of the stress field(s) during deformation. Nonetheless, for reasons discussed earlier the SFF are considered useful for determining windows of regional s_1 orientations.

Most SFF are discontinuous on the outcrop. Most occur along crossbeds and do not extend beyond the given length of the crossbed surface. Displacements along SFF are generally less than 10 CM. The overlapping crystal fibers are usually quartz sandwiched between thin films of chlorite. Some fibers are curved and are indicators of rotations in the relative displacement direction on the fault surface during SFF development. Other slip surfaces

such as polished ripple marks and bedding surfaces with a thin film of lineated phyllosilicates were observed but not measured even though these lineations appeared to parallel those of SFF.

EVA are intimately associated with SFF. Pinnate EVA apparently developed on pre-existing SFF such that both recorded the same displacement sense (eg. figure 16a). Occasionally a SFF cut across a pre-existing EVA presumably as a late stage fault in the progressive evolution of the shear zone (figure 16b). Thus EVA may form both in advance of SFF or during subsequent slip on SFF (Hobbs et al., 1976, pp. 294-295). Also, SFF and EVA apparently may form at about the same time as indicated by shear zones in the Green Pond characterized by an SFF at one end and an EVA at the other (figure 16c). This intimate relation between the two features suggests that the conditions that lead to the formation of one or the other must be very similar and that the variation in physical conditions must be very localized. Perhaps in this case there were differences in material strength along the crossbedding surface such that the SFF developed along the weaker portion. The EVA may have developed along the stronger or more tightly sealed portion where shear strain was most effectively accommodated in a distributed zone as opposed to a discrete plane. The development of EVA at fault tips (figure 16d) further supports the

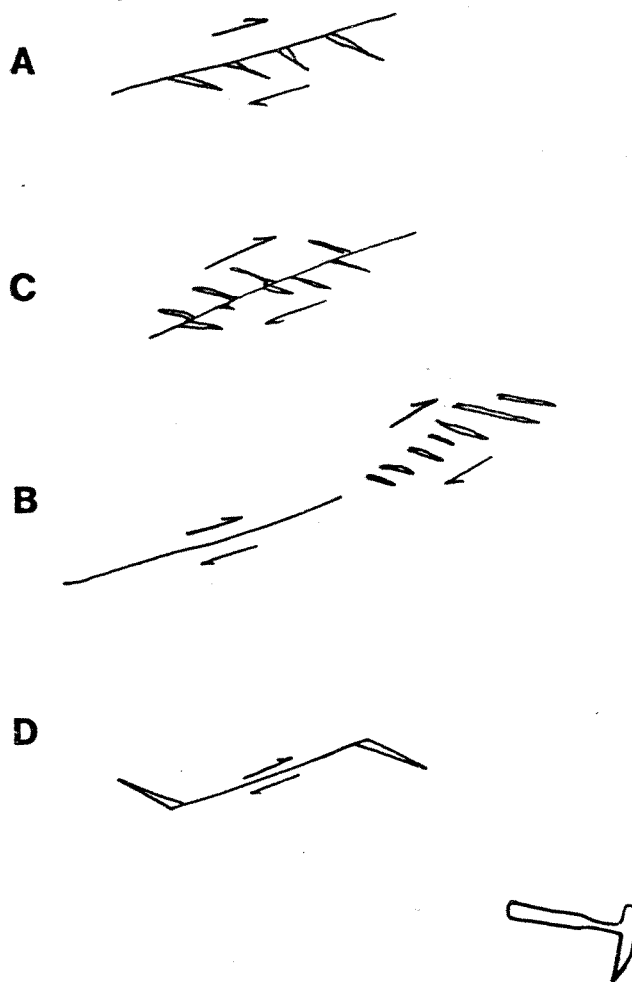


FIGURE 16. SFF AND EVA ASSOCIATIONS IN THE GREENPOND.

premise that there is a delicate balance of physical conditions that leads to the formation of one feature in preference to the other.

SFF Methodology

Assumptions: Since most SFF in the Green Pond formed along planes of anisotropy and only a few formed as apparent conjugates, a range of possible s_1 orientations from the fault surface was determined for many of the SFF. However, in the regional analysis a specific angle to the SFF was assumed for the purpose of 1) simplicity in the analysis and 2) consistency with the approach to EVA analysis. The conventional assumption of 30 degrees was utilized as well as the assumption that s_2 lies in the plane of each fault and perpendicular to the fiber lineation figure 10. Although imprecise, measurements of paleostress directions from SFF provide at least general information on the regional paleostress directions. Also, curved fibers are considered useful because they give an indication of the sense of rotation in the local stress field.

Measurement Techniques: For each SFF the following was measured, 1) attitude of the fault surface, 2) pitch of the fiber lineation, 3) sense of relative displacement, and 4) sense of rotation of curved fibers (assuming syntaxial growth). All were measured with a high degree

of confidence (ie. error of less than 15 degrees). The displacement sense was determined by observing fiber overlap orientation and by using the "rough-smooth" technique described earlier.

DESCRIPTION OF PALEODYNAMIC RESULTS

GENERAL TRENDS

In an attempt to resolve the dynamic history of the Green Pond outlier EVA and SFF data were used following the methodology discussed in the last section. Over 200 EVA and 130 SFF were used to determine more than 330 independent stress directions over an area incorporating 80 square miles within the outlier. The data was then grouped into summary plots and stereograms to characterize four southeast dipping limbs, three northwest dipping limbs and two hinge zones. The locations of seventeen sites where data were collected are shown on the accompanying map (figure 17). The positions of each in the fold structure are indicated in the two-point perspective diagram of figure 18.

Results from each site displays one or more clusters of sl orientations and many have a linear distribution in the stereograms. Although clusters from one site to the next do not always match one another, compilation plots produce distinct patterns which are relatively consistent from one part of the fold structure to the next. These patterns are first summarized below and then regionwide modes are discussed in more detail.

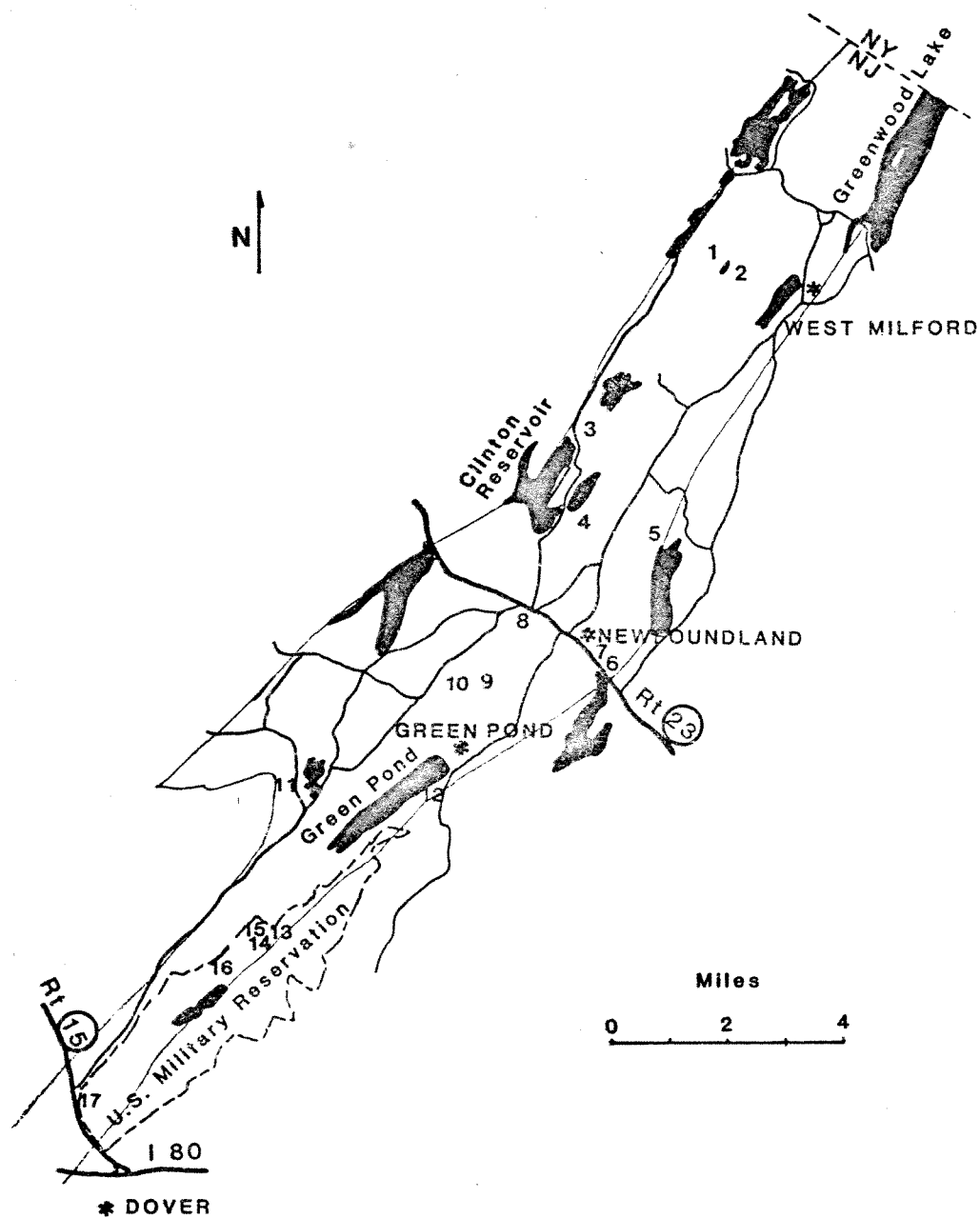


FIGURE 17. ROAD MAP SHOWING PRINCIPAL SITES WHERE EVA AND SFF DATA WERE COLLECTED.

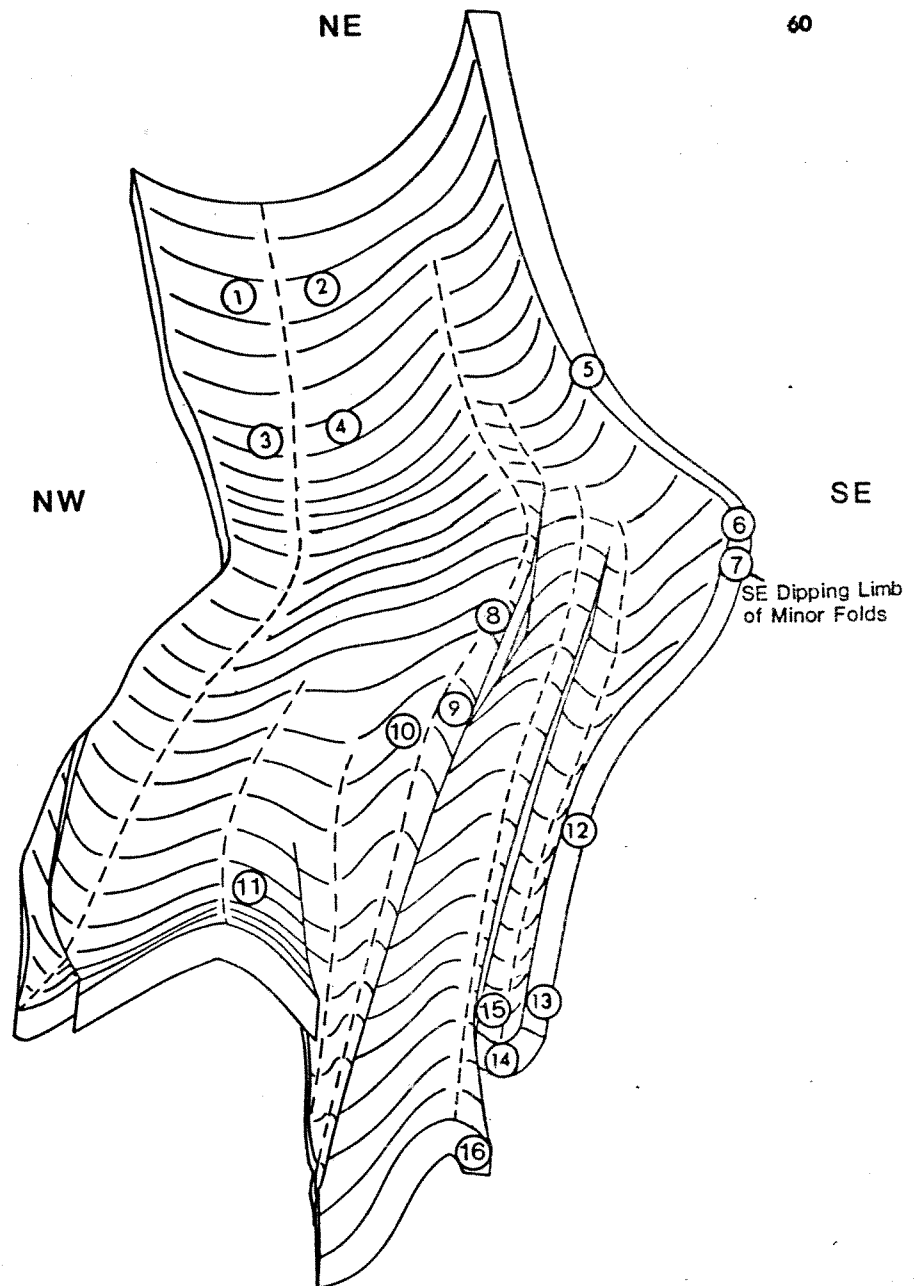


FIGURE 18. THREE-DIMENSIONAL REPRESENTATION OF THE GREEN POND FORMATION SHOWING THE POSITIONS OF SITES IN THE FOLD STRUCTURES. SITES 1-4 ACTUALLY OCCUR ON MODERATE TO STEEPLY DIPPING LIMBS OF THE SKUNNEMUNK CONGLOMERATE AND, IN PART, THE BELLVALE SANDSTONE. ALMOST ALL OF THE REMAINING DATA COMES FROM THE GREEN POND FORMATION.

Cumulative s_1 plots are shown for southeast dipping limbs (figure 19a), hinge zones (figure 19b), and northwest dipping limbs (figure 19c). In each plot note the overall symmetry about the generally NE-SW strike of axial surfaces and bedding. This symmetry is defined by two major trends in the s_1 distribution which lie in vertical s_1 - s_3 planes roughly oriented NW-SE and NE-SW with s_2 horizontal. In addition, a significant though less pronounced s_1 trend is oriented N-S as expressed by the slight assymetry in the s_1 distribution that is particularly evident in the EVA plots. Because regionwide s_1 trends may have significance for regionally applied stress directions, rose diagrams were also constructed to illustrate s_1 trends at each site for both SFF (figure 20a) and EVA (figure 21a) data. In the cumulative plots SFF data (figure 20b) record a variation restricted largely to the NW and SE quadrants and records largely one modal trend, whereas, EVA data (figure 21b) span all quadrants and records all three modal trends described above (NW-SE, N-S, NE-SW) with maximums oriented NW-SE and N-S. The maximums are analyzed separately.

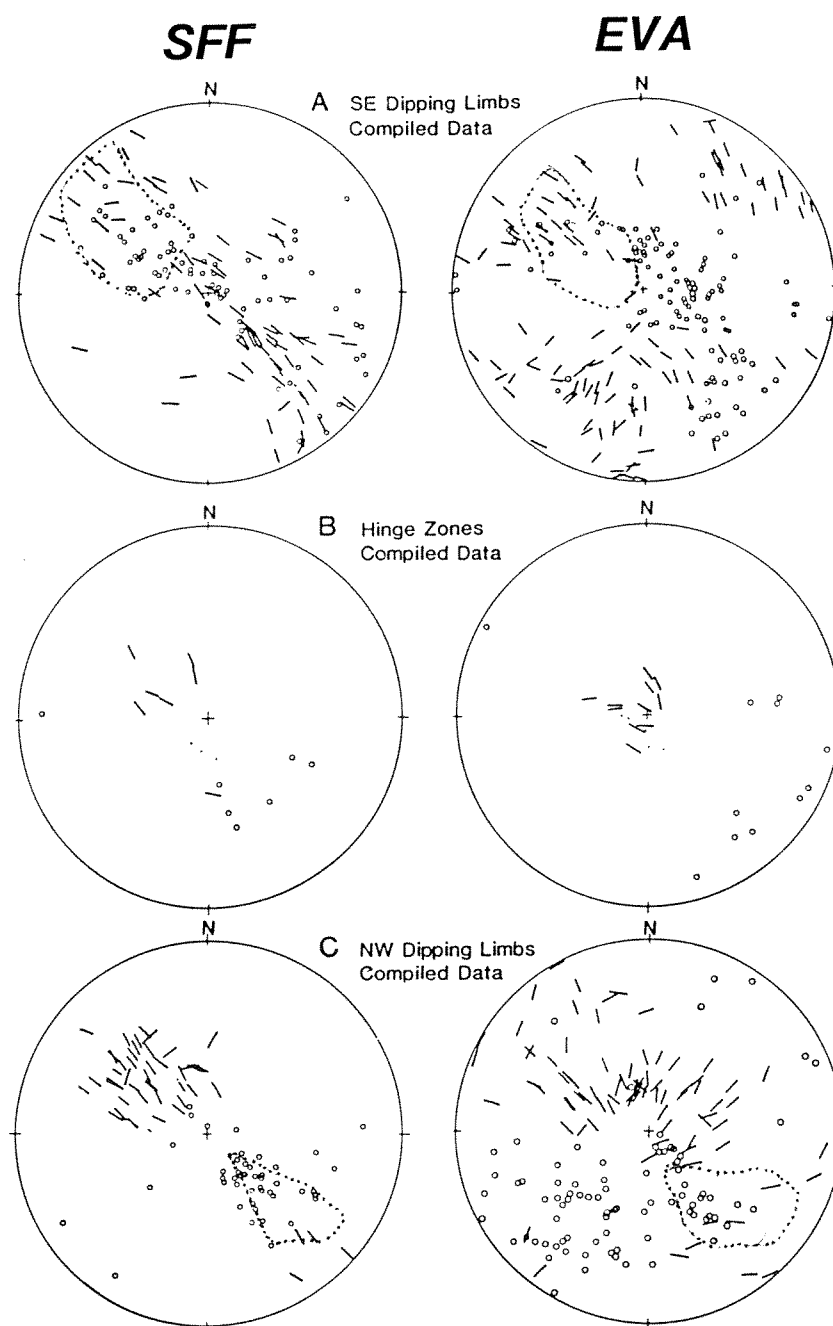


FIGURE 19. CUMULATIVE S1-S3 PLOTS FOR ALL SFF AND EVA DATA: A) FROM SE DIPPING LIMBS, B) FROM HINGES, C) FROM NW DIPPING LIMBS (SHORT LINE=S1, CIRCLE=S3, DOTTED LINE= FIELD OF POLES TO BEDDING).

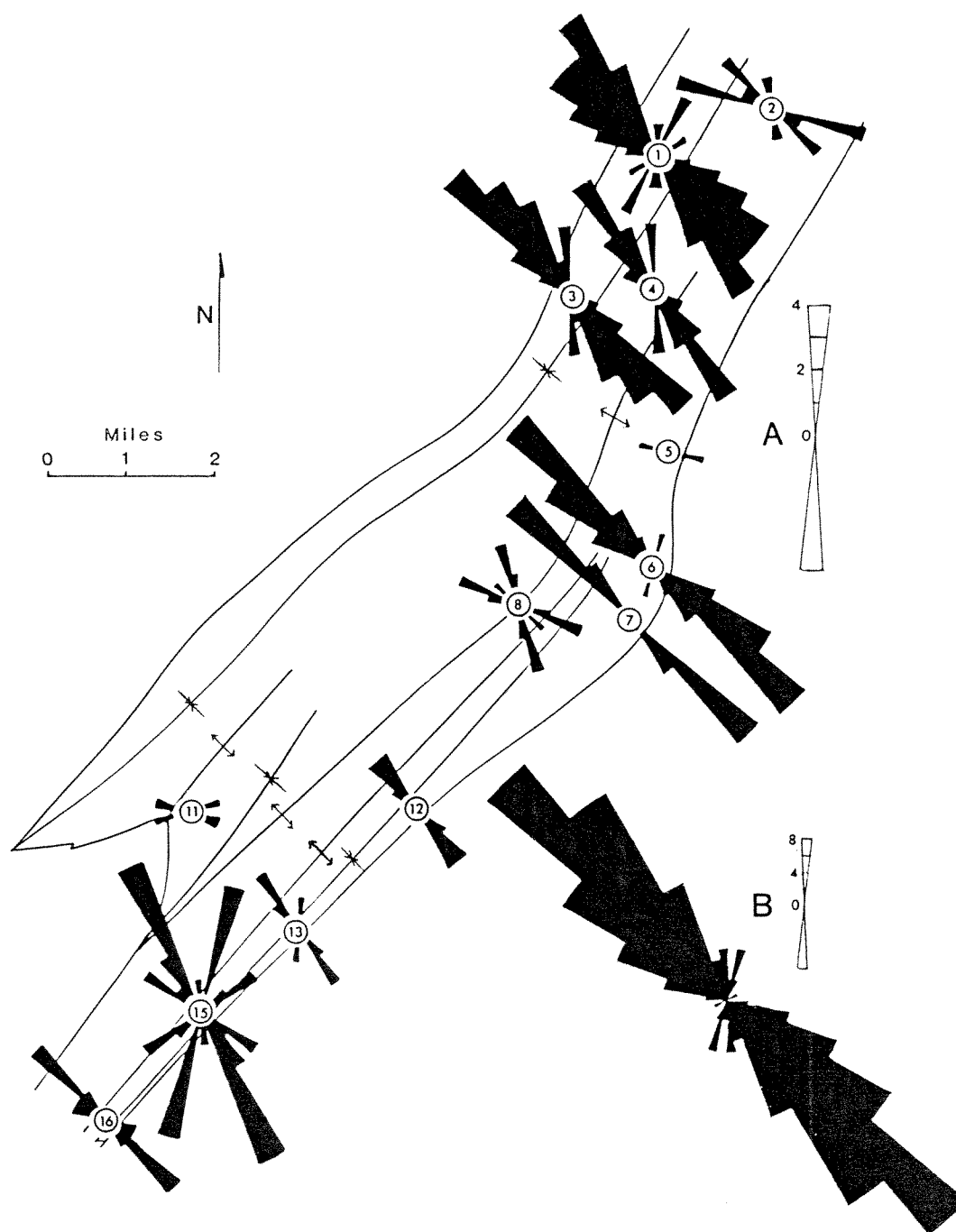


FIGURE 20. S1 TRENDS FROM SFF: A) AT INDIVIDUAL SITES, B) CUMULATIVE PLOT OF ALL SFF.

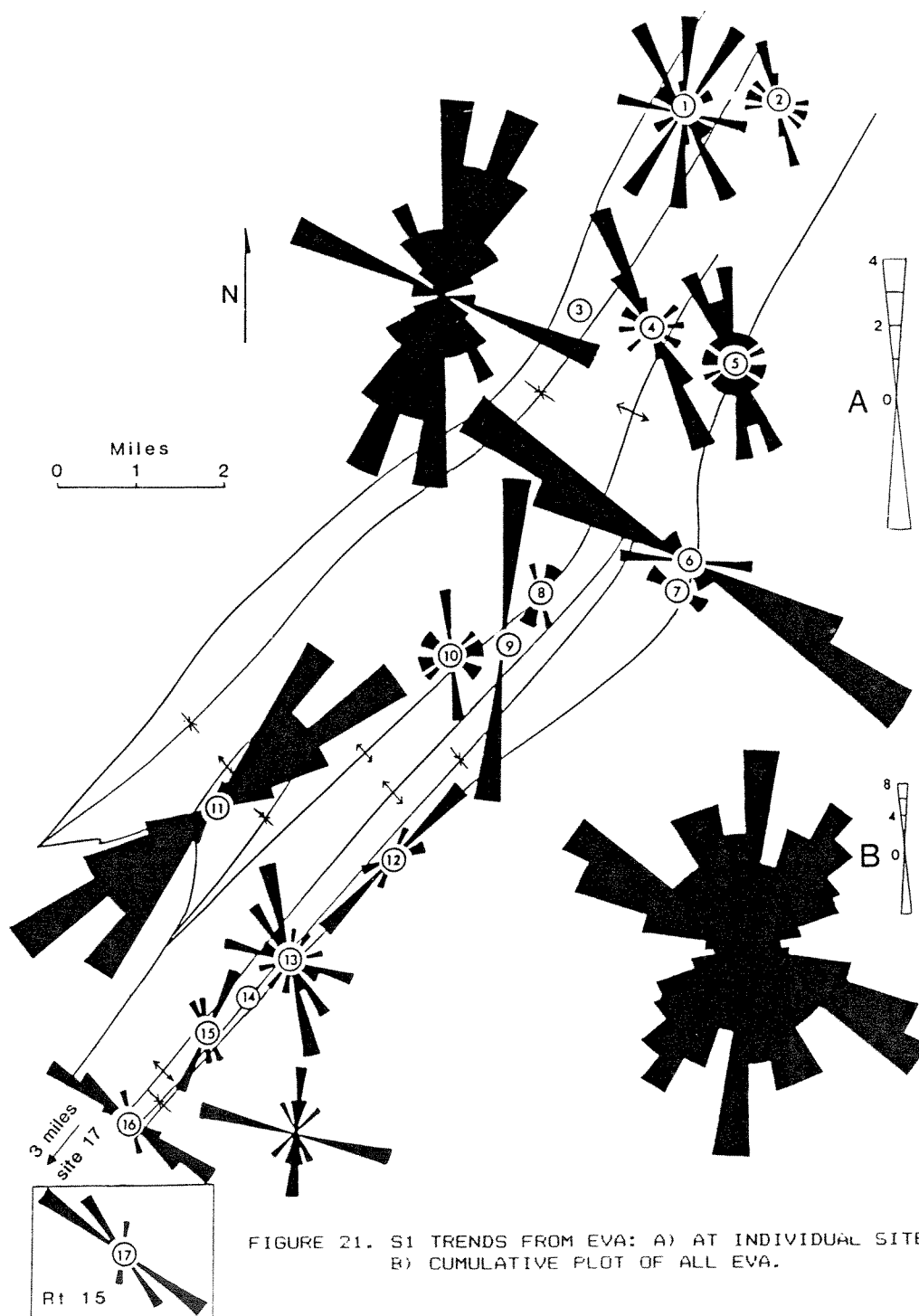


FIGURE 21. S1 TRENDS FROM EVA: A) AT INDIVIDUAL SITES, B) CUMULATIVE PLOT OF ALL EVA.

NW-SE S1 TREND ORIENTED NORMAL TO FOLD HINGES

Results

Initial inspection of the NW-SE s1 trending data reveals nonrandom but complex distributions. These distributions, in addition to field relationships relevant to the deformation history, are described below.

First, since s1 trends of the SFF data are largely confined to the NW-SE modal trend, it appears that the SFF record only part of the stress history of the outlier, whereas, the EVA record a more complete stress history. this may reflect that SFF development was largely restricted to slip on pre-existing planes of weakness such as bedding. Orientations of crossbeds generally parallel the NE-SW strike of bedding in the Green Pond Formation (Thompson, PhD). This is an orientation which may have been less vulnerable to slip in a rotated stress system. In contrast to SFF, EVA appear to be less effected by bedding surfaces and therefore are more likely to record a rotated stress system.

Secondly, where both EVA and SFF record NW-SE trending s1 at the same site, the s1 directions (ie. plunges) are approximately parallel. This relationship is most apparent where a large population of both features in the same outcrop record a reasonably uniform stress system such as that illustrated in figure 22. This strongly

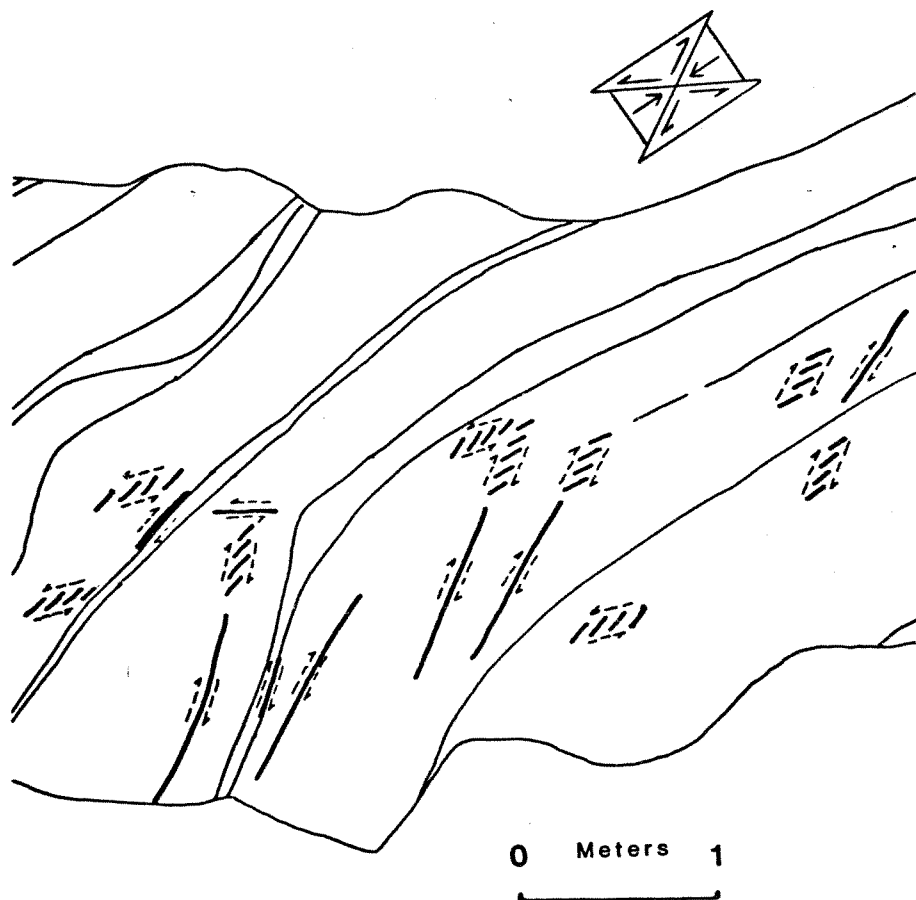


FIGURE 22. OUTCROP DRAWING OF NUMEROUS EVA AND SFF WITH COMMON S1 ORIENTATIONS (ROUTE 23, NEWFOUNDLAND, NEW JERSEY).

supports coeval development of these features. In some cases one can see on the outcrop (such as that in figure 22) that SFF surfaces terminate into EVA each giving the same s_1 direction (figure 16c) also suggesting coeval development. Thus, SFF and EVA with NW-SE trending s_1 orientations appear to have formed during the same general period of deformation.

Thirdly, the specific orientations of s_1 (ie. plunge) vary systematically with respect to positions in the fold structure. At hinge zones of major folds s_1 is consistently normal to bedding and vertical (figure 19b). This is in contrast to limbs which record a wide range of s_1 plunge orientations as shown in stereograms which show all SFF and all EVA for SE and NW dipping limbs (figure 19a and 19c). Note that in the plots for fold limbs a gap in the distribution of s_1 orientations occur in orientations plunging steeply in the direction opposite of bedding dip. That is, the " s_1 gap" plunges steeply in the NW quadrant for SE dipping limbs and in the SE quadrant for NW dipping limbs. The significance of this for stress variations through time will be discussed later. At present, it is sufficient to note that the s_1 orientations are unique and vary in systematic ways for each position in the fold structure (ie. hinges, SE dipping limbs, and NW dipping limbs). For these and other reasons presented below it is believed that the NW-SE trending stress system

reflects the main folding event. The fact that the trend is generally perpendicular to hinge lines further supports this interpretation.

Fourthly, the variation in s_1 orientations on a given fold limb appears to be systematic with respect to bedding. The bulk of the data consists of s_1 oriented: from a position nearly parallel to bedding (eg. EVA at site 7, figure 23a) through a range of intermediate values towards a horizontal position (eg. SFF at site 7, figure 23b) to a subhorizontal position oriented normal to bedding for steep limbs (site 17, figure 23c). This range of orientations produces the s_1 gap introduced earlier and is apparent at some individual sites (eg. figure 23b) as well as for data compiled for single limbs (eg. SFF in figure 23d, sites 1 and 3). This systematic variation suggests the possibility that s_1 rotated with respect to bedding during progressive folding. Evidence for relative timing occurs at sites 6 and 7 where an exceptional exposure of minor folds demonstrates this variation (figure 24) (more extensive drawing of features along this outcrop in the appendix). At this site several EVA shear zones are deformed. That is, the shear zone is bent or curved in a manner consistent with its enveloping shear or bedding surface and indicates that it too was buckled during the folding process. Thus, some of these features clearly predate at least some of the buckling history

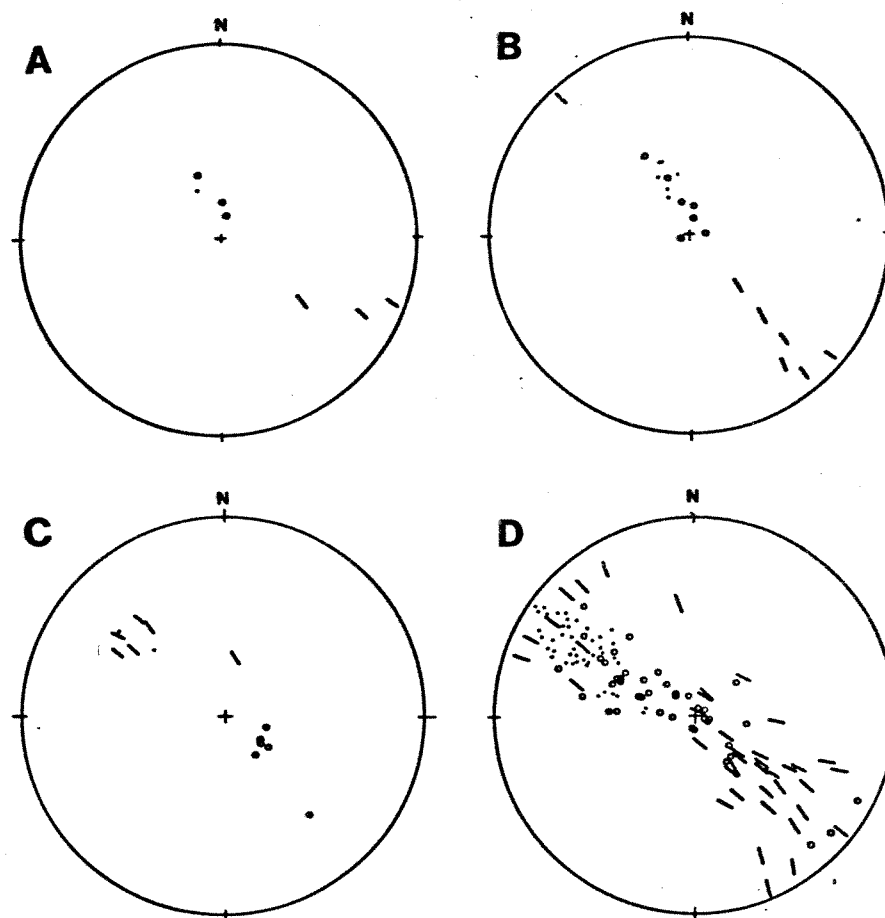


FIGURE 23. STEREOGRAMS EXEMPLIFYING S1 PATTERNS FOR NW-SE TRENDING DATA (EXAMPLES FROM SE DIPPING LIMBS): A) EVA-SITE 7 (MINOR FOLD), B) SFF-SITE 7 (MINOR FOLD), C) EVA-SITE 17, D) SFF-SITES 1 AND 3 COMBINED.

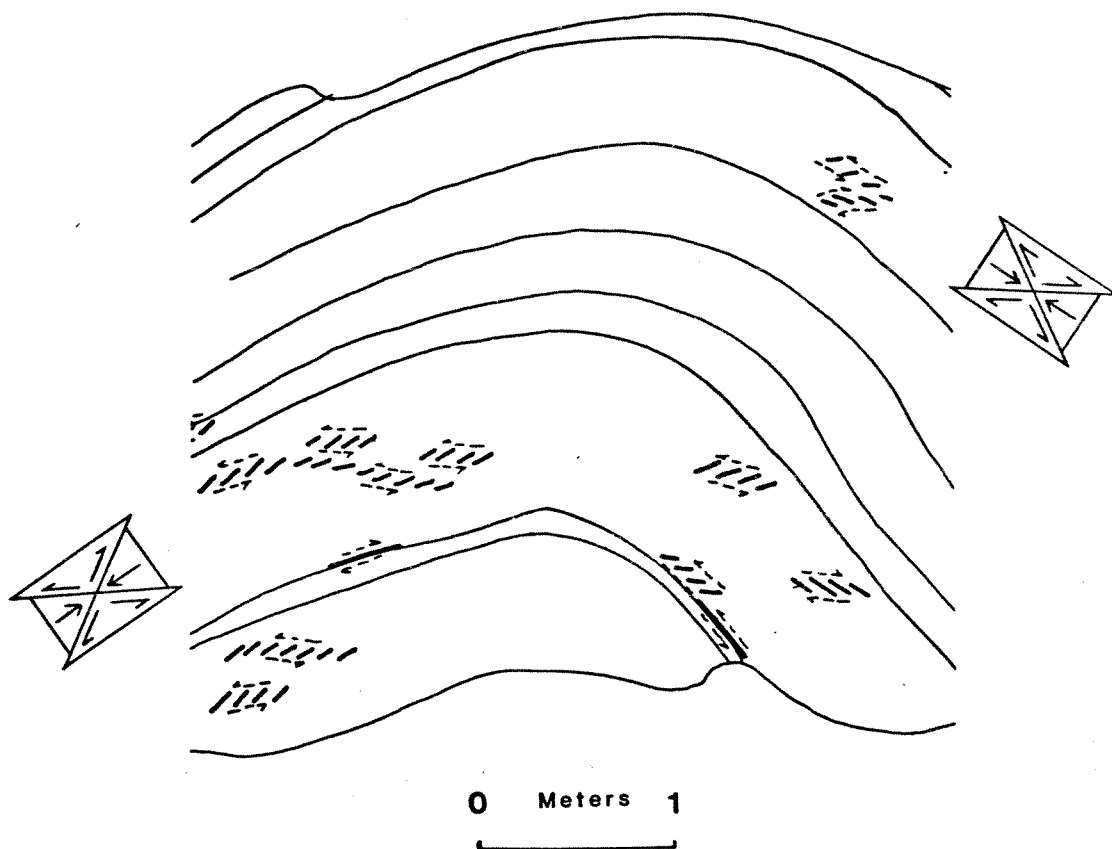


FIGURE 24. OUTCROP DRAWING OF EVA AND SFF ON A MINOR FOLD (ROUTE 23, NEWFOUNDLAND, NJ).

while others appear to have developed later in the folding history. Furthermore, since at this same site only EVA shear zones recording bedding parallel s_1 are found to be deformed it appears that s_1 was parallel to bedding in the early stages of folding and subsequently rotated to higher angles to bedding.

The numerous EVA and SFF that record NW-SE trending, but bedding parallel s_1 orientations, are restricted to fold limbs. Since hinge zones consistently do not have EVA and SFF that indicate s_1 of this orientation it appears that although these features formed during the early stages of folding they did not accomodate layer parallel shortening prior to buckling. This may be important for contrasting the style of deformation in the Green Pond with that reported for the Valley and Ridge.

A Model for the Stress History of Folding

The available field evidence and the systematic variations in s_1 orientations presented in the accompanying stereograms leads one to conclude that both EVA and SFF with NW-SE trending s_1 orientations developed during the main folding deformation. Furthermore, variations in the plunge of s_1 on limbs appear to reflect rotations of s_1 during folding in a manner consistent with the following model:

- 1) In the early stages of, but not prior to, folding SFF and EVA recorded a bedding parallel compression directed NW-SE and normal to hinges. These early features were then subsequently rotated with a few being deformed along with their enclosing beds during later stages of folding.
- 2) As folding proceeded s_1 orientations progressively rotated to higher angles to bedding while maintaining the NW-SE trend. On stereograms this is identified by a linear continuum of s_1 orientations between bedding parallel positions to the horizontal and likely represents an incremental record of s_1 orientations during intermediate stages of folding (figure 25).
- 3) Late stage folding is characterized by subhorizontal s_1 orientations which occur at high angles to bedding (eg. on limbs dipping greater than 50 degrees and with interlimb angles less than 90 degrees).

This pattern is similar to that predicted from dynamic models of buckling by Dieterich and Carter (1969) and Dieterich (1970). Their models predict that when layers of high viscosity contrast are subjected to an externally applied horizontal stress field, s_1 on fold limbs will rotate with respect to bedding during buckling. Computer generated simulations (figure 26) show that S_1 rotates out of a bedding parallel orientation

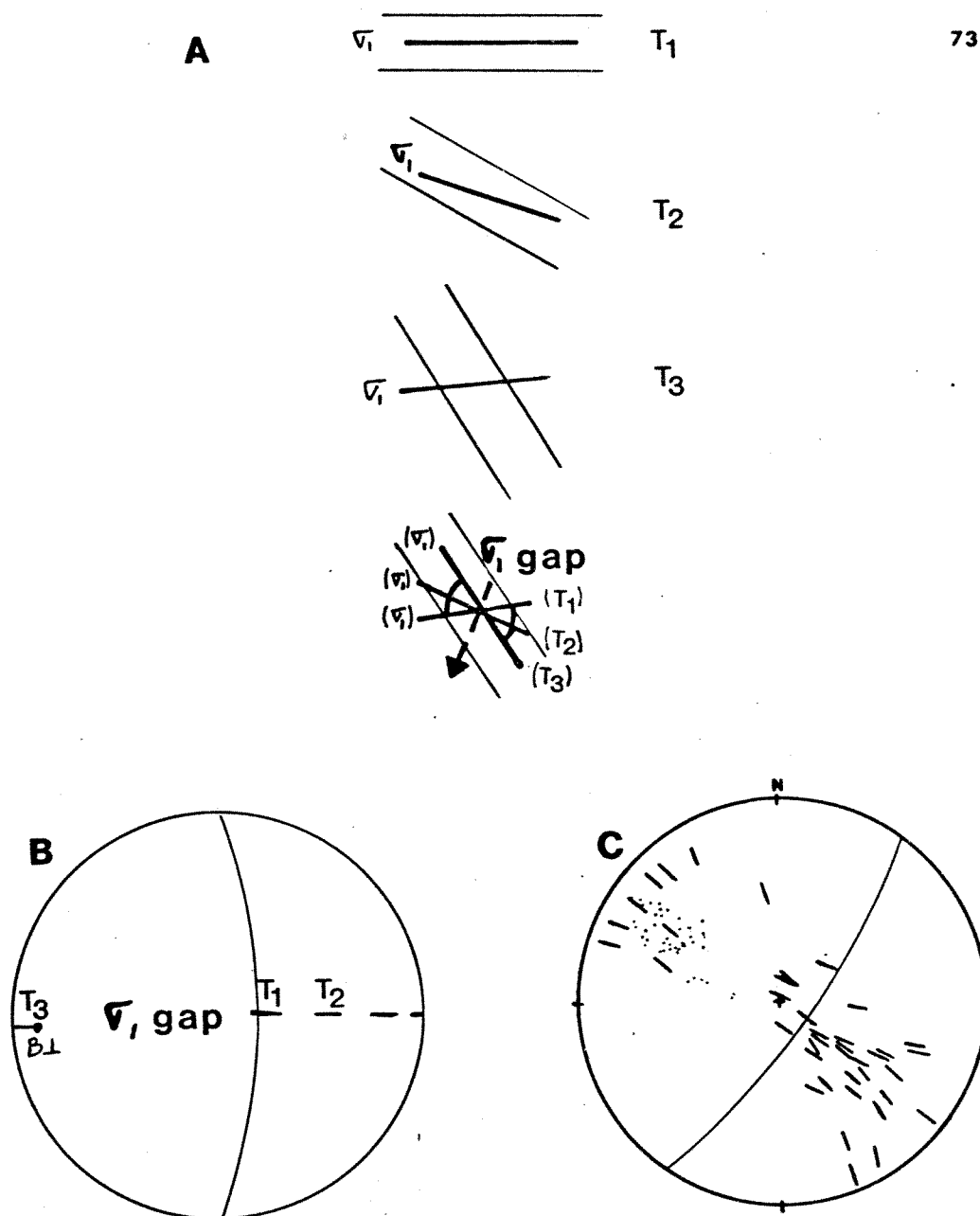


FIGURE 25. A MODEL FOR THE STRESS HISTORY OF FOLDING AND DEVELOPMENT OF THE "S1 GAP": A) CROSS-SECTION OF FOLD LIMBS SHOWING ROTATION OF SIGMA 1 RELATIVE TO BEDDING, B) STEREOGRAM SHOWING SIGMA 1 PATTERN AND RELATIVE TIMING, C) SFF-SITES 1 AND 2 COMBINED (SHORT LINE=SIGMA 1, DOT=POLE TO BEDDING).

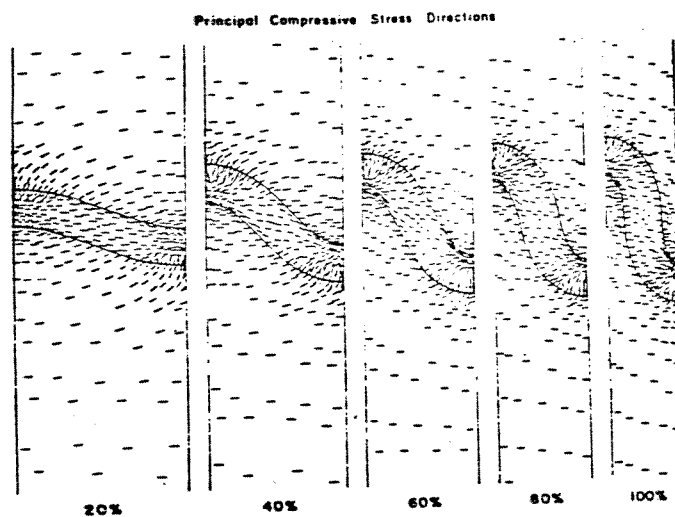


FIGURE 26. COMPUTER GENERATED S1 TRAJECTORIES DURING PROGRESSIVE FOLDING OF LAYERS WITH HIGH VISCOSITY CONTRAST (FROM DIETERICH AND CARTER, 1969).

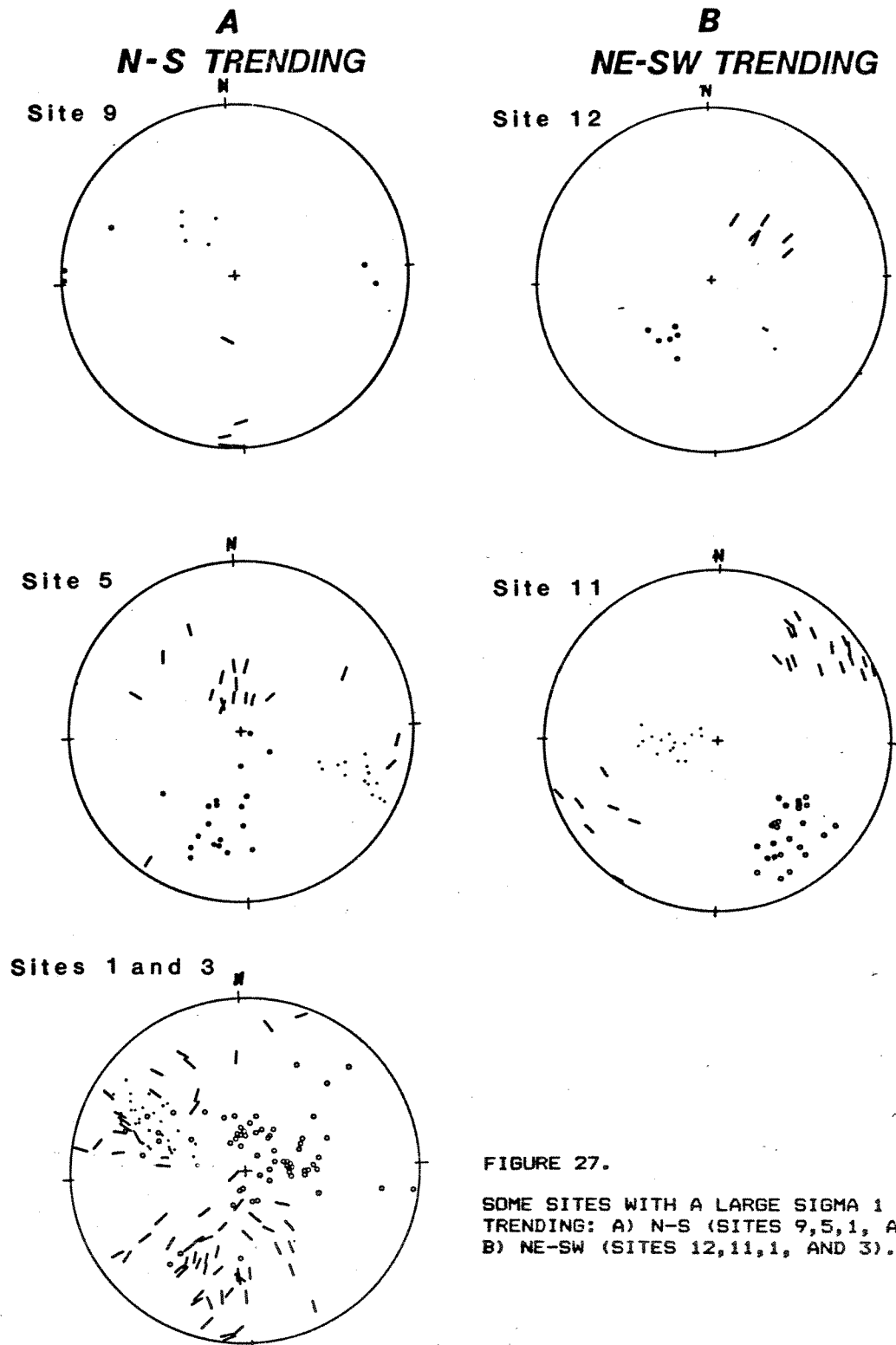
into progressively steeper angles to bedding during progressive folding until, for steeply dipping limbs, s_1 is oriented subperpendicular to bedding and subhorizontal.

S_1 TRENDS ORIENTED OBLIQUE TO FOLD HINGES AND THOSE ORIENTED PARALLEL TO FOLD HINGES

Results

Much of the remaining dynamic data from the Green Pond outlier does not appear to fit the simple model of progressive folding just described. For example, most of the other data indicate s_1 orientations that are not normal to fold hinges. Nonetheless, a number of other field relations and patterns in the data indicate that these data cannot be considered simply spurious results. These other modes may record an important change in the regional stress field which either occurred very late in the fold history or post-dated folding.

First, as described earlier, two other s_1 modal trends occur in the data, N-S (eg. figure 27a) and NE-SW (eg. figure 27b). These two modal trends lie in a continuous range of s_1 trends between NW-SE and NE-SW. One thing that is clear is that there is practically no evidence for E-W trending compression in the Green Pond



outlier. This absence, in and of itself, would be difficult to explain if the other modes were simply representing spurious or secondary fields during the main folding event.

Secondly, s_1 orientations that are inconsistent with the NW-SE trend are recorded by more than one-half of all the EVA data. This suggests that EVA record either spacial variations in the orientations of s_1 (ie. secondary stress fields) during the main folding event or a unique period of oblique compression reflecting temporal variations in the orientation of the regional stress field.

Thirdly, several sites record incompatibilities of s_1 trends in the same rock layer. This proximity of incompatible s_1 trends can be seen between SFF data and EVA data where each has a unique trend (eg. site 12, figures 20 and 21), and within the EVA data where a variation, or at least two distinct trends, are recorded by EVA (eg. sites 1 and 3, figures 20 and 21). In addition, pinnate EVA have been observed (site 3) branching off of SFF with a geometry such that each feature records a different s_1 orientation. The SFF record a NW-SE trending s_1 orientation while the pinnate EVA record a range of s_1 orientations trending NW-SE to NNW-SSE with a prominent NNW-SSE s_1 trend. The fact that nonparallel s_1 trends occur in the same rock suggests that

a temporal shift occurred in the stress field for those rocks. In these cases cited, the features that record the NW-SE trend apparently developed at a different time than the features recording the other modal s_1 trends. Thus, it appears that rotations occurred in the stress fields with time. Do these rotations reflect local variations only or do they reflect rotations in the regional stress field? Arguments presented below suggest the latter alternative.

Fourthly, at several sites throughout the Green Pond outlier some curved fibers have been found on SFF that indicate rotations in the local stress fields during progressive SFF development (plate 1). These fibers consistently record a clockwise rotation in the s_1 trend from NW-SE positions towards NNW-SSE. Therefore, a temporal clockwise rotation in the stress field did occur at least locally.

A fifth point, is that a curvilinear continuum of s_1 plunges occurs at site 3 with NNW-SSE trends oriented oblique to the NE-SW trending axial surface (note SE quadrant of figure 28b). Could this be related to progressive folding under an oblique stress field? One would expect that folding within a horizontally applied external stress field oriented oblique to hinge lines would produce a curvilinear s_1 distribution as shown in figure 28a (modeled using results from Dieterich and



PLATE 1. QUARTZ FIBERS ON A SFF SURFACE (SITE #1).
TWO STAGES OF DISPLACEMENT ARE INDICATED.
THE FIRST TRENDS NW AND THE LATER TRENDS
MORE NORTHERLY.

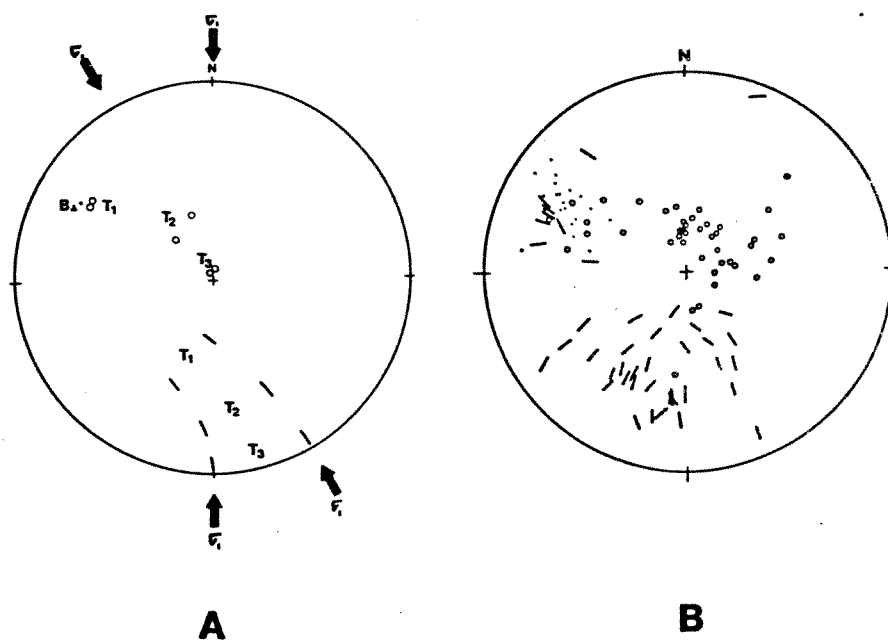


FIGURE 28. A) CURVILINEAR S1 DISTRIBUTIONS MODELED BY SUBJECTING A FOLD LIMB TO OBLIQUE HORIZONTAL COMPRESSION DURING PROGRESSIVE FOLDING. S1 "PATHS" ARE SHOWN FOR TWO ORIENTATIONS OF OBLIQUE COMPRESSION (LINE=S1, CIRCLE=S3). B) EVA-SITE 3; NNW-SSE TRENDING SIGMA 1 AND SIGMA 3 "PATHS" COMPARE WITH THOSE IN THE MODEL.

Carter, 1969). Therefore, at least a partial late stage history of progressive folding within an oblique stress field may have occurred in the main syncline .

Sixth, on the same fold just described a "cross" cleavage has been recognized for the first time in the outlier. It covers at least 1 square kilometer in the environs of Terrace Pond and has not yet been fully traced out. This cleavage crosses both limbs of the main syncline and strikes N 85 E (figure 29). Several EVA were observed in the same region with s_1 orientations normal to cleavage (plate 2). Although cleavage records a finite strain rather than the more or less instantaneous stress represented by EVA and SFF the compatibility of the shortening direction (ie. normal to cleavage) with the s_1 direction from EVA in the same area suggests a mutual relation in time. Both the cleavage and the EVA independently support the interpretation that a noncoaxial deformation occurred in the Green Pond outlier. The dominant cleavage of the rocks in the Green Pond strike roughly parallel to axial traces of the folds which trend N 30 E - N 55 E. The cross cleavage strikes at a high angle to the dominant structural trend and, hence, reflects a clockwise rotation in the finite shortening direction. Thus the two cleavages may be used to argue that noncoaxial deformation affected the outlier and that, more specifically, a clockwise rotation occurred in the

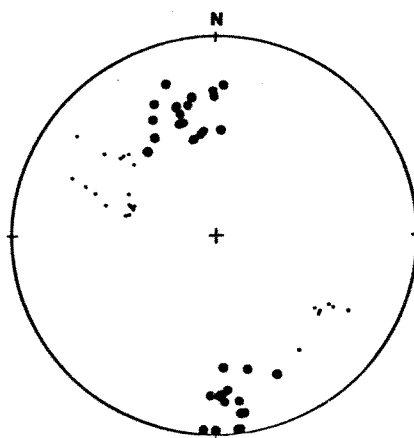


FIGURE 29. POLES TO CROSS-CLEAVAGE (LARGE DOTS) AND BEDDING (SMALL DOTS) FROM SITES 1 AND 2 OF THE MAIN SYNCLINE. NOTE THE DISCORDANCE OF TRENDS.

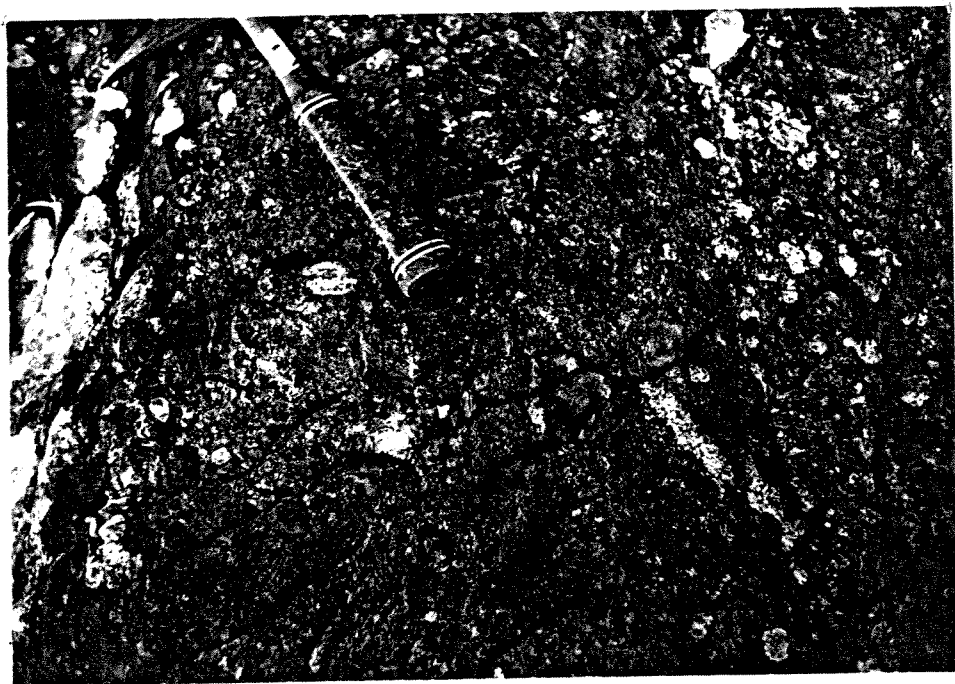
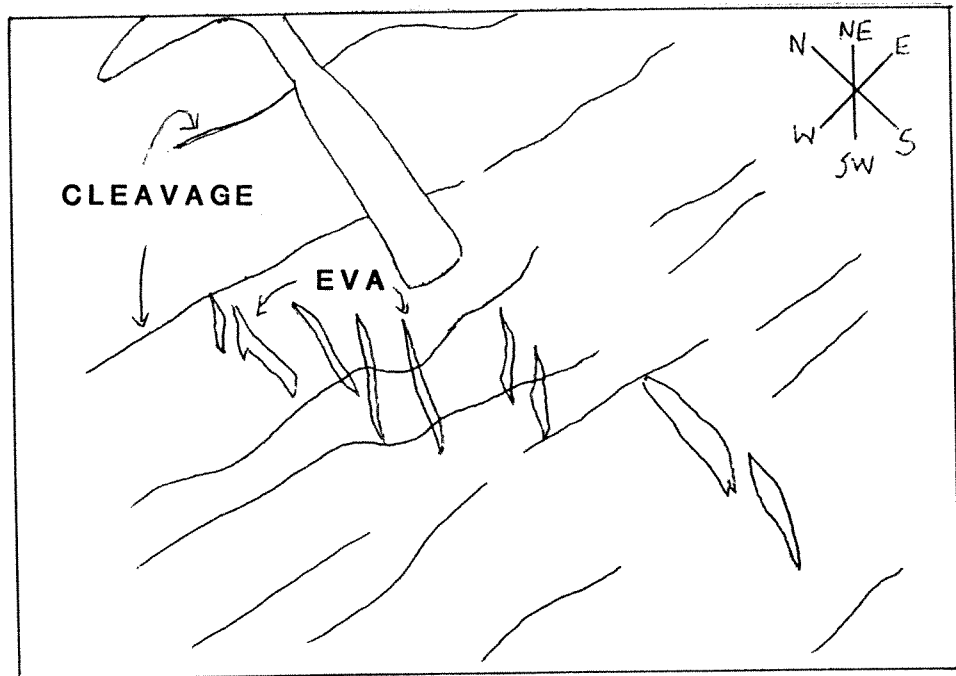


PLATE 2. EVA ORIENTATIONS INDICATE MAXIMUM COMPRESSION DIRECTED N-S AND NORMAL TO CLEAVAGE CONSISTENT WITH COEVAL DEVELOPMENT DURING A PERIOD OF OBLIQUE COMPRESSION AND SHORTENING (SITE #1).

bulk shortening strain during either the late stages of folding or after it.

Lastly, a large number of EVA data record s1 orientations with NE-SW trends. The timing of these EVA relative to folding is uncertain, although, in one outcrop the veins of an EVA with a NE-SW s1 trend cross-cuts crystal fibers of and SFF with a NW-SE s1 trend. This suggests that hinge parallel compression post-dated at least some of the major folding. The mechanisms that led to hinge parallel compression are also unclear. The EVA formation may be related to the development of fold terminations and/or to lengthwise buckling of folds. Also, since s1 trends are exactly parallel to the strike of axial traces of the folds it seems reasonable to suggest that significant folding of the outlier predated and later controlled the development of these EVA. One way to explain the data is to visualize the Green Pond as a series of cylindrical folds with layers of high competency. These corrugated competent layers, could act as a strong stress guide effectively rotating external fields into parallelism with the fold axes. At present the most reasonable interpretation is that when the fold was responding to the oblique N-S regional field, further rotations locally occurred due to a control of the fold structure.

Two-Stage Stress History Model

The dynamic data and field relations appear to indicate that rotations in the stress field(s) occurred at least locally and that these rotations were consistently clockwise from NW-SE towards N-S (figure 30). In addition, the two cleavage trends in the main syncline strongly argues for two noncoaxial deformations. The parallelism of each of the inferred shortening directions with the two NW-SE and N-S sl modal trends supports their correlation and collectively makes a strong case for two periods of noncoaxial deformation. The fact that N-S sl trending data can be found from many different parts of the outlier suggests that this noncoaxial history is regional in scope. Therefore, it is concluded that a two-stage noncoaxial deformation history occurred in the Green Pond outlier involving a clockwise rotation of the regional stress field and locally the finite axis of shortening. The deformation history is envisioned as follows:

Stage I: major folding was initiated under a semi-regional compressive stress field oriented NW-SE (and subhorizontal) as recorded by both SFF and EVA. At this time the dominant NE-SW trending folds and cleavage developed.

**SHORTENING DIRECTIONS
FROM MESOSTRUCTURES**

DEFORMATION	SFF	EVA	CLEAVAGE
STAGE I (Major Folding)	NW N 	NW N 	NW N
STAGE II (Late Folding and/or Post Folding)			

FIGURE 30. SUMMARY OF NONCOAXIAL DEFORMATION RECORDED BY STRUCTURES IN THE GREEN POND OUTLIER INDICATES A CLOCKWISE ROTATION OF THE MAXIMUM SHORTENING AND COMPRESSION DIRECTION FROM NW-SE TO ALMOST N-S.

Stage II: The semi-regional stress field rotated clockwise to a nearly N-S direction. This direction was an unfavorable orientation for slip on bedding surfaces such that SFF development was reduced significantly and any additional slip on bedding surfaces resulted in curved fibers. Since EVA are less effected by rock anisotropies (eg. bedding) these features continued to develop throughout the period of oblique compression. Stage II post-dated most folding but probably occurred during the later stages of folding in the main syncline resulting in the E-W trending cleavage and the distinctive NNW-SSE to N-S modal sl trends recorded by EVA.

TECTONIC MODEL FOR THE GREENPOND OUTLIER

Any model for the structural development of the Green Pond must account for the noncoaxial deformation. Since the stage II deformation is recognized for the first time in the outlier no previous work explains this aspect. The model proposed for stage II deformation is one of oblique compression that induced strike-slip motion on pre-existing fractures in the crystalline basement beneath the Green Pond strata. Strike-slip motion on echelon faults or irregular fault surfaces would have created pull-apart basins that downdropped the Green Pond and at the same time result in locally distributed compressional deformation (figure 31). This would provide a single

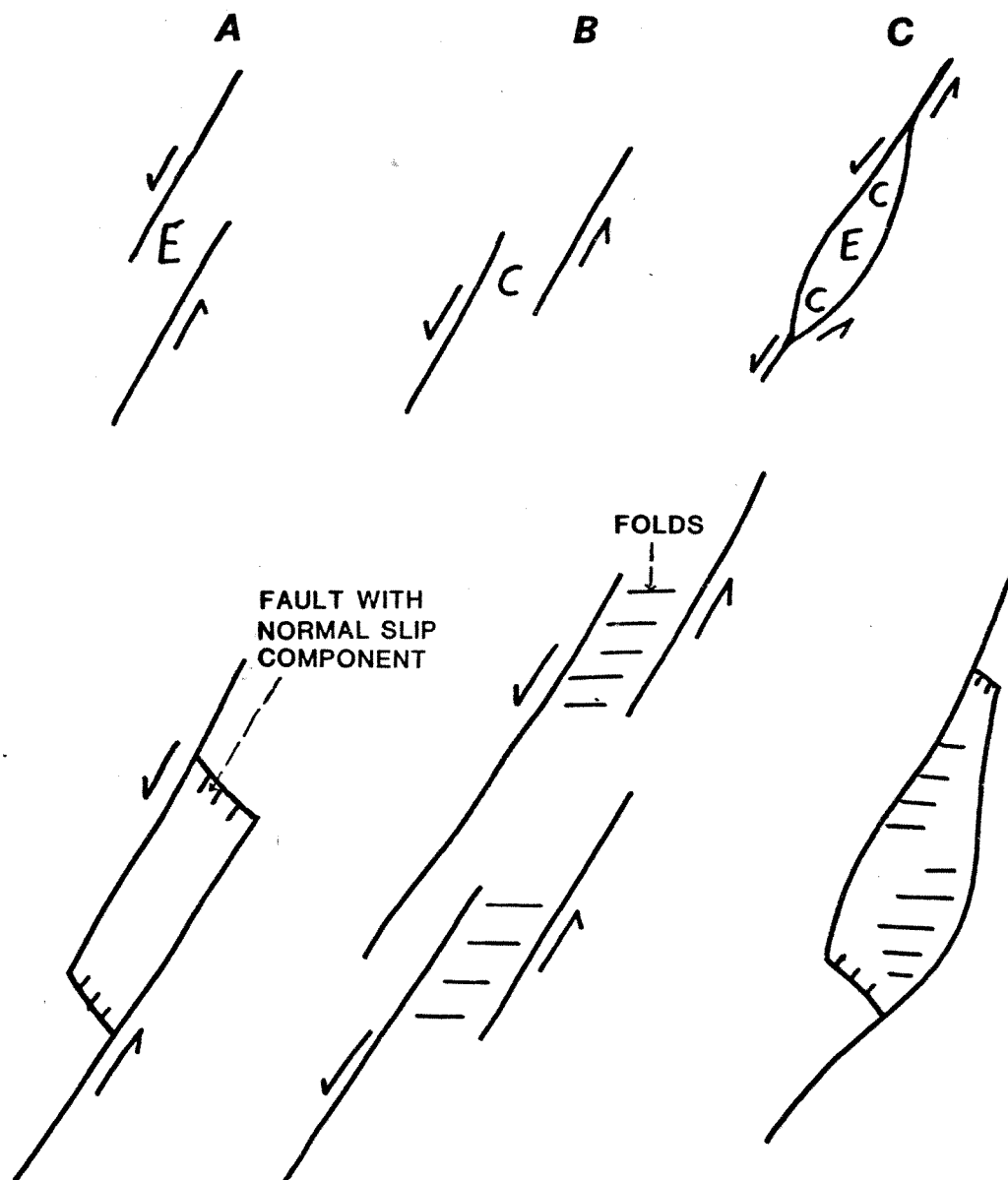


FIGURE 31. THREE POSSIBLE MODELS OF STAGE II DEFORMATION IN THE GREEN POND OUTLIER RELATED TO STRIKE-SLIP FAULTING DURING N-S DIRECTED COMPRESSION (E=EXTENSION, C=COMPRESSION).

mechanism to account for stage II deformation and the numerous faults in the area.

The Green Pond outlier, an elongate sliver of folded lower and middle Paleozoic strata, was downdropped into the surrounding Precambrian along at least three high angle faults. These faults occur on the SE and NW borders in New York which forms a graben (Sanders et al., 1991, p110). Downdropping also occurred along a fault in the southeastern region which passes through a U.S. Military Reservation (U.S.G.S open file report). Although a significant normal component of displacement apparently occurred along each of these faults, it is possible, though not known, that significant strike-slip components occurred as well. At least two other uncharacterized faults occur in the southern region. Previously (Ratcliff, 1980) it has been suggested that the downdropping occurred during the Triassic rifting event. Since little, if any, data exist on the exact nature of these faults or their time of movement this model is highly speculative. Since the faults run almost exactly parallel to the fold axes and to the dominant cleavage, a later normal faulting event seems somewhat unsatisfactory, unless of course it involves reactivation of older basement faults. In either case we might conclude that faulting played an important role during folding of the Green Pond. In a region near the state line the NW border fault may dip eastward at

less than 40 degrees (Gunderson, oral communication) which raises the possibility that the downdropping occurred along a pre-existing thrust. Furthermore, recent gravity data collected across the Green Pond outlier (Toskos, M.S) at the northern end of Clinton Reservoir suggest that basement and cover is juxtaposed along a high angle fault located beneath the central anticline. This supports the hypothesis that deformation in the cover rocks is, at least in part, controlled by adjustments between basement blocks. The model therefore would account for the oblique deformation and the existing fault data without calling on a later rifting event to explain the present structural position of the outlier within the Precambrian highlands. Much work is needed before this model can be considered more than a speculation but it serves as a legitimate alternative to previous models, as it accounts for the oblique deformation.

TIMING OF DEFORMATION: ALLEGHENIAN?

Three major orogenic events are commonly thought to have occurred in the central Appalachians. They are the Taconic (generally Middle to early Late Ordovician, 450-470 m.y.), the Acadian (mostly Middle Devonian, but including Early Devonian, 360-400 m.y.), and Alleghenian (Pennsylvanian and (or) Permian, 230-280 m.y.) (Drake,

1980). Since the structural analysis of this study occurred in Silurian and Devonian age rocks the Taconic orogeny had no contribution to the deformation described. The youngest rock affected by the deformation is Middle Devonian in age, hence, records the Acadian orogeny and/or the Alleghenian orogeny.

The Middle Devonian age is based largely on marine fauna collected by Kummel and Weller (1902) and Willard and Cleaves (1933) from the Bellvale Sandstone and Marcellus Shale. A partial list of index Brachiopods are listed in table 3. Plant fossils have also been found in the Bellvale Sandstone (Martin, 1871; Smock, 1884; Prosser, 1892). Although a Middle Devonian age was suggested, Devonian plant taxonomy was poorly understood at the time and no recent workers in the region have reinterpreted the assemblage in light of modern taxonomy.

The age of stage I and stage II deformations in the Green Pond is uncertain. In New York an Acadian thermal event is recorded in the Precambrian (Gunderson, oral communication) located near the NW border of the Green Pond outlier. If Acadian deformation extended into the Late Devonian then the outlier would have likely recorded it. On the other hand, Acadian deformation may have ended in the Middle Devonian at about the same time that the Bellvale Sandstone and Skunnemunk Conglomerate were being deposited. These two formations were part of a

TABLE 3. BRACHIOPODS OF MIDDLE DEVONIAN AGE COLLECTED FROM THE LOWER BELLVALE SANDSTONE AND THE MARCELLUS SHALE BY KUMMEL AND WELLER (1902) AND WILLARD AND CLEAVES (1933).

Athyris spiriferoides

Camarotoechia sappho

Chonetes coronatus

Leiorhynchus laura

Spirifer audaculus

prograding delta whose sediments were derived from an uplifted terrane to the east presumably caused by the Acadian orogeny (Barnett, 1976). Consequently, a Middle Devonian Acadian deformation in the Green Pond requires the unlikely conditions of voluminous deposition (>1.5 KM), burial to at least one additional KM, lithification, low-grade metamorphism, cleavage development, folding, and thrusting during the Middle Devonian. Therefore, although Acadian orogenesis may have occurred in the Green Pond outlier, middle Devonian fold and thrust development appears to be highly unlikely.

Northwest of the outlier noncoaxial Alleghenian structural trends in Carboniferous rocks of eastern Pennsylvanian have been recently traced to the Valley and Ridge of westernmost New Jersey (Geiser and Engelder, 1983). Also, deformation in the Valley and Ridge and Great Valley just west of the outlier has been considered Alleghenian based on similarity of structural style with that in Carboniferous rocks to the west (ie. decollement related folds, thrusts and cleavage involved in thin-skin tectonics) (Drake, 1980). Similarly, The two-stage noncoaxial structural trends in the Green Pond may correspond to the two phases of Alleghenian deformation further west and represent an easternmost trace of Alleghenian effects in New Jersey. Regional correlation would provide evidence for wholly Alleghenian age fold and

thrust development in the Green Pond and is therefore described in more detail in the following section.

RELATION TO CENTRAL APPALACHIANS

The previously described structures are developed within an outlier of Siluro-Devonian strata within the Highlands province (Reading Prong) of the Central Appalachians. As such, structures are not directly traceable across intervening ranges of Precambrian gneisses into equivalent and younger age strata of the Valley and Ridge and Plateau provinces. Yet, certain relations, especially with regards to the noncoaxial nature of late Paleozoic deformation within the Highlands, Valley and Ridge, and Plateau provinces strongly argues for direct correlation. These relationships are described below.

In the Alleghenian Plateau of eastern Pennsylvania and southern New York two noncoaxial phases of Alleghenian deformation appear to be well documented by Geiser and Engelder (1983) (figure 32,#1). The two phases correspond to regional development of cross cutting folds (figure 33) and cleavage (figure 34). For example, the Lackawana syncline in eastern Pennsylvania developed generally along a NE-SW trend whose eastern limb was subsequently refolded along E-W trends indicating a clockwise rotation of the overall shortening direction. Since both deformations folded middle Carboniferous rocks in the syncline the two structural trends correspond to two stages of Alleghenian

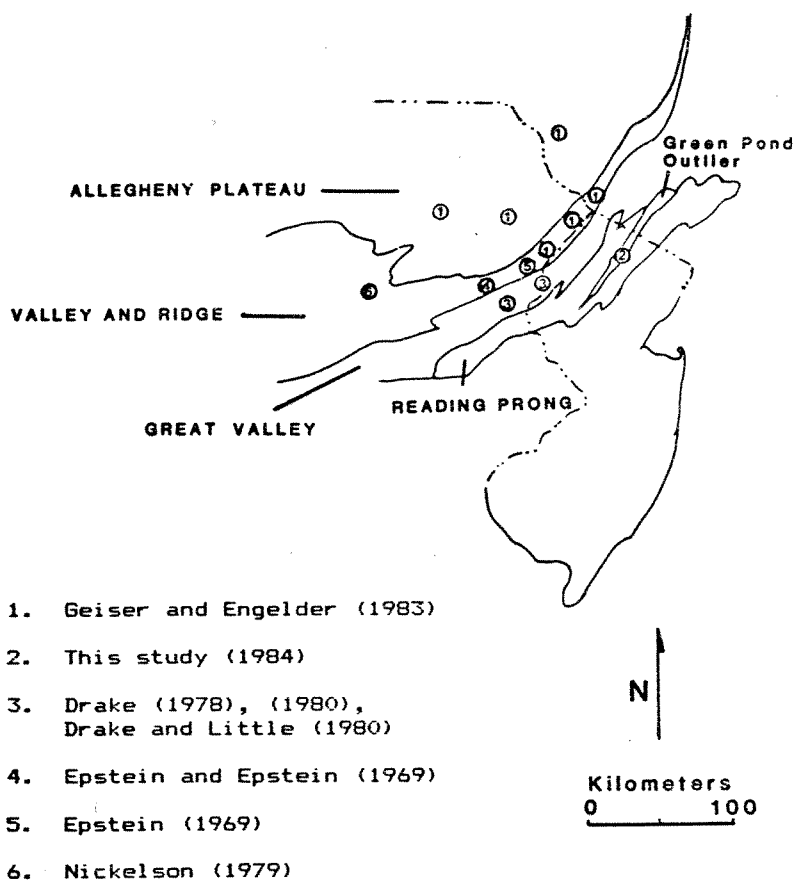
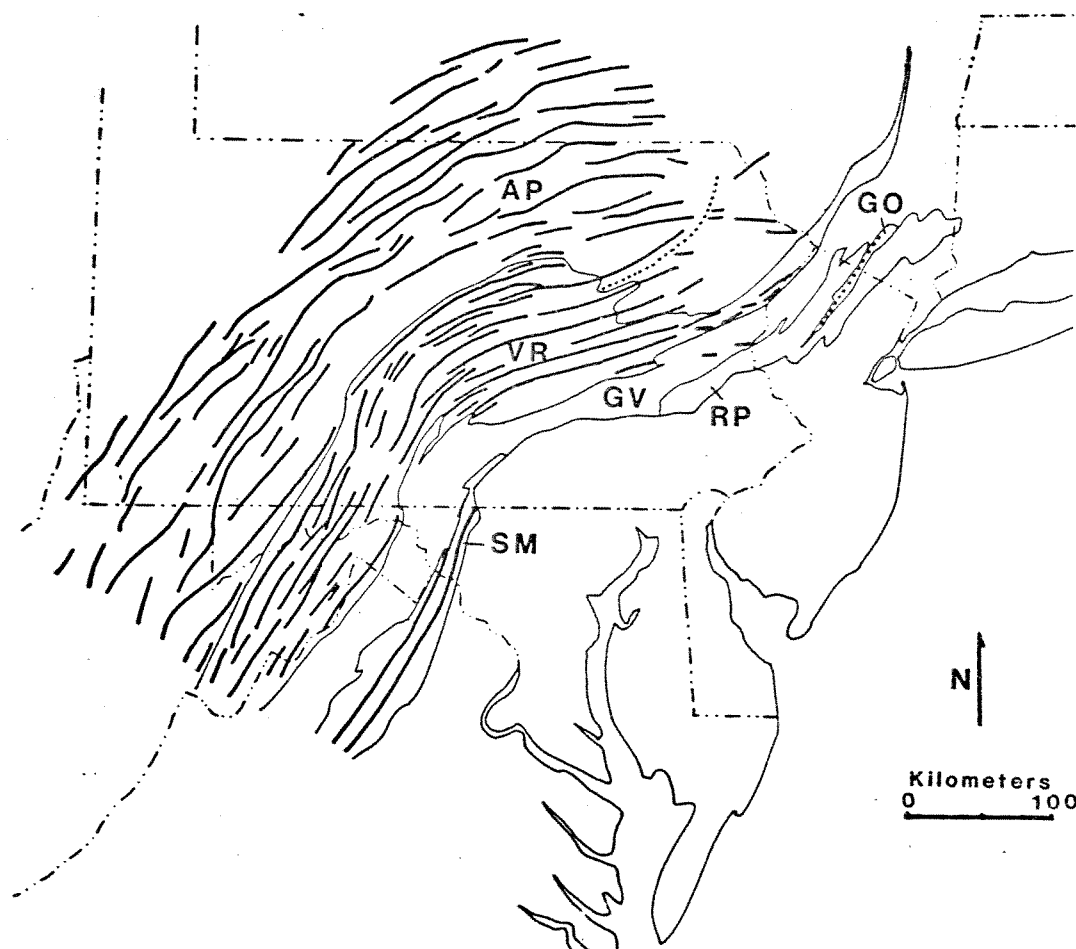


FIGURE 32. SITES OF PREVIOUS STUDIES THAT HAVE REPORTED NONCOAXIAL STRUCTURAL TRENDS OF PROBABLE ALLEGHENIAN AGE.



GO Green Pond Outlier	GV Great Valley
AP Allegheny Plateau	RP Reading Prong
VR Valley and Ridge	SM South Mountain

FIGURE 33. FOLD TRACES IN THE CENTRAL APPALACHIANS (PRIMARILY AFTER GEISER AND ENGELDER, 1983, AND COHEE ET AL., 1976). DOTTED LINES= LACKAWANA SYNCLINE AND GREENPOND "SYNCLINE".

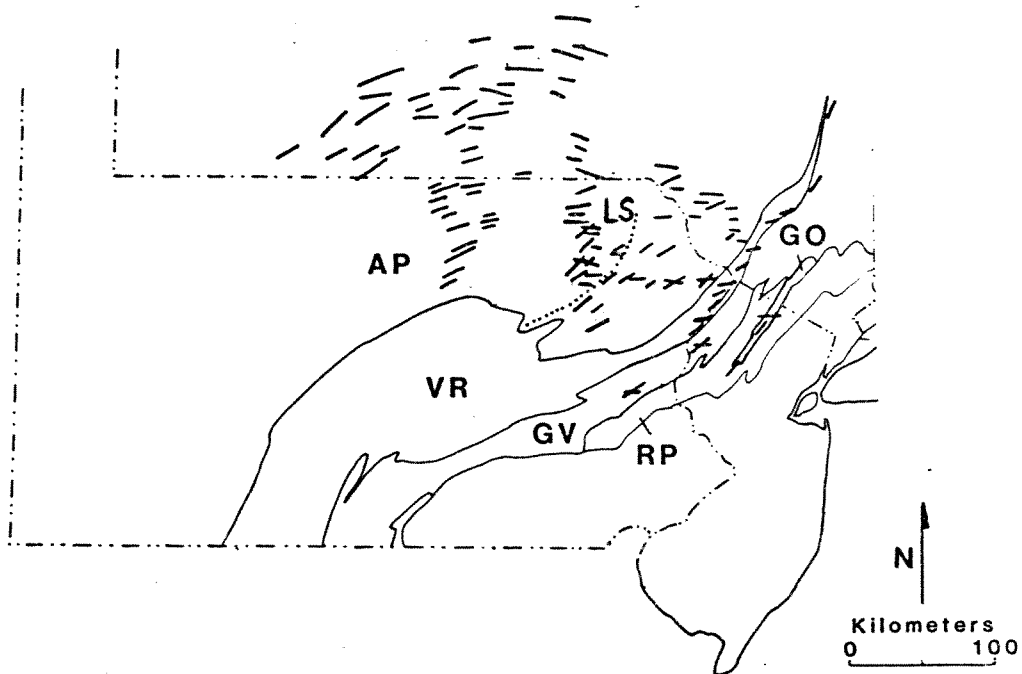


FIGURE 34. CLEAVAGE TRENDS IN THE NORTHERN CENTRAL APPALACHIANS (PRIMARILY AFTER GEISER AND ENGELDER, 1983).

deformation. Phase I structures of the "Lackawana phase" are late Carboniferous or younger and phase II structures of the "Main phase" are early Permian or younger.

In the Green Pond outlier of northern New Jersey a two-stage structural history is also apparent (this study) (figure 32, #2) and may correlate with the "Lackawana" and "Main" phases of deformation just described. Folding that produced the main syncline in the Green Pond was initiated along a NE-SW trend and is associated with a NE-SW trending axial plane cleavage. The syncline was subsequently affected by an E-W trending cleavage cutting across the fold structure. This corresponds to a clockwise rotation in the shortening direction. Also, paleostress directions determined from numerous EVA and SFF indicate compression directed NW-SE and N-S and a probable clockwise rotation in the stress field. This rotation is compatible with the two shortening directions and suggests that a clockwise rotation in the regional stress field caused the clockwise rotation in the shortening axis. Since the two structural trends deform Middle Devonian and older rocks the ages of deformation may be Alleghenian and/or late Acadian. In the light of this uncertainty regional correlation of structures is critical evidence for timing. Indeed the two structural trends in the Green Pond outlier of New Jersey are compatible with those of eastern Pennsylvania, both in

orientations and relative timing, suggesting a probable Alleghenian age for the two-stage history of the Green Pond.

If this correlation is real then Alleghenian noncoaxial deformation is extrapolated well into the Highlands province for the first time. Of course, the credibility of such a correlation depends in part on tracing these two structural trends across the intervening Precambrian ranges and Great Valley into the Valley and Ridge. A detailed study of this problem is beyond the scope of this work, however, several studies done by other workers in the Great Valley and Valley and Ridge report two noncoaxial structural trends considered to be Alleghenian deformation. The locations of these studies are indicated in figure 32 and some details of each are summarized below.

In the Precambrian of the Reading Prong thrust faults which generally strike NE-SW have been mapped in the area of the New Jersey-Pennsylvania border south of the Green Pond outlier (Drake, 1969). Also in this area, but along the western margin of the Reading Prong (figure 32, #3), allochthonous klippe of Precambrian lie in subhorizontal thrust contact on top of Cambro-Ordovician rocks of the Great Valley (Drake and Little, 1980). Since many of these thrust faults cut across Taconic age folds in the Cambro-Ordovician rocks the thrusts are thought to

represent a late Paleozoic deformation and have been interpreted as Alleghenian age structures (Drake and Little, 1980). Their overall strike is NE-SW compatible with the earlier phase of deformation but as of yet no E-W trending structures compatible with the later "Main" phase have been discovered in the Precambrian to my knowledge. However evidence for this later phase does occur in the adjacent Cambro-Ordovician rocks as described below.

In the Cambro-Ordovician rocks of the Great Valley three phases of folding and associated cleavage have been recognized (Drake and Little, 1980) (figure 32, #3). The first phase is related to nappe development during the Taconic orogeny and resulted in ENE (N 60 E) trending folds and slaty cleavage in the Martinsburg Formation (Drake, 1978). The second and third folding phases overprint the Taconic structures and are considered noncoaxial phases of Alleghenian deformation (Drake, 1978; Drake and Little, 1980; Drake, 1980). Of the latter two folding phases the first developed in association with a strain slip cleavage along a NE trend (N 40 E) and fold hinges of the second and last phase trend nearly E (N 80 E) parallel to a locally and poorly developed cleavage. These orientations are compatible with those in the Green Pond outlier and the Lackawana syncline. These structural relations can be seen in the Paulins Kill Valley just east of the Delaware Water Gap where a tectonic window into a

Taconic nappe is framed by the Portland thrust. This thrust is thought to be a major Alleghenian decollement that was subsequently deformed by both N 40 E and N 80 E sets of folds (Drake, 1978). The folds of the last phase (N 80 E) control, at least in part, the configuration of the tectonic window (ie. a general E-W trend) both in the Paulins Kill Valley and in other tectonic windows in the same nappe exposed in this area (Drake, 1978). Thus, it appears that the second phase of Alleghenian deformation extended eastward at least as far as the Great Valley.

Noncoaxial deformation is also evident west of the Great Valley in the Valley and Ridge of New Jersey and Pennsylvania. Here folds and cleavage in the Siluro-Devonian rocks are dominately NE-SW trending. This deformation is considered Alleghenian in age based on similarity of structural style with younger rocks further west (Drake, 1980) and is compatible with phase I deformation. Evidence for a period of oblique compression is the presence of small E-W trending folds north of the Lehigh River in Pennsylvania (figure 32, #4) (Epstein and Epstein, 1969, figure 54), a nearly E-W trending cleavage located in northwest New Jersey and in the Hudson Valley of New York (figure 32, #1) (Geiser and Engelder, 1983, figure 3), and curvature of axial surfaces into ENE-WSW trends in the Delaware Water Gap area of New Jersey and Pennsylvania (figure 32, #5) (Epstein, 1969). Also, the

cross fold flexure that controlled, in part, the formation of the water gap (Epstein, 1969) may also have formed during a period of oblique compression.

Finally, in figures 33 and 34, it appears that E-W trending folds and cleavage have been reported across the Pocono Plateau of eastern Pennsylvania and southern New York (Geiser and Engelder, 1983) spanning the remaining distance to the Lackawana syncline and completing the regional traverse westward from the Green Pond outlier in New Jersey. Along this traverse it has been shown that noncoaxial structural trends (NE-SW and E-W) considered to be phases of Alleghenian deformations can be traced in a discontinuous fashion from the Green Pond outlier across the Great Valley, Valley and Ridge, and Pocono Plateau to the Carboniferous rocks of the Lackawana syncline where the phases are clearly Alleghenian in age. Although only NE-SW trending thrusts in the Reading Prong have been identified and considered Alleghenian in age, the cross cleavage and EVA orientations in the Green Pond outlier provide the first evidence of phase II deformation within the Precambrian of the Highlands province. Indeed, based on the regional correlation just described, it appears that noncoaxial Alleghenian deformations extend eastward well into the Reading Prong of New Jersey. Furthermore, the relative timing is consistent for all provinces with the NE-SW trend being overprinted by the E-W trend and

corresponding to a clockwise rotation in the finite shortening direction from NW-SE to N-S. It should also be noted that available dynamic information is compatible with the kinematic information. Namely, cross joints and conjugate wrench faults in Carboniferous rocks south of the Lackawana syncline (figure 32, #6) are thought to indicate a NW-SE compression (Nickelson, 1979) that produced phase I structures (Geiser and Engelder, 1983) and N-S striking joints to the north are thought to record N-S compression during development of phase II structures (Geiser and Engelder, 1983). This appears to correlate with orientations and relative timing of the compression directions interpreted from dynamic data in the Green Pond outlier (this study) suggesting that the Alleghenian noncoaxial structural trends which record a clockwise rotation in the regional finite strain for eastern Pennsylvania and northern New Jersey developed in response to a contemporaneous clockwise rotation in the regional stress field.

AN INDENTOR MODEL FOR THE COLLISION OF
GONDWANALAND AND LAURASIA AND DEVELOPMENT
OF ZONES OF NONCOAXIAL DEFORMATION

Alleghenian deformations in the Central Appalachians are thought to record the final convergence and suturing of Gondwanaland and Laurasia in the late Paleozoic (Lefort and Van Der Voo, 1981). To understand the kinematics of continent-continent collision it is useful to look at a modern day analog such as the India-Asia collision. The kinematics of this collision has been modeled by Tapponnier and Molnar (1976) , Molnar and Tapponnier (1977), and Tapponnier et al. (1982) as the consequence of a rigid die (India) indenting a plastic-rigid material (Asia). This plane strain model incorporates slip-line theory which predicts trajectories of maximum shear stress (paralleling slip lines) as well as principal stress trajectories through the relatively plastic material (eg. Asia) (Tapponnier and Molnar, 1976). The general pattern of strike slip faults in Asia is strikingly similar to that predicted by the model. This model has also been applied to the Gondwanaland-Laurasia collision to explain the distribution of major Carboniferous strike-slip faults in north Africa and North America (Lefort and Van Der Voo, 1981). Unfortunately, their model does not explain the development of noncoaxial deformation recorded in eastern

Pennsylvania and New Jersey as well as in other areas (Mosher, 1983).

In addition to strike-slip faults, both the Himalayas and the Appalachians have well developed fold and thrust belts. These structures reflect a "thin-skinned" tectonic response of a continent-margin orogenic zone during the collisional process. Their development differs from the response observed in experiments by Tapponnier et al. (1982), in that, deformation is accommodated principally by underthrusting of one collisional margin under the other giving rise to a zone of thickened crust.

Assuming that the mechanical processes necessary to propagate the Appalachian fold and thrust belt do not vary significantly around the New York promontory and Pennsylvania reentrant, variations in space and time of its development, should reasonably reflect variations in space in time of underthrusting of the Laurasia craton under Gondwanaland during collision. Superposition of folds and cleavages in regions having undergone noncoaxial Alleghenian deformation can likewise be used to test various geometric and kinematic models for collision based on a modified indenter model which allows for some underthrusting.

Convergence of a rectilinear margin of Gondwanaland with the North American margin would logically bring the New York promontory into initial contact, and then as

deformation proceeded the reentrants would eventually make contact. In order that a rectilinear margin adjust to fit the North American margin significant deformation must occur in the region of the promontory. As either the promontory or Gondwanaland is deformed the contact zone migrates into the reentrant. Deformation would continue on the promontory but it would be expected to continually reflect changes in margin geometry. Progressive development of fit during contact between the two cratons can logically explain the distribution in space and time of noncoaxial deformation. Figure 35 illustrates a simple three stage model that explains the development of noncoaxial deformation observed on the New York promontory.

Stage one (figure 35b): A rigid North American craton makes initial contact with a relatively plastic Gondwanaland at the New York promontory. This results in underthrusting and northwest directed fold and thrust development in response to principally a NW directed compression. This stage could have produced the NE-SW trending structures of phase I Alleghenian deformation.

Stage two (figure 35c): Vertical thickening of the collisional zone in the promontory area builds progressive resistance to continued underthrusting due to gravity forces. Internal deformation (along slip lines?) begins to allow the Gondwanaland margin to change shape and to

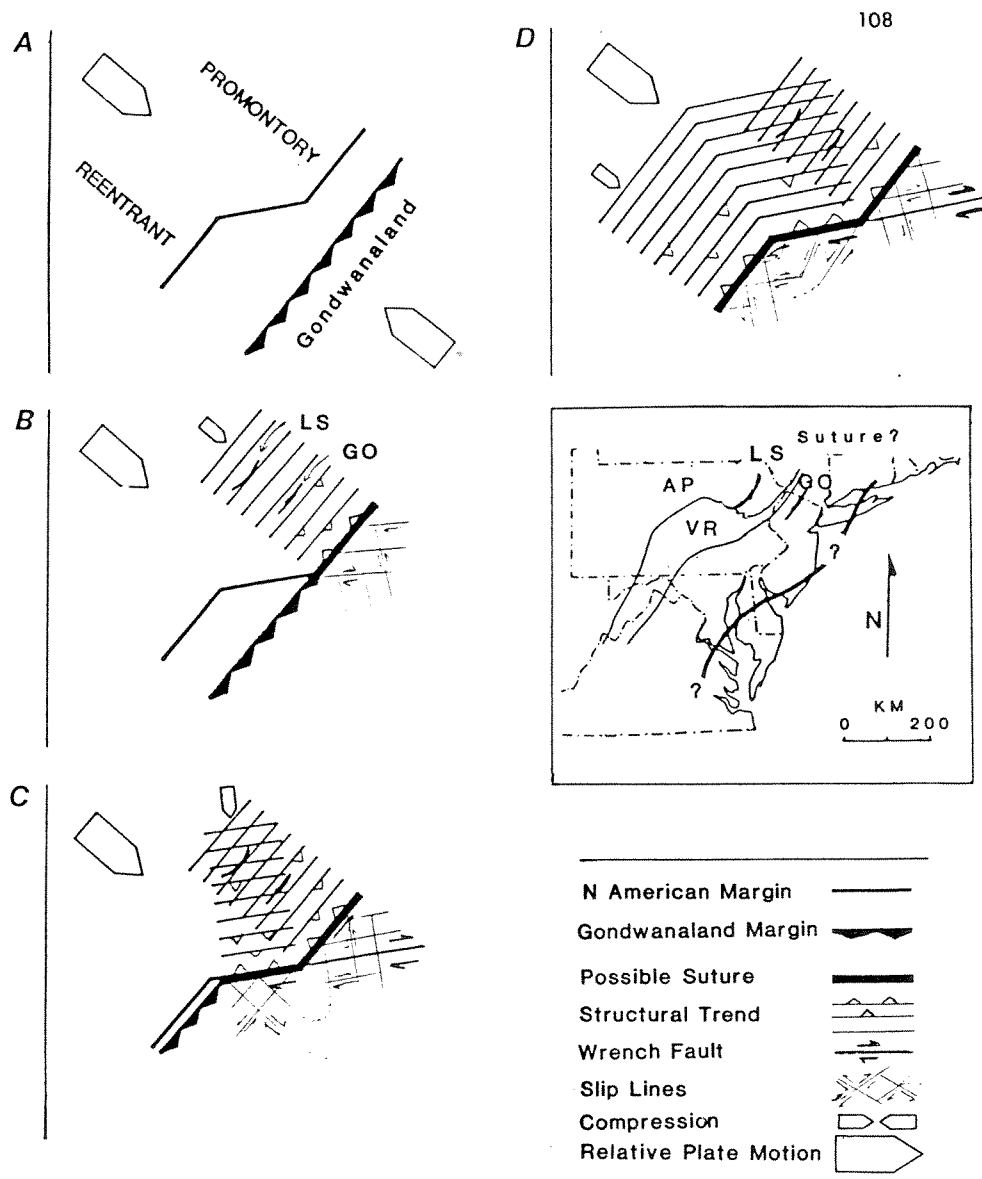


FIGURE 35. CONTINENT-CONTINENT COLLISION MODEL FOR THE NEW YORK PROMONTORY AND PENNSYLVANIA REENTRANT: A) CONVERGING CONTINENTAL MARGINS OF GONDWANALAND AND LAURASIA, B) INITIAL CONTACT ON LEADING EDGE OF PROMONTORY MARGIN, C) SUBSEQUENT CONTACT ALONG THE PROMONTORY SIDE(S), D) CONTACT AND OCEAN CLOSURE IN THE REENTRANT.

move into the Pennsylvania embayment. This could have involved motion along E-W trending right-lateral strike-slip faults and have been coincident with northerly directed fold and thrust development on the New York promontory. Both faulting and folding would likely reflect a corresponding clockwise rotation in the stress field. This stage could have produced the E-W trending structures of phase II Alleghenian deformation.

Consequently, it is suggested that deformation around the promontory subsequent to initial contact with the African craton produced the clockwise rotation in the stress field and corresponding axes of shortening observed in the Green Pond outlier and eastern Pennsylvania. The kinematics of this deformation (stage II) is considered analogous to the development of fold and thrust belts that parallel wrench faults along the India-Asia suture (figure 36a).

Tapponnier and Molnar (1976) note that the direction of thrust faulting (normal to wrench faults) that led to crustal thickening in the Himalayas is approximately parallel to the orientation of the compressive stress predicted for the plastic material (Asia) (figure 34b). The same India-Asia analog was used by Geiser and Engelder (1983) to explain Alleghenian deformations in eastern Pennsylvania.

Stage three (figure 35d): As the African craton makes contact with the reentrant and margin adjustments cease to

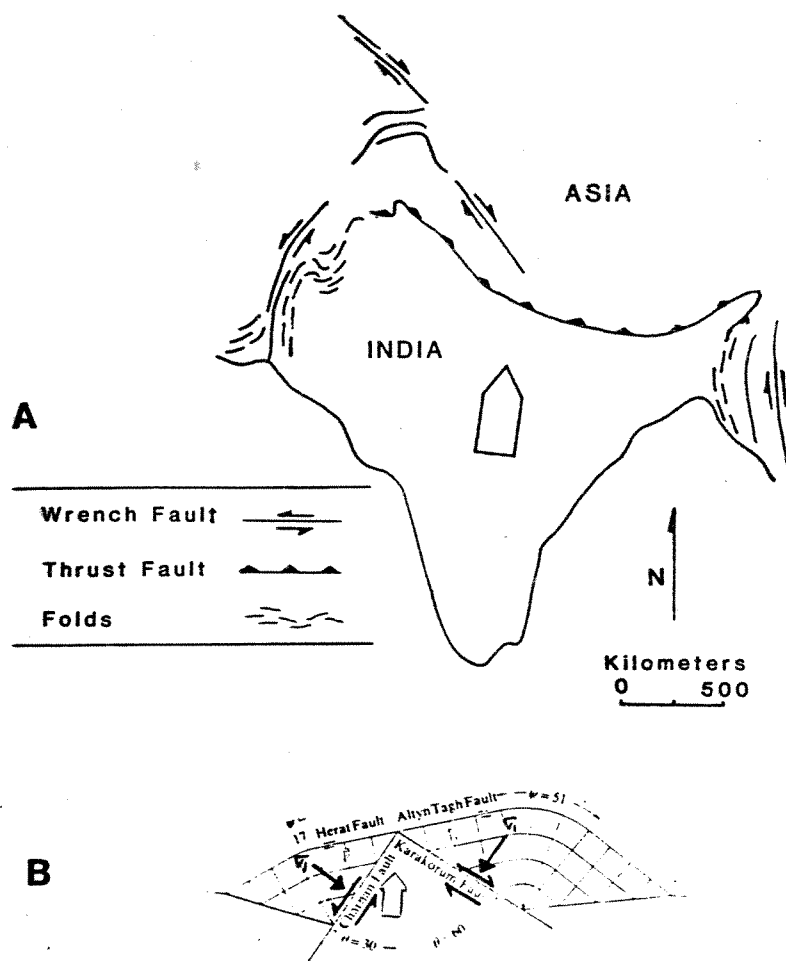


FIGURE 36. A) FOLD AND THRUST DEVELOPMENT ON THE INDIAN CRATON ORIENTED PARALLEL TO WRENCH FAULTS ALONG THE INDIA-ASIA SUTURE, B) SLIP LINES PREDICTED IN RIGID INDENTOR MODEL (AFTER TAPPONNIER AND MOLNAR, 1976).

occur, deformation proceeds by underthrusting in the reentrant as it first occurred on the promontory. This could have produced the nearly N-S trending structures south of Pennsylvania (eg. the South Mountain Anticlinorium, Cloos, 1950), which can be seen in figure 33.

This model is consistent with the regional geology in three ways. First, major E-W striking right-lateral strike-slip faults cross north Africa (eg. South Atlas fault, Tizi n'Test fault) along which Gondwanaland is thought to have converged into the North American craton (Mattauer et al., 1972; Arthaud and Matte, 1977; Lefort and Van Der Voo, 1981; Mosher, 1983). This is consistent with stage two deformation mentioned above. Furthermore, in a Permo-Triassic reconstruction Lefort and Van Der Voo (1981) (figure 37) suggest that this right-lateral fault system extends westward across the African continental shelf and into the Pennsylvania reentrant where some E-W trending right lateral strike-slip faults of possible Alleghenian age also have been reported (eg. Breesewood fault, Carbaugh-Marsh Creek fault: Root, 1973; Root and Hoskins, 1977).

Secondly, evidence from regional Appalachian geology supports the assumption that the North American craton behaved more rigidly than the African craton during continental collision. Major displacements (>50 KM)

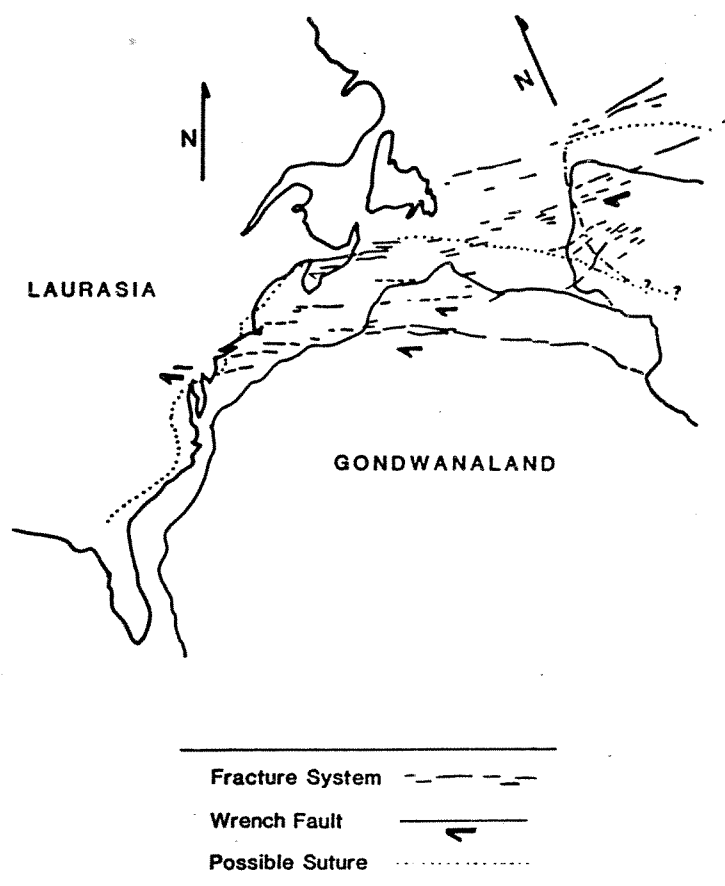


FIGURE 37. A MAJOR RIGHT-LATERAL WRENCH FAULT SYSTEM
ON A PERMO-TRIASSIC RECONSTRUCTION
(ADAPTED FROM VAN DER VOO, 1981).

occurred on individual faults in north Africa (eg. South Atlas fault) while displacements on the Pennsylvania extension of this fault system was <4 KM (eg. Carbaugh-Marsh Creek fault). Also, it is thought that the North American cratonic margin has maintained its general geometry since rift development in the late Precambrian to Cambrian. This argument is based on geophysical anomalies, the distribution of rift related volcanics (Rankin, 1976), and on systematic variation in thicknesses of Paleozoic sedimentary strata (Thomas, 1977). Thus, it appears that during continent-continent collision the development of the Valley and Ridge structural trends mimicked the geometry of the pre-existing cratonic margin. At the same time, the African craton appears to have internally deformed to accomodate the promontories and reentrants of the North American cratonic margin. This condition implies that rigid-indentor models for continent-continent collision must assume that the North American craton acted as the rigid die in a manner analogous to the Indian craton. The rigid indentor model proposed is consistent with this condition.

Thirdly, noncoaxial deformation of Alleghenian age has been reported on every major promontory in the Central and Southern Appalachians. This is a condition predicted by the three-stage model above. Figure 38 shows the location of each promontory and gives references for

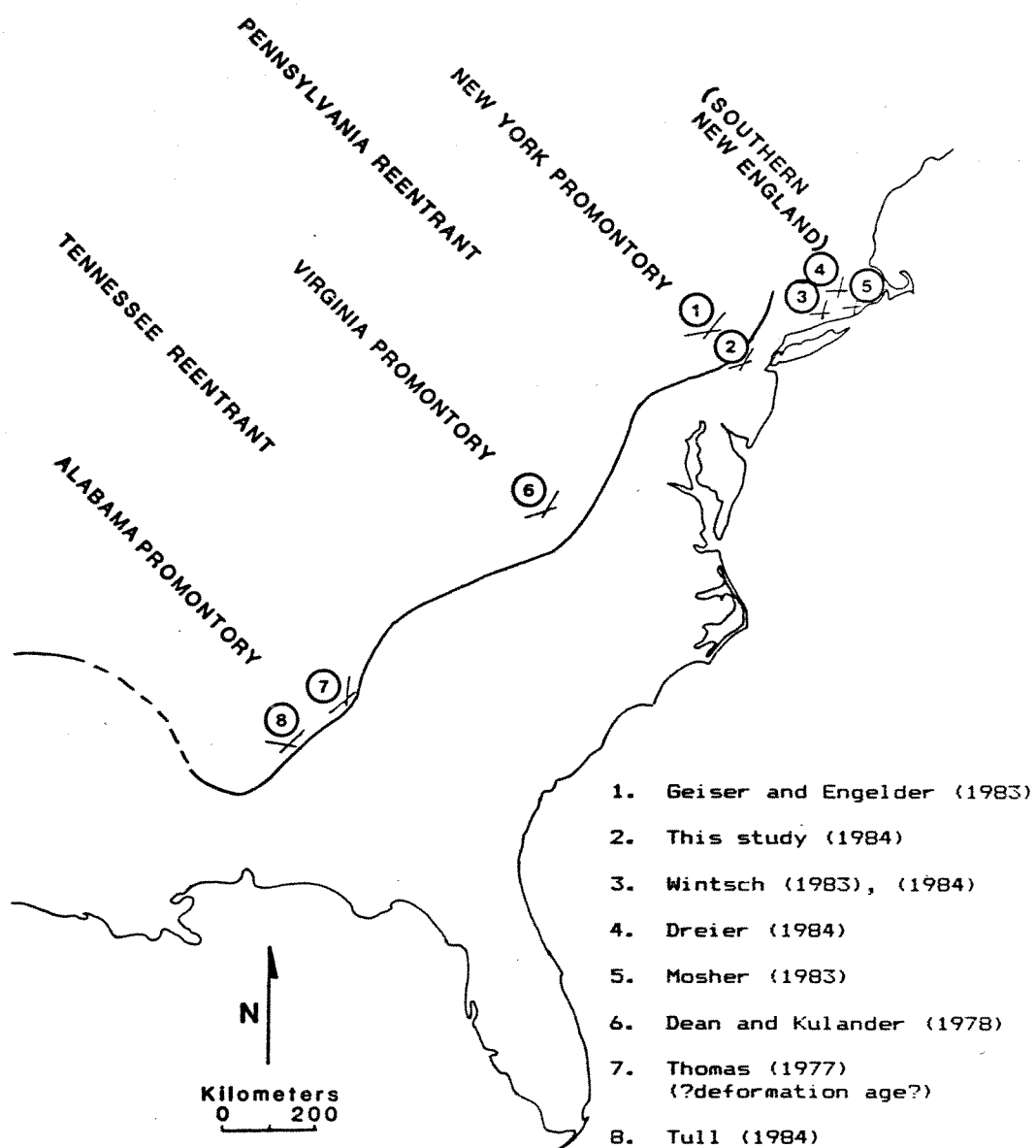


FIGURE 38. NONCOAXIAL STRUCTURAL TRENDS OF PROBABLE ALLEGHENIAN AGE REPORTED ON PROMONTORIES IN THE CENTRAL AND SOUTHERN APPALACHIANS.

noncoaxial deformation at each. In each case crosscutting structural trends indicate a rotation in the shortening direction consistent with the three stage model. On the Alabama promontory and in southern New England, the noncoaxial deformation occurred on the south facing sides producing a clockwise rotation in the shortening direction in a manner analogous to the model in figure 35. However, it has been locally reported that a later third phase of Alleghenian deformation caused an additional counterclockwise rotation in the shortening direction (Tull, 1984; Mosher, 1983). This condition could occur on promontories following ocean closure in neighboring reentrants as stress trajectories are restored to a uniform direction across the suture. According to the rigid indenter model, stress trajectories along irregular margins rotate out of uniformity during movement into embayments prior to closure. Once closure and complete suturing between cratons is established stress trajectories should restore to a uniform direction consistent with the late stage counterclockwise rotations observed. The fact that a late stage counterclockwise rotation is not reported in the New York promontory may simply be because stress magnitudes were not restored to levels sufficient to initiate a late phase of deformation.

CONCLUSIONS

Echelon vein arrays and slickenfiber faults are semi-brittle and brittle shear zones with known displacement directions. Each records a relatively instantaneous principal stress field at the time of its formation. They have been used to approximate paleostress directions during folding of the Siluro-Devonian strata of the Green Pond outlier in northern New Jersey. SFF record a strong NW-SE trending compression directed perpendicular to the NE-SW trend of major folds and dominant cleavage. Results from EVA are more variable, ranging from NW-SE to NE-SW with a strong regionwide N-S directed compression. The development of those EVA which record compression directed oblique to the dominate structural trend are likely to correlate in time with the development of a second cleavage striking E-W. The two structural trends combined with dynamic data leads one to conclude that a two-stage noncoaxial deformation history occurred in the Green Pond outlier of northern New Jersey.

Stage I represents the period of major fold and cleavage development. During this stage the development of numerous SFF and many EVA on fold limbs recorded a progressive folding history as follows. First, when folding began numerous SFF and EVA recorded layer parallel shortening with sl lying in the bedding plane and oriented NW-SE. Progressive folding of fold limbs rotated these

early features preserving their local parallelism to bedding. Continued folding eventually developed new EVA with their s_1 oriented at low angles to bedding. Finally in the later stages of folding numerous EVA and SFF developed with their s_1 at high angles to bedding and subhorizontal. The general order of these features fits well with changing stress patterns predicted by various models for the stress history of progressive folding. In addition, the vertical s_1 recorded by SFF and EVA at hinges fits these models.

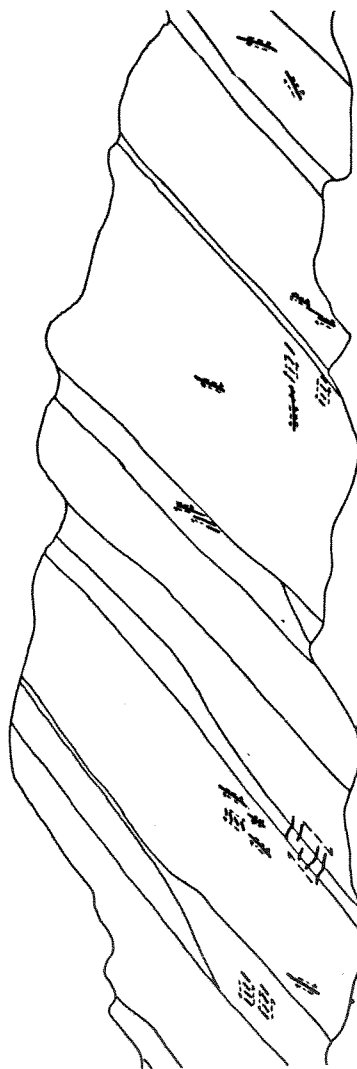
Stage II deformation corresponds to the development of numerous EVA which record compression trending NNW-N parallel to the shortening direction of the cross cleavage. The clockwise rotation of the stress field from NW towards N produced curved fibers on SFF and resulted in incompatible s_1 orientations of SFF and EVA in the same rock. Numerous EVA record this stage of oblique compression because their development, unlike SFF, is not strongly controlled by pre-existing bedding surfaces.

The two stages of noncoaxial deformation in the Green Pond correlates with two phases of Alleghenian deformation on the Allegheny Plateau in eastern Pennsylvania where northwest directed shortening ("Lackawana phase") was also followed by north directed shortening ("Main phase"). These two structural trends are also recorded in the intervening Great Valley and Valley and Ridge of

northwestern New Jersey. Thus, it is concluded that a two-stage Alleghenian deformation history occurred in northern New Jersey on the basis of regional correlation of structures.

Coaxial deformation is recorded in the Pennsylvania reentrant indicating that the zone of noncoaxial deformation is restricted to the New York promontory. This is considered a natural consequence of shortening along an irregular and relatively rigid cratonic margin during collision with Gondwanaland. As a tentative hypothesis the following is proposed. When the New York promontory made initial contact with the continental margin of Gondwanaland the NE-SW trending structures were formed (stage I) as a consequence of underthrusting of Gondwanaland beneath Laurasia. As collision proceeded the African craton internally deformed around the promontory and into the Pennsylvania reentrant involving, in part, right-lateral motion on E-W trending wrench faults. This produced the E-W trending stage II structures which coincides with clockwise rotation of the stress field recorded by the dynamic data in the Green Pond outlier. Similar structural development has occurred in the fold and thrust belt on the Indian cratonic margin as a response to margin adjustments during continental collision with Asia. This model may be useful, in a general way, to explain the presence of Alleghenian age

noncoaxial deformation that appears to exist on every major promontory in the central and southern Appalachians.



APPENDIX. OUTCROP DRAWINGS ALONE

- Anderson, E.m., 1951, The Dynamics of Faulting, second edition, Oliver and Boyd, 206 pages.
- Arthaud, F., and P. Matte, 1977, Late Paleozoic strike-slip faulting in southern Europe and northern Africa: results of a right-lateral shear zone between the Appalachians and the Urals, Geological Society of America, Bulletin 88, pp 1305-1320.
- Barnett, S. G., 1976, Geology of the Paleozoic Rocks of the Green Pond Outlier, Geologic Report Series No. 11, New Jersey Geological Survey, 9 pages.
- Barnett, S.G, 1976, Geologic Map of the Greenpond Outlier, New Jersey.
- Beach, A., 1975, The geometry of en-echelon viens, Tectonophysics, V 28, pp 245-263.
- Beach, A., 1977, Vein arrays, hydraulic fractures and pressure solution structures in a deformed flysch sequence, S. W. England, Tectonophysics, V 40, pp 201-225.
- Beach, A., 1980, Numerical models of hydraulic fracturing and interpretation of syntectonic viens, Jour. of Struc. Geol., V 2,N 4, pp 425-438.
- Bristol, D., Tullis, J., and T. Tullis, 1984, Nature of distributed faulting in the Dighton Conglomerate of SE Massachusetts, Geological Society of America Abstracts with Programs, V 16, N 1, p 6.
- Burger, R.,III, and M.D. Thompson, 1970, Fracture analysis of the Carmichael Peak Anticline, Madison County, Montana, Geological Society of America Bulletin, V 81, pp 1831-1836.
- Casey, M., 1980, Mechanics of shear zones in isotropic dilatant materials, Jour. of Struc. Geol., V 2. N 1/2, pp 143-147.
- Cloos, E, 1932, "Feather joints" as indicators of the direction of movements on faults, thrusts, joints, and magmatic contacts, National Academy of Science Proceedings, V 18, pp 387-395.
- Cloos, E., 1950, General Geology of South Mountain Anticlinorium, Guidebooks to the Geology of Maryland, Johns Hopkins Press, pp I1-I10.

- Cloos, E., 1971, *Microtectonics Along the Western Edge of the Blue Ridge, Maryland and Virginia*, Johns Hopkins Press.
- Cohee, et al., 1968, *Tectonic map of the United States*, U.S. Geological Survey, Washington, D.C..
- Compton, R.R., 1966, Analyses of Pliocene-Pleistocene deformation and stresses in northern Santa Lucia Range California, *Geological Society of America Bulletin*, V 77, pp 1361-1380.
- Dalziel, I.W.D., and G.L. Stirewalt, 1975, Stress history of folding and cleavage development, Baraboo syncline, Wisconsin, *Geological Society of America Bulletin*, V 86, pp 1671-1690.
- Daubree, A., 1897, *Etudes synthetiques de geologie experimentale*, Paris.
- Davis, G.H., 1984, *Structural Geology of Rocks and Regions*, John Wiley and Sons, 492 pages.
- Dean, S.L., and B.R. Kulander, 1978, Kinematic analysis of folding and pre-fold structures on the southwestern flank of the Williamsburg anticline, Greenbrier County, West Virginia, *Geological Society of America Abstracts with Programs*, V 9, pp 132-133.
- Dennis, J.G., 1972, *Structural Geology*, Ronald Press Company, 532 pages.
- Dieterich, J.H., 1970, Computer experiments on mechanics of finite amplitude folds, *Can. Jour. of Earth Sciences*, V 7, pp 467-477.
- Dieterich, J.H., and N.L. Carter, 1969, Stress-history of folding, *American Journal of Science*, V 267, pp 129-154.
- Donath, F.A., 1961, Experimental study of shear failure in anisotropic rocks, *Geological Society of America Bulletin*, V 72, pp 985-989.
- Drake, A.A., Jr., 1969, Precambrian and lower Paleozoic geology of the Delaware Valley, New Jersey-Pennsylvania, in, Subitzky, S., ed., *Geology of Selected Areas in New Jersey and Eastern Pennsylvania and Guidebook of Excursions*, pp 51-131.

- Drake, A.A., Jr., 1978, The Lyon Station-Paulins Kill nappe—the frontal structure of the Musconetcong nappe system in eastern Pennsylvania and New Jersey, U. S. Geological Survey Professional Paper 1023, 20 pages.
- Drake, A.A., Jr., 1980, The Taconides, Acadides, and Alleghenides in the central Appalachians, in Wones, D. R., ed. Proceedings, "The Caledonides in the USA", I.G.C.P. Project 27-Caledonide Orogen, Virginia Polytechnic Institute and State University Memoir 2, pp179-187.
- Drake, A.A., Jr., and P.T. Lyttle, 1980, Alleghanian thrust faults in the Kittatiny Valley, New Jersey, in, Field Studies of New Jersey Geology and Guide to Field Trips, Manspiezer, W., ed., pp 92-115.
- Dreier, R.B., 1984, The Blackstone Series: Evidence for Alleghanian deformation in an Avalon terrane, Geological Society of America Abstracts with Programs, 19th Annual Meeting, Northeastern Section, V 16, N 1, p 13.
- Durney, D.W., and J.G. Ramsay, 1973, Incremental strains measured by syntectonic crystal growths, in Gravity and Tectonics, De Jung, B. A., Scholter and Roberter, eds., John Wiley and Sons, pp 67-96.
- Etchecopar, A., Vasseur, G., and M. Daignieres, 1981, An inverse problem in microtectonics for the determination of stress tensors from fault striation analysis, Journal of Structural Geology, V 3, N 1, pp 51-65.
- Epstein, J.B., 1969, Structural control of wind gaps and water gaps and of stream capture in the Stroudsburg area, Pennsylvania, and New Jersey, in Subitzky, ed., Geology of Selected Areas in New Jersey and Eastern Pennsylvania and Guidebook to Excursions, pp 206-213.
- Epstein, J. and A. Epstein, 1969, Geology of the Valley and Ridge province between Delaware Water Gap and Lehigh Gap, Pennsylvania, in, subitzky, ed., Geology of Selected Areas in New Jersey and Eastern Pennsylvania and guidebook of excursions, pp 132-205.
- Fletcher, R.C., and D.D. Pollard, 1981, Anticrack model for pressure solution surfaces, Geology, V 9, pp 419-424.
- Friedman, K., and D.W. Stearns, 1971, Relations between stresses inferred from calcite twin lamellae and macrofractures, Teton Anticline, Montana, G. S. A. Bull., V 82, pp 3151-3162.
- Fyfe, W.S., Price, N.J., and A.B. Thompson, 1978, Fluids in the Earth's Crust, Elsevier Scientific Publishing Company, 383 pages.

- Geiser, P., and T. Engelder, 1983, The distribution of layer parallel shortening fabrics in the Appalachian foreland of New York and Pennsylvania: evidence for two non-coaxial phases of the Alleghenian orogeny, *Geological Society of America Memoir* 158, pp 161-175.
- Griggs, D.T., and J. Handin, 1960, *Rock Deformation*, Geological Society of America Memoir 79.
- Hancock, P.L., 1964, The relations between folds and Late-formed joints in South Pembrokeshire, *Geology Magazine*, V 101, N 2, pp 174-184.
- Hancock, P.L., 1972, The analysis of en-echelon veins, *Geology Magazine*, V 109, N 3, pp 269-276.
- Handin, J., 1969, On the Coulomb-Mohr failure criterion, *Journal of Geophysical Research*, V 74, pp 5343-5348.
- Hallbauer, D.K., Wagner, H., and N.G.W. Cook, 1973, Some observations concerning the microscopic and mechanical behavior of quartzite specimens in stiff, triaxial compression tests, *Int. Jour. Rock Mech. and Mining Sci.*, V 10, 713-726.
- Hobbs, B.E., W.D. Means, and P.F. Williams, 1976, *An Outline of Structural Geology*, John Wiley and Sons, 571 pages.
- Hubbert, M.K., and W.W. Rubey, 1959, Role of fluid pressure in mechanics of overthrust faulting, Part I, *Geological Society of America Bulletin*, V 70, pp 115-166.
- Kirby, M.W., 1981, *Sedimentology of the Middle Devonian Bellvale and Skunnemunk Formations in the Green Pond outlier in northern New Jersey and southeastern New York*, Masters thesis, Rutgers University, New Brunswick, New Jersey, 100 pages.
- Knipe, R.J., and S.H. White, 1979, Deformation in low grade shear zones in the Old Red Sandstone, S. W. Wales, *Journal of Structural Geology*, V 1, N 1, pp 53-66.
- Kummel, H.B., and S. Weller, 1902, The rocks of the Green Pond mountain region, Annual report of the state geologist, New Jersey Geological Survey, pp 1-51.
- Lajtai, E.Z., 1971, A theoretical and experimental evaluation of the Griffith theory of brittle fracture, *Tectonophysics*, V 11, pp 129-156.
- Lajtai, E.Z., 1969, Mechanics of second order faults and tension gashes, *Geological Society of America Bulletin*, V 80, pp 2253-2272.

- Lefort, J.P., and R. Van Der Voo, 1981, A kinematic model for the collision and complete suturing between Gondwanaland and Laurussia in the Carboniferous, *Journal of Geology*, V 89, pp 537-550.
- Marshak, S., Geiser, PA, Alvarez, W. and T. Engelder, submitted April, 1981, Mesoscopic fault array of the Northern Umbrian Apennines fold belt, Italy: A case of conjugate shear by pressure solution slip, *Geological Society of America Bulletin*.
- Martin, H., 1871, *Proc. N.Y. Lyceum Natural History*, V 1, pp 259-260.
- Mattauer, M., Proust, F., and P. Tapponnier, Major strike-slip fault of late Hercynian age in Morocco, *Nature*, V 237, pp 160-162.
- Means, W.D., 1976, *Stress and Strain: Basic Concepts of Continuum Mechanics for Geologists*, Springer-Verlag New York Inc., 339 pages.
- Molnar, P, and P. Tapponnier, 1977, Relation of the tectonics of eastern China to the India-Eurasia collision: application of slip-line field theory to large-scale continental tectonics, *Geology*, V 5, pp 212-216.
- Mosher, S., 1983, Kinematic history of the Narragansett Basin Massachusetts and Rhode Island: constraints on late Paleozoic plate reconstructions, *Tectonics*, V 2, N 4, pp 327-344.
- New Jersey Geological Survey, *Geologic Overlay Series*, Sheet Number 22, Trenton, New Jersey.
- Nickelson, R.P., 1979, Sequence of structural stages of the Allegheny Orogeny at the Bear Valley Strip Mine, Shamokin, Pennsylvania, *American Journal of Science*, V 279, pp 225-271.
- Pollard, D.D., Segall, P., and P.T. Delaney, 1982, Formation and interpretation of dilatant echelon cracks, *Geological Society of America Bulletin*, V 93, pp 1291-1303.
- Prosser, C.S., 1892, Notes on the geology of Skunneunk Mtn., Orange Co., New York, *New York Academy of Science Transactions*, V 11, pp 132-149.
- Ragan, D.M., 1973, *Structural Geology: An Introduction to Geometric Techniques*, second edition, John Wiley and Sons, 208 pages.

- Ramsay, J.G., 1980, The crack and seal mechanism of rock deformation, *Nature*, V 284, N 13, p 135.
- Ramsay, J.G., 1980, Shear zone geometry: a review, *Journal of Structural Geology*, V 2, pp 83-99.
- Ramsay, J.G., 1967, *Folding and Fracturing of Rocks*, McGraw-Hill Book Company, 568 pages.
- Ramsay, J.G., and R.H. Graham, 1970, Strain variation in shear belts, *Canadian Journal of Earth Sciences*, V 7, pp 786-813.
- Rankin, D.W., 1976, Appalachian salients and recesses: late Precambrian continental breakup and the opening of the Iapetus ocean, *Journal of Geophysical Research*, V 81, N 32, pp 5606-5619.
- Ratcliffe, 1980, Brittle faults (Ramapo fault) and phylonitic ductile shear zones in the basement rocks of the Ramapo seismic zones New York and New Jersey, and their relationship to current seismicity, pp 278-311 in Manspeizer, Warren, ed., *Field studies of New Jersey geology guide field trips*, New York State Geological Association, 52nd Annual Meeting, Newark, New Jersey, 398 pages.
- Rickard, M.J., and L.K. Rixon, 1983, Stress configurations in conjugate quartz-vein arrays, *Journal of Structural Geology*, V 5, N 6, pp 573-578.
- Rispoli, R., 1981, Stress fields about strike-slip faults inferred from stylolites and tension gashes, *Tectonophysics*, V 75, pp T29-T36.
- Rispoli, R., and G. Vasseur, 1983, Variation with depth of the stress tensor anisotropy inferred from microfault analysis *Tectonophysics*, V 93, pp 169-184.
- Roering, C., 1969, The geometrical significance of natural en-echelon crack arrays, *Tectonophysics*, V 5, N 2, pp 107-123.
- Root, S.I., 1970, Structure of the northern terminus of the Blue Ridge in Pennsylvania, *Geological Society of America, Bulletin*, V 8, pp 815-830.
- Root, S.I., and D.M. Hoskins, 1977, Latitude of 40 degree north fault zone, Pennsylvania: a new interpretation, *Geology*, V 5, pp 719-723.

- Rowlands, D., 1982 pers. comm., Doctoral research in progress concerning structure of the Greenpond outlier, University of South Carolina.
- Sanders, J.E., Friedman, G.M., and C.A. Sternbach, 1981, Extinct and active continental margin deposits and their tectonic-switchover products: Appalachian Orogen ("eastern overthrust belt") -Catskill Plateau-Newark Basin Atlantic Coastal Plain, pp 106-232 in Hobbs, G., ed., Field guide to the geology of the Paleozoic, Mesozoic, and Tertiary rocks of New Jersey and the central Hudson Valley eastern Section Meeting of the A.A.P.G., Atlantic City, New Jersey, 232 pages.
- Shainin, V.E., 1950, Conjugate sets of en echelon tension fractures in the Athens Limestone at Riverton, Virginia, Geological Society of America Bulletin, V 61, pp 509-517.
- Smock, J.C., 1884, Report of the State Geologist of New Jersey for 1884, New Jersey Geological Survey, pp29-56.
- Tapponnier, P., and P. Molnar, 1976, Slip-line field theory and large-scale continental tectonics, Nature, V 264, pp 319-324.
- Tapponnier, P., Peltzer G., Le Dain A.Y., Armijo R., and P. Cobbold, Propagating extrusion tectonics in Asia: new insights from simple experiments with plasticine, Geology, V 10, pp 611-616.
- Thomas, W.A., 1977, Evolution of Appalachian-Quachita salients and recesses from reentrants and promontories in the continental margin, American Journal of Science, V 277, pp 1233-1278.
- Thompson, A.F., 1957, Petrology of the Silurian quartzites and conglomerates in New Jersey, unpublished Ph.D. thesis, Rutgers University, New Brunswick, New Jersey.
- Toskos, T., 1984, Structural and gravity transect along the New Jersey Highlands and adjacent Valley and Ridge, in northern New Jersey, Masters thesis, Rutgers University, New Brunswick, New Jersey, 156 pages.
- Tull, J.F., 1984, Polyphase late Palaeozoic deformation in the southeastern foreland and northwestern Piedmont of the Alabama Appalachians, Journal of Structural Geology, V 6, pp 223-234.

- Turner, F.J, and L.E. Weiss, 1963, Structural Analysis of Metamorphic Tectonites, McGraw-Hill Book Company, Inc., 544 pages.
- Willard, B. and A.B Cleaves, 1933, Hamilton Group of central Pennsylvania, Geological Society of America Bulletin V 44, pp 757-782.
- Wintsch, R.P., 1983, A temperature-strain-path as a memory of late Hercynian intraplate deformation, Geological Society of America, Abstracts with Programs, 18th Annual Meeting, Northeastern Section, V 15, N 3, p 196.
- Wintsch, R.P., 1984, A tectonic model for the late Paleozoic of southeastern New England, Geological Society of America Abstracts with Programs, 19th Annual Meeting, Northeastern Section, V 16, N 1, p 71.
- Wise, D.U., Dunn, D.E., Engelder, J.T., Geiser, P.A., Hatcher, R.D., Kish, S.A., Odom, A.L., and S. Schamel, Fault-related rocks:suggestions for terminology, Geology, V 12, pp 391-394.

VITA: JAMES P. MITCHELL

- 1955 Born August 21 in Richmond, Virginia.
1973 Graduated from J.F.K. High School,
Richmond, Virginia.
1973-77 Attended College of William and Mary,
Williamsburg, Virginia. Geology Major.
1977 B.S., College of William and Mary.
1978-81 Teacher, High School Earth Science,
Richmond, Virginia.
1981-84 Attended Rutgers University, New Brunswick,
New Jersey.
1984 Mitchell, Jim and Randy Forsythe, Paleostress
directions during folding of the Green Pond
outlier, N.J. Highlands, Geological Society
of America Abstracts with Programs, NE Section
Annual Meeting, Volume 1, page 51.
1985 M.S. Geology.